INSTITUTE OF GEOSCIENCE
Center of Applied Geoscience (ZAG)

Master Thesis

Master of Science in
Applied Environmental Geoscience

Ahmed Elshall

Practical Design Optimization of Pump and Treat Systems at Complex Real-world Sites using Evolution Strategies

Supervisor

Dr. Michael Finkel

Tübingen, October, 2009

TO MY FATHER AND MOTHER

ACKNOWLEDGEMENT

I am indebted to the innumerous manifestations that have explicitly or implicitly contributed to this work in particular the unreserved kindness of my parents, family and friends. I am especially thankful for my thesis supervisor Dr. Michael Finkel for providing a Research Assistant job opportunity, which then continued to be this master thesis, and particularly for maintaining an obliging work atmosphere over the last one and half years. In addition, I would like to extend many thanks to the D-Site for providing the needed tools and facilities. For the most part, I am grateful to the AEG coordinator Dr. Peter Merkel, professors and students for making the AEG Master Course a great learning experience. Finally, I would like to acknowledge the Evolution Ecology Forum in Tuebingen for supporting this thesis through their generous Evolutionary Grant Award.

TABLE OF CONTENTS

ABBREVIATIONS

ACL	Alternate Concentration Level
APM	Additive Penalty Method
BTEX	Benzene, Toluene, Ethylbenzene and Xylene
C	Case
CHC	Chlorinated hydrocarbon
CMA-ES	Covariance Matrix Adaptation Evolution Strategies
CAT Unit	Catalysis Unit (PCR-MBS + GAC Air Filter)
CCC	Cross Capture Coefficient
COC	Contaminant of Concern
DC	Differentiated Capture
DCA	Dichloroethane
DCE	Dichloroethene
DCM	Dichloromethane
DCO	Direct Cost Optimization
DNAPL	Dense Non-aqueous Phase Liquid
EPA	Environmental Protection Agency
ES	Evolution Strategy
GAC	Granular Activated Carbon
GAC Unit	Granular Activated Carbon (aqueous unit)
GSA	Grouped-Scenarios Approach
H	Henry's Coefficient [-]
HMOC	Hybrid Method of Characteristics
IDCO	Indirect Cost Optimization
ISA	Individual-Scenarios Approach
LNAPL	Light Non-aqueous Phase Liquid
MBS	Membrane Based Stripping
MCL	Maximum Concentration Level
MMOC	Modified Method of Characteristics (backward tracking)
MOC	Method of Characteristics (forward-tracking)
MPM	Multiplicative Penalty Method
MR	Model Run
NAPL	Non-aqueous Phase Liquid
NDC	Non-differentiated Capture
NPV	Net Present Value [€]
OF	Objective Function
OFI	Objective Function Improvement
OR	Optimization Run
PAH	Polyaromatic Hydrocarbon
PDC	Particle Distribution Configuration
PTS	Pump and Treat System
PTSDC	Pump and Treat System Design and Cost
PCE	Perchloroethene
PCR	Palladium Catalytic Reduction
PVC	Polyvinyl Chloride
Sc	Scenario

S/O	Simulation-Optimization
RMS	Residual Mean Squared
TCA	Trichloroethane
TCE	Trichloroethene
TR	Time Ratio (of the out-site to in-site particles travel time)
VC	Vinyl chloride
VSP	Variation of Search Points
WB	Western Boundary

1 Introduction

1.1 Practical Design Optimization of Remediation Systems

A study in 2004 by the U.S. Environmental Protection Agency (EPA) estimated the remaining remediation cost for contaminated soil and ground water in the U.S. to be $ 209 billion. The study further mentions that out of the implemented remediation systems, 65% are Pump and Treat Systems (PTS). However, most of existing PTSs are not operating as designed and have not been optimized since installation (U.S. EPA, 2002). To design new PTSs or to upgrade the existing ones, simulation-optimization (S/O) methods are gaining ground over traditional approaches. In study by Becker et al. (2006) conducted on three sites operated by the U.S. Department of Defense to evaluate the benefits of S/O algorithms against traditional trial and error modeling approaches, the results show that the solutions found by S/O methods are 5%-50% cost efficient than those obtained by trail-and-error with an average cost reduction of ≈20%. Accordingly, reducing the cost of the existing and future PTSs through the utilization of S/O methods is becoming an active research area with the aim of increasing the robustness of these methods and the reliability of the candidate solutions.

The gap between theoretical studies and practical applications of design optimization of problems involving flow and transport phenomena is subsurface systems continues to converge as more practical studies are emerging. The applicability and benefits of S/O approach in the design of PTS for complex real-world sites are documented in several studies (e.g. Liu et al., 2000; Zheng and Wang, 2002; Becker et al., 2006; Peralta et al., 2008). Other studies extend the implementation of the S/O to other remediation technologies such as bioremediation (e.g. Yoon and Shoemaker, 1999), soil vapor extraction (e.g. Herke et al., 1999) and surfactant-enhanced aquifer remediation (e.g. Schaerlaekens et al., 2006; He et al., 2008b), or other hydrogeological applications such as balancing the needs of agricultural irrigation and environmental protection (e.g. Wu et al., 2007; Rana et al., 2008), groundwater management (e.g. Bayer et al., 2009), and pumping at costal aquifers (e.g. Park and Aral, 2004; Kourakos and Mantoglou, 2009). Although these technologies and applications seem quite different, yet the underlying research objective is similar.

Two interlinked issues are significant when addressing the practicality of S/O approach, which are finding an optimal reliable solution at a reasonable amount of time. Finding a global optimal or near optimal solution is more or less a function of the optimization algorithm. However, a more critical issue is the reliability of the candidate solution. Although the reliability of the solution has been extensively researched on a theoretical level, only few works present practical cases studies. Tiedeman and Gorelick (1993) developed a contaminant capture design for a Superfund site with a vinyl chloride plume under uncertain hydraulic conductivity and recharge using stochastic S/O approach. Medina et al. (1996) developed a system that is capable of accounting for uncertainty by guiding the user in the selection of appropriate transport model and by presenting tradeoffs between different remediation costs and probability of failure. Massmann et al. (1991) implemented a full decision analysis approach, which is further developed by Russell and Rabideau (2000). Ensuring the reliability of the solution is done as part of the optimization process, and can be further complimented by several post-processing processes. However, effective practical implementation of these

approaches is subject to the computational efficiency, since each optimization iteration evokes several simulation models such as flow, transport, particle tracking and so on.

Several solutions are being developed to alleviate this computational burden. The use of parallel computer (e.g. Kobayashi et al., 2008) is the most obvious solution, yet this option is generally implausible for many practitioners. Clearly, the best option is to use a powerful optimization algorithm (e.g. Mulvey et al., 1995; Bayer and Finkel, 2004; Yuen and Chow, 2009) or an improved search strategy (e.g. Guan and Aral, 1999; Babbar and Minsker, 2006; Espinoza and Minsker, 2006; Guo et al., 2007; Sinha and Minsker, 2007; Ayvaz and Karahan, 2008). Also, these powerful optimization algorithm and enhanced search techniques can be further complemented with response functions, which act as surrogates for the simulation models as the optimization advance (e.g. Zheng and Wang, 2002; He et al., 2008a). For example, Yan and Minsker (2006) shows that an adaptive neural network genetic algorithm saved 85-90% of the simulation model runs through a dynamic learning process. Improving the computational efficiency of the stochastic methods used to account for uncertainty (e.g. Bayer et al., 2008) is another area for research aiming at decreasing the design time of the S/O problems.

Other issues of practical implications are also discussed in literature. A study by Ren and Minsker (2005), which discusses the formulation of the objective function, illustrates that a more realistic cost function with detailed cost items may yield more accurate results, but requires more development time. Another study by Endres et al. (2007) shows that accounting for nonequilibrium adsorption in granular activated carbon (GAC) treatment model will result in more realistic cost and better-engineered system. A study by Finkel et al. (2008) demonstrates that the dis-joint capture and separate treatment of different plume types that exist in close proximity can considerably reduce the PTS cost.

In conclusion, two recent review articles (Mayer et al., 2002; Qin et al., 2009) acknowledge that many efforts have been made in the area of design optimization of remediation systems. Yet the effective design of various remediation systems are still challenging for practitioners (Qin et al., 2009), and "more work remains before comprehensive, efficient and robust solution methods exist to solve the most challenging applications in subsurface science" (Mayer et al., 2002).

1.2 Thesis Overview in connection with Previous Studies

This thesis implements several innovative concepts to design a robust, reliable and cost efficient PTS that can capture and treat multiple contaminant plumes in groundwater by using an Evolution Strategies (ES) optimization algorithm. This is done through the combined application of the optimization algorithm with several models that can simulate the ground water flow and contaminant transport, design and dimension the treatment unit, and calculate the cost of the PTS.

A heavily contaminated site in Italy, which contains complex plumes of petroleum and chlorinated hydrocarbons that exist in close proximity, is used in this study. PTS is selected to be the best available remediation solution for this contaminant situation. The PTS has several pumping wells installed at various locations in the aquifer. The function of these wells is to hydraulically contain the contaminant plumes within the site boundaries or to achieve a full

aquifer restoration. The pumped water is treated by various treatment technologies, and the treated water is either re-injected into the aquifer or discharged. If the PTS design objective is to hydraulically control the plume, then the wells should be located in a way to minimize contaminant extraction in order to decrease the water treatment cost. If the design objective is to achieve a full aquifer restoration, then the wells should be located in a way that ensures maximum removal rates. In this case study the management decision is not to achieve a full aquifer restoration, but rather to hydraulically contain the plumes within the site premise at the minimum cost.

Although pump-and-treat systems are no longer considered the best or most popular choice among groundwater remediation systems because of the time required to achieve cleanup goals and the ineffectiveness of the system, yet they are still useful especially in areas with significant contamination (Khan et al. 2004) and when other more effective and efficient technologies are inapplicable. PTS is chosen for this site because it is dominated by 1,2- Dichloroethane (DCA), so no efficient in-situ remediation technology is available for this contaminant situation. Due to its low octanol water partitioning coefficient K_{ow}, sorption of 1,2-DCA onto GAC is inefficient and the associated cost is high (Finkel et al., 2008). Also, Dehalogenation of 1,2-DCA will not occur under ambient conditions in the aqueous phase. Instead, elevated temperature up to 400 C° is needed to achieve high reaction rate, which can only be achieved in gaseous phase. Accordingly, no in-situ treatment system can fulfill this condition, so an ex-situ treatment system is needed. Thus PTS is found to be the most suitable remediation technology for this site.

Again the management decision is not to hydraulically contain the plumes within the site premise at the minimum cost. IMES GmbH (2002) developed a flow and transport models for this site to find a cost efficient solution for this pump and treat hydraulic capture system using a trail-and-error approach. As a better alternative, this study implements an optimization algorithm, which automates the problem solving process and guide the search process to find an optimal solution in a reasonable amount of time. Evolution strategies optimization, which is an experience-based heuristic optimization algorithm, is chosen for this task.

Evolution Strategies as indicated by its name is oriented toward natural evolution by mimicking the characteristic features of evolution theory to solve optimization problems. The algorithm is implemented as a computer code in which a population of abstract representations (genome) of candidate solutions (individual) evolves toward a better solution. The evolution starts from a population of randomly generated individuals. After the fitness of the individuals of a population are independently assessed based on an objective function (OF), multiple individuals are selected based on their fitness, and mutated to act as the parents of the new population. Every population denotes a generation, which keeps evolving until reaching the stopping criterion.

As a continuation of the previous studies (Bayer and Finkel, 2007; Finkel et al., 2008), the innovative optimization algorithm CMA-ES (Hansen and Ostermeier, 2001; Hansen et al., 2003) - derandomized evolution strategies with covariance matrix adaptation - is selected for this design optimization problem. The object of the optimization is the well configuration (i.e. layout and pumping rate) that hydraulically control the existing groundwater contamination. CMA-ES algorithm along with other models is used to evaluate the fitness of any particular well

configuration. This fitness is then used by the CMA-ES algorithm for the optimization process to propose a new candidate solution. The groundwater flow and contaminant migration is simulated with public domain simulation codes (MODFLOW, MODPATH and MT3DMS). A pump and treat system design and cost (PTSDC) code developed by (Lantschner, 2005) is used to design and dimension the treatment unit, and calculate the cost of the PTS. The S/O tools used in the study follows Finkel et al. (2008). A schematic for the tools used in this study and their respective outputs is presented in Figure 1.1.

The results of Finkel et al. (2008) show that the mathematical optimization with CMA-EA invoking the simulation codes is adequate and efficient for the given task (i.e. CMA-ES optimization succeeded in reaching a well configuration that separately captures the two contaminant plumes at lower economic costs compared to reference configurations that are set only on the basis of expert knowledge).

Using the same flow and transport models, particle configuration and PTSDC code developed previously, this master thesis features several new concepts in order to overcome the most significant problems in identifying optimal technical solutions in practice. Special consideration is given to the issue of robustness of the identified solutions and the computational efficiency of the optimization process. Major research topics addressed in this thesis are as follows:

1. Develop a practical stopping criterion
2. Analyze the optimization search capacity under different parameter settings
3. Examine the effectiveness of adding time of contaminant migration in groundwater as an additional constraints in the objective function to restrict the capture zone to the site premise
4. Account for data uncertainty by representing the groundwater flow situation using four different equally probable conceptual hydrogeological scenarios in which two approaches are examined, namely, individual-scenarios approach (ISA) and grouped-scenarios approach (GSA)
5. Compare the two different search strategies, namely the indirect cost optimization (IDCO) and direct cost optimization (DCO) in which the formal is stepwise procedure (technical optimization + economic assessment of technically optimal solutions), while the later is a one-step full economic optimization

Each of the above five objectives is discussed the in the next sub-section. Then the specific thesis tasks are presented in the last sub-section.

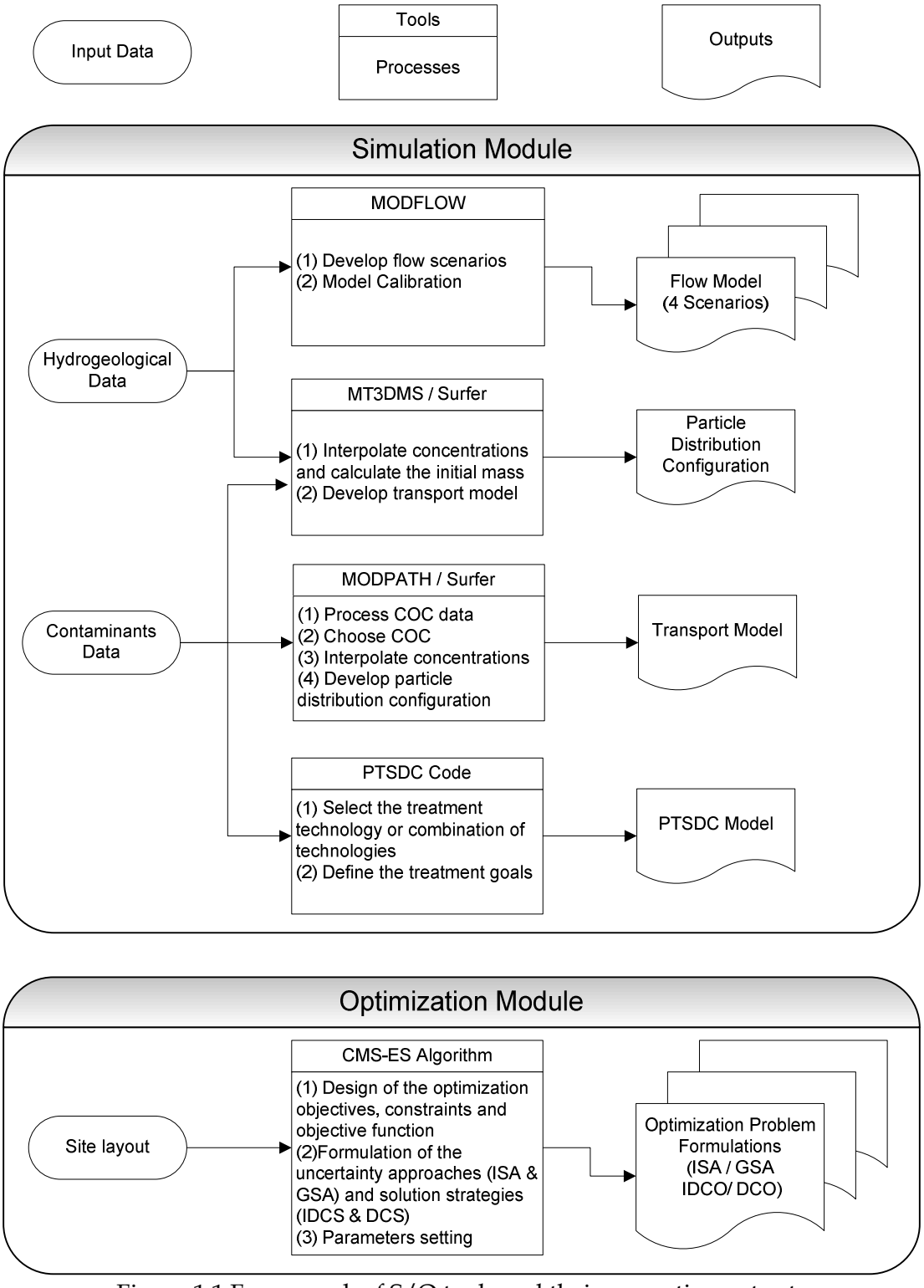

Figure 1.1 Framework of S/O tools and their respective outputs

1.3 Thesis Objectives

1.3.1 Develop a Practical Stopping Criterion

Two built-in stopping criteria are examined in this study in order to develop a new practical stopping criterion. The number of generations is the CMA-ES default stopping criterion in which the search ends when a predefined number of generation evaluation is reached. This stopping criterion is not practical since the required number of generations is a function of the problem complexity, and thus it is not known in advance. Accordingly, if this number is not accurately defined, the optimization can prematurely terminate or conversely continue running without any significant improvement in the OF values.

The variation of search points (VSP) is another built-in stopping criterion in which the search stops if variation of the search points becomes considerably smaller in all coordinates than a predefined scalar value $tolX$, which is defined as $S / \sqrt{n}$, where n the number of problem dimensions and S is a scalar number with a default value S= 1E-7. Since the practical meaning of the VSP stopping criterion is not clear a priori, a new stopping criterion is thought.

By analyzing the number of generations required to reach a solution in which no further significant improvement in the OF values is occurring, a practical stopping criterion is developed. The study propose the objective function improvement (OFI) stopping criterion, which terminates the search when the improvement of the OF values reaches a certain predefined minimum value. Also, the built-in VSP stopping criterion is normalized the to the newly developed OFI stopping criterion to give it a practical meaning.

1.3.2 Evaluate the Optimization Search Capacity

A second objective of this study is to make the search capacity more robust and explorative by increasing the number of individuals λ per generation. The increase in the number of the model runs (MR) due to the increase in the λ is evaluated, and is weighted against the improvement in the solution to assess if such increase is worthwhile.

1.3.3 Constrain the Capture Zone to the Site Premise

To avoid any legal and financial liability the plume must not only be captured and contained, but rather the capture zone should be located within the site boundaries. In other words, the proposed well configuration should ensure that all particles routes from the original position to the pumping wells are within the site premise. Using the particle configuration developed using MODPATH, this study accounts for the time ratio (TR) of the out to in-site travel time for all the particles to restrict the capture zone to the site premise. Thus, TR acts as an additional constraint in the objective function. A third objective in this thesis is to formulate and evaluate the performance of this new constraint.

1.3.4 Account for Uncertainty

Most studies addressing the parameters uncertainties in the design and operation of PTS are limit to uncertainty in hydraulic conductivity (Aly and Peralta, 1999; Ndambuki et al., 2000; Hilton and Culver, 2005; Ricciardi et al. 2007; Ko et al., 2008; Kourakos and Mantoglou, 2008). In addition to uncertainties in hydraulic conductivity, few other studies address other uncertain parameters such as recharge (Tiedeman and Gorelick, 1993), plume distribution (Bau and Mayer, 2008) and longitudinal and transverse dispersion coefficients (Guan and Aral 2005). In a study by Aksoy and Culver (2004) addressing chemical heterogeneity, sorption distribution coefficient K_d and the mass transfer rate are treated as spatial variables.

Accounting for uncertainty is usually carried out using stochastic methods, yet these methods are limited to sites that have enough data points that enable the generation of the statistical properties of the parameter understudy. A second limitation of the stochastic methods is that some parameters cannot be addressed stochastically. For example, the uncertainty in this case study is resulting from the unavailability of data of the layers thickness in the model domain outside the site boundary. Also, water table depth and flow at certain boundaries are uncertain. Such points can only be addressed deterministically. Regardless of these two limitations, stochastic methods are generally computational demanding, and thus their application in practical problems is still limited.

Accounting for uncertainties is carried out using individual-scenarios approach (ISA) or grouped-scenarios approaches (GSA). In ISA, the solution is obtained based on the critical scenarios, which are the scenarios that have effect on the optimal solution depending on desired reliability level. Critical realizations are identified through using initial designs and safety threshold (e.g. Mantoglou and Kourakos, 2007), or can be incorporated into the optimization algorithm through a self adaptive method (Hilton and Culver, 2005; Kourakos and Mantoglou, 2008). On the other hand, in grouped-scenarios approach several scenarios, which represent the uncertainty, are examined simultaneously resulting in a single design that incorporate the data of the multiple scenarios (e.g. Ricciardi et al., 2007).

Using the 4 hydrogeological scenarios developed by IMES GmbH both the ISA and GSA are tested. The optimization runs on each scenario individually resulting in 4 optimal well configurations. Using ISA, each well configuration is later post-proceeded on the other scenarios to evaluate its performance thereon, and thus the critical scenario can be identified. A more robust approach is the GSA where the optimization runs on the four scenarios simultaneously resulting in one optimal well configuration, which is valid for the four scenarios. The difference between these two approaches can be visualized in Figure 1.2

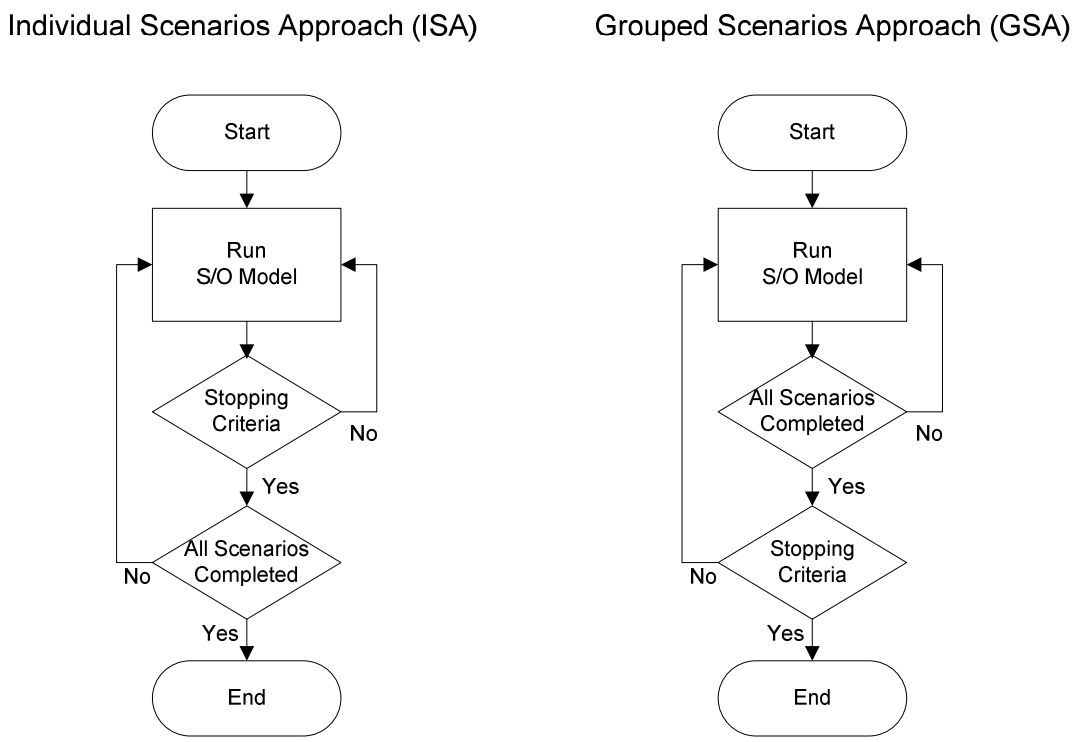

Figure 1.2 Flowcharts for ISA and GSA

1.3.5 Assess Different Optimization Strategies

Two optimization strategies are implemented in this study, which are indirect cost optimization (IDCO) strategy and direct Cost Optimization (DCO) strategy. The IDCO is a two-steps procedure strategy in which the outcome of the simulation and optimization models is an objective function (OF) value, which is a real number that contains data from the flow simulation and particle tracking. The lower the OF value, the better is the solution. Mainly, the OF value incorporate data about the following objectives/constraints:

1. Restriction of the pumping wells to the site premise
2. Capturing the plume fringe
3. Constraining the capture zone to the site premise
4. Disjoint capture of the two plume types
5. Minimizing the pumping rate

In the second step, the well configuration with the minimum OF is selected and is then post-processed using the transport model to obtain the amount of mass removed for each contaminant, and then the PTSDC model is used to design and calculate the total cost of the PTS. Figure 1.3 shows a flowchart for this two-steps strategy.

In contrast to the IDCO, the DCO is a one-step procedure in which the cost is directly optimized. Each flow simulation and particle tracking run is used to evaluate the following constraints:

1. Restriction of the pumping wells to the site premise
2. Capturing the plume fringe
3. Constraining the capture zone to the site premise

If the proposed well configuration fulfilled these three constraints then the transport and PTSDC models are invoked to calculate the total cost, otherwise the OF function value is converted to a cost value. Either ways, the calculated cost value is passed to the optimization algorithm as shown in Figure 1.3.

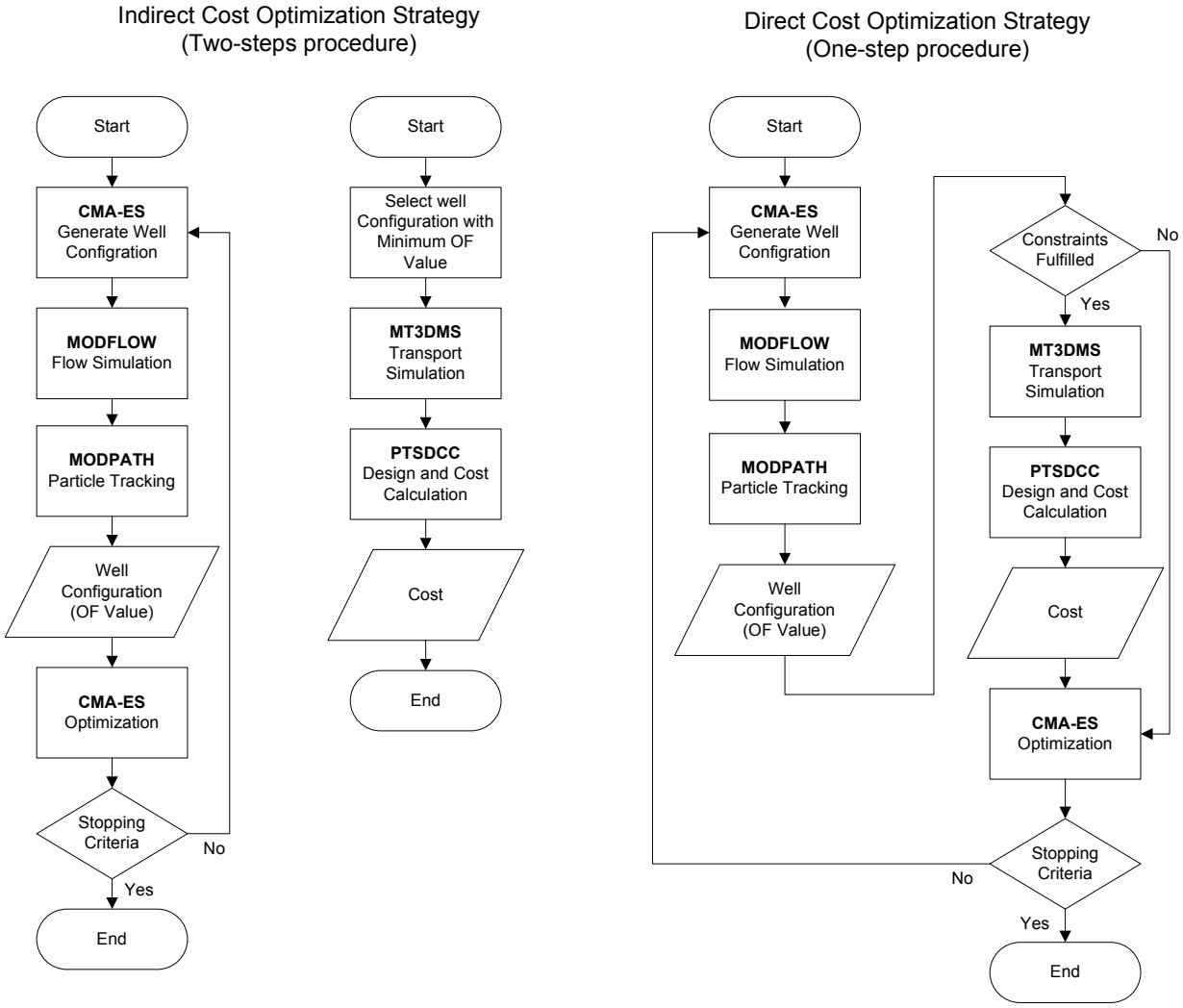

Figure 1.3 Flowcharts for IDCO and DCO strategies

The formulation of the objective function for these two strategies is discussed in the Methodology section and their performance is evaluated and compared in the Results and Discussion section.

1.4 Thesis Tasks

Because of the stochastic features of the evolutionary algorithms, any randomly initialized optimization run (OR) shows a different search and provide different results even if the parameter settings are not changed (Bayer and Finkel, 2004). Thus to provide a reliable basis for the analysis the optimization is performed repeatedly using several randomly initialized attempts for each task under study. In doing so the stochastic influences on the evaluation and interpretation of the results is reduced.

Each optimization problem formulation using a specific approach (GSA or ISA), strategies (IDCO or DCO), set of scenarios, stopping criteria and so on is termed case. The cases used to study the 5 thesis objectives are presented in Table 1.1 with the following being the specific thesis tasks:

1. Develop Stopping Criteria (Case: 4, 5 and 6)
2. Normalize the VSP stopping criterion to OFI stopping criterion (Case 9)
3. Explore the Optimization Search Capacity (Case: 4, 5 and 6)
4. Evaluate the performance of the travel time ratio (TR) constraint (Case: 1 and 2)
5. Evaluate differentiated capture (DC) objective (Case: 7 and 8)
6. Compare Individual and Grouped Scenarios Approaches (Case: 1 and 3)
7. Compare IDCO and DCO strategies (Case: 10 and 11)

Table 1.1 Summary of all the cases used in this thesis to evaluate different objectives

C#	Task	Case Name	OR	OS	Sc.	OA	Stopping Criterion	λ	TR	DC
1	4 & 6	ISA-TR	5	IDCO	All	ISA	308 generations	13	Yes	Yes
2	4	ISA-NTR	5	IDCO	All	ISA	308 generations	13	No	Yes
3	6	GSA	5	IDCO	All	GSA	308 generations	13	Yes	Yes
4	1 & 3	GSA- 13λ	2	IDCO	All	GSA	750 generations	13	Yes	Yes
5	1 & 3	GSA- 20λ	2	IDCO	All	GSA	750 generations	20	Yes	Yes
6	1 & 3	GSA- 23λ	2	IDCO	All	GSA	750 generations	23	Yes	Yes
7	5	GSA-DC	5	IDCO	All	GSA	$OFI_{50G} < 0.1\%$	23	Yes	Yes
8	5	GSA-NDC	5	IDCO	All	GSA	$OFI_{50G} < 0.1\%$	23	Yes	No
9	2	IDCO-S_n	7	IDCO	Sc 1	-	Several S values	13	Yes	Yes
10	7	IDCO	11	IDCO	Sc 1	-	S < 0.03	13	Yes	Yes
11	7	DCO	11	DCO	Sc 1	-	S < 0.03	13	Yes	No

Abbreviations: C#: Case Number, OR: Optimization Runs, OS: Optimization Strategy, IDCO: indirect cost optimization, DCO: direct cost optimization, Sc.: Scenario , OA.: Optimization Approach, ISA: Individual-Scenarios Approach, GSA: Grouped Scenarios Approach, OFI_{50G}: Objective function improvement in the range of the last 50 generations, TR: Time ratio constraint, NTR: No time ratio constraint, DC: differentiated capture, NDC: Non-differentiated capture. λ: Individuals per generation(i.e. Model Runs= λ x Generations), S: scalar number, which is part of $tolX = S / \sqrt{n}$, where tolX is a predefined value for the VSP stopping criterion.

2 Case Study Description

2.1 Site Description

This study is conducted on a petrochemical plant located close to a wetland of high ecological value, which is hydraulically connected to the Mediterranean Sea as shown is Figure 2.1. The site area is approximately 2 km², and is surrounded by urban and industrial area, agricultural land, salt industry and wetland. The groundwater flow direction is toward the wetland.

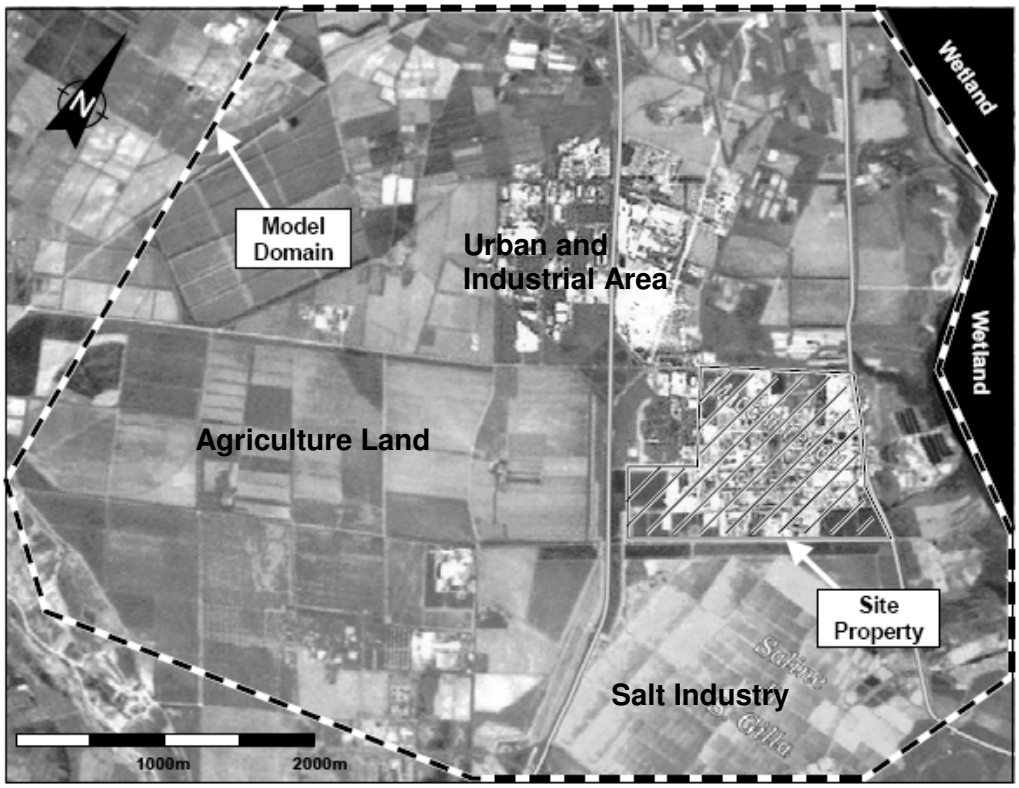

Figure 2.1 Site plan [Source Finkel et al., 2008]

The plant is located on coastal plain overlying terrace alluvial sediments with a thickness of around 20 m. The alluvium consists of very heterogeneous Pleistocene-age deposits ranging from conglomerates to gravels and silty clay with an overall intermediate hydraulic conductivity. Three main levels constitute the subsurface stratigraphical sequence in the study area:

- An upper level consisting of sand and silty gravel with local lenses of silty clay reaching a maximum thickness of approximately 20 m
- An intermediate level consisting of clay and silt present in the whole area with variable thickness
- A lower layer consist of alternating sub-layers of gravel and clay

However, during the construction of the petrochemical plant the original morphology of the upper layer changed by site leveling. Also, the natural drainage networks and two small streams with about 3 m thick were filled with high permeable filling material.

The local hydrogeology is characterized by a phreatic aquifer overlying the impervious silty clay layer. A second deep aquifer is located in the gravely and sandy layers, which is confined by the overlying silty clay layer. In this study only the top phreatic aquifer is considered.

The hydraulic conductivity values in the alluvial aquifer are heterogeneous with a mean value of approximately 3E-04 m/s. The corresponding Darcy groundwater velocity is around 60 m/year. The mean annual precipitation in the region is 470 mm out of which 75% is concentrated in autumn and winter, and only 3 % in summer.

Groundwater recharge has both a natural and anthropogenic origin. Its natural component has two sources: infiltration from precipitation and local infiltration from the runoff coming from the granite hills located at the West. Net recharge from precipitation is very low. The second recharge source, which causes groundwater potential anomalies on the site, is an artificial local recharge. Its source could be leakage in supply lines.

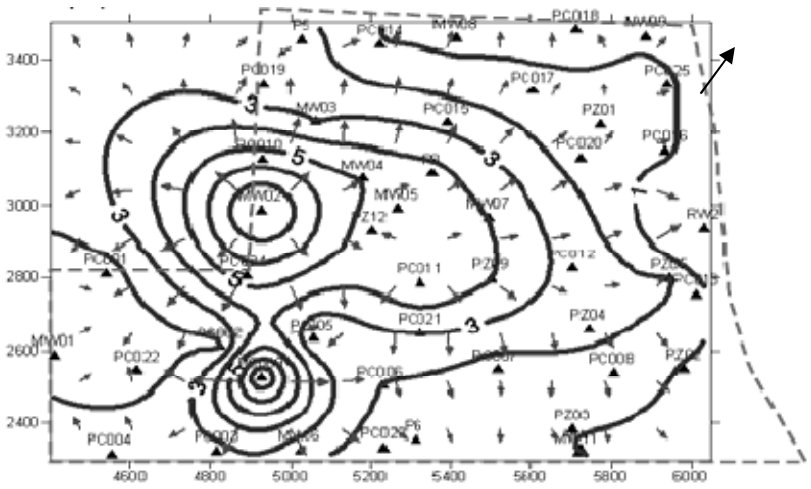

Figure 2.2 Flow directions in the site premise [source: Lantschner, 2005].

The water table in the site area has a depth of less than 10 m. The mean hydraulic gradient is 0.6%. A watershed associated to an anomalous zone of artificial recharge separates the flow directions toward the wetland in the North, and the agriculture land and slat industry in the South as shown in Figure 2.2.

2.2 Contaminant Situation

The main products of the plant until the year 2000 were chlorine (with sodium hydroxide as by-product), acrylonitrile, 1,2-dichloroethane (DCA), perchloroethylene (PCE), trichloroethylene (TCE), organic solvents, vinyl chloride, PVC, polyethylene and poliolefines. The main raw materials used for production were ammonia, propylene, hydrochloric acid, chlorine, ethylene and dichloroethylene (DCE). The installed production capacity was of approximately 800,000 tons/year.

IMES GmbH (2002) characterized the contaminant situation by two different contaminate classes, which are chlorinated hydro carbons (CHC), and benzene, toluene, ethylbenzene and xylene (BTEX). Two major groundwater contaminant plumes in close proximity to one another are identified at the site area. The one in the South East is almost completely composed of C-1 and C-2 chlorinated hydrocarbon compounds with a clear predominance of 1,2-DCA (concentrations up to 240 mg/l). The Northern plume is mostly composed of BTEX compounds with Benzene presenting the highest concentrations (up to 4.2 mg/l). Also, this plume has some minor CHC contamination on North side. Figure 2.3 illustrates the overall BTEX and CHCs concentrations at the site.

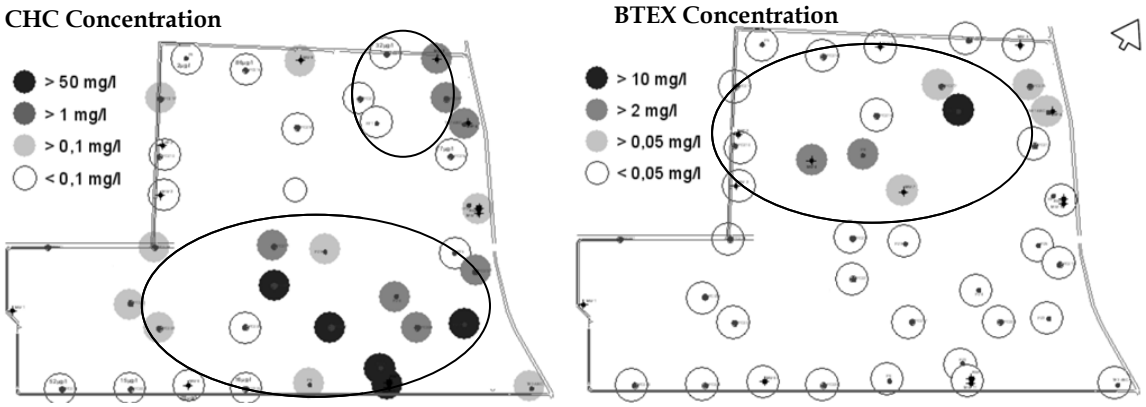

Figure 2.3 Site plan showing concentrations of CHC (left figure) and BTEC (right figure) [source: Lantschner, 2005]

A complete analysis of the chemical compounds detected in GW samples from 46 installed monitoring wells is shown in Annex (Table A.1). Electrical conductivity in the wells ranged from 340 to 17000 µS/cm and pH values from 4.2 to 10.1.

From the chemical analysis, priority compounds of concern (COCs) are selected. The selection of the COCs is based on the maximum concentration of the contaminants at the site premise. Secondary criteria are (1) the ratio of the maximum concentration and the allowable maximum concentration level (MCL) in groundwater according to the Italian law, and (2) the mobility of the contaminant. The mobility is assessed by considering the mobility of the chemical group. For example, Polyaromatic hydrocarbon (PAH) compounds are not taken into account since they generally have very low mobility. Table 2.1 presents the selected 11 COCs with their corresponding maximum concentrations at the monitoring wells, and the allowable legal limits according to Italian laws of groundwater (DM 471/99), drinking water (DLgs31/2001) and Surface water (Testo Unico 2006).

Table 2.1 Maximum concentration, initial mass, allowable legal limits according to the Italian laws of groundwater (MCL DM471/99), drinking water (MCL DM471/99) and surface water (MCL Testo Unico/2006)

Compound	Maximum Concentration [µq/l]	MCL DM471/99 [µg/l]	MCL DM471/01 [µg/l]	MCL Testo Unico 2006 [µg/l]
Benzene	4200	1	1	Total Aromatic Organic Solvents ≤ 200
Toluene	4900	15	-	
1,1,2-TCA	2500	0.2	-	Total Chlorinated Solvents ≤ 1000
1,2-DCA	240	3	3	
Chloroform	5500	0.15	-	
DCM	2050	NS	-	
PCE	3000	1.1	-	
TCE	5100	1.5	-	
1,1-DCE	2780	0.05	-	
1,2-DCE	3100	60	-	
VC	7000	0.5	0.5	

The selected COCs with their corresponding concentration are the base for developing the particle distribution configuration and transport models. In addition, MCLs for ground water according to DM471/99 are used as the target concretions for the design of the water treatment units.

3 Methodology

3.1 Simulation and Optimization Codes

3.1.1 Flow Code

The underlying governing equation describing horizontal groundwater flow is a non-linear partial deferential equation as follows:

$$S\frac{\partial h}{\partial t} - \nabla.(\boldsymbol{T}\nabla h) = N \quad (3.1)$$

Where N is the net recharge, **T** is the transmissivity vector, S is the storage coefficient. Assuming a mean isotropic hydraulic conductivity tensor $\bar{\boldsymbol{K}}$ equation 3.1 becomes a linear equation for the steady state condition as follows:

$$-\nabla.(\bar{\boldsymbol{K}}\nabla h^2) = 2N \quad (3.2)$$

A code is computer program that contains an algorithm to solve a mathematical model. MODFLOW (McDonald and Harbaugh, 1988) code is selected to numerically simulate the horizontal groundwater steady-state flow with source and sink terms since no analytical solution is available.

Code selection, is followed by model design in which the flow code is used as a tool to convert the conceptual model into a mathematical model. This step includes the grid design, setting boundary and initial conditions, inputting the aquifer parameters and defining all the other modeling parameters to simulate the flow conditions as detailed in Section 3.2.1.

The model is calibrated before it is used to simulate the flow conditions. The objective of calibration is to make the model capable of reproducing the field measured heads. Parameter ESTimation (PEST) is used as a calibration code. During the parameter estimation process, the PEST searches for the optimum parameter values that minimize the deviations between model-calculated and observed values. The deviation is expressed in this study by the residual mean squared (RMS).

$$\mathrm{RMS} = \sqrt{\frac{1}{n}\sum(x_{\mathrm{measured}} - x_{\mathrm{mod\,eled}})^2} \quad (3.3)$$

The smallest global RMS corresponds to the optimal values because as indicated by Eq.3.3 larger deviations are weighted more than small deviations, since the difference between the measured and model head is squared. In addition, squaring the difference yields an absolute difference, so the positive and negative parameters do not cancel out. In addition, RMS corresponds to standard deviation of randomly varying quantities, so some statistical tests are applied to indicate whether a certain RMS value represents significant or insignificant differences between the measured and modeled parameter. Moreover, parameter values can be

treated differently by assigning a different weight for each, yet this option is not used in this study.

After calibration, the model is said to be ready for simulating the flow conditions using the candidate well configuration proposed by the optimization code. The flow conditions are further used for particles tracking and transport simulation.

3.1.2 Particles Tracking Code

Assuming that advection is the dominant transport mechanism, path lines are used to represent the contaminant migration following Mulligan and Ahlfeld (1999). Multiple particles are used to define the plume boundary. To ensure that the plume is captured, a sufficient number of particles must be used to represent the plume and all particles must terminate at an extraction well.

Particles tracking is performed using MODPATH code (Pollock, 1994). The ground water flow equation (3.1) is solved to determine the velocity field, which is used to trace each particle. A particle path line is the trace of particle position overtime (Mulligan and Ahlfeld, 1999), which is determined as:

$$\int_{so}^{sf} ds = \int_{to}^{t} v_s dt \tag{3.4}$$

Where s is the particle coordinate along the pathline, v_s is the particle velocity at location s, t is time and s_o and s_f are initial and final particle locations respectively.

3.1.3 Transport Code

Transport simulation is performed to estimate the mass removed for each COC by the candidate well configuration, which is a prerequisite for the design and dimensioning of the treatment facility.

The transport of sorbing and reactive compounds in porous media is governed by advection, dispersion and mass transfer processes as expressed by the transport equation:

$$\mathrm{R}\frac{\partial c_w}{\partial t} + \boldsymbol{v}.\nabla c_w - \nabla.(\boldsymbol{D}\nabla c_w) = (c_{in} - c)\frac{q_{in}}{n_e} + n_e r \tag{3.5}$$

The first terms in equation 3.5 describes the change in aqueous phase concentration c_w with time t for a single compound assuming equilibrium sorption, which is expressed by the retardation factor R. This change in concentration is due to advection (second term), dispersion (third term) and source and sink terms (right hand side). The source and sink terms include mass fluxes of dissolved compounds transported with internal volumetric sources and sinks and potential reaction terms.

Mass transfer can occur as equilibrium or kinetic reaction, and the partitioning processes can be described linearly or non-linearly. The longer the water remains in contact with the sorbent the more the concentration approaches equilibrium. Kinetics plays no role and equilibrium

concentration exists, if the characteristic time for groundwater flow is larger than that of the mass transfer process.

Sorption isotherm defines the relationship between the dissolved concentration c and sorbed mass s at a given pressure and temperature. The partitioning between these two phases is described by a linear relationship such as the linear partitioning law (Eq. 3.6), or by a non-linear relationship such as Freundlich and Langmuir isotherms.

$$s = K_d c \tag{3.6}$$

Where K_d $[L^3M^{-1}]$ is the partitioning coefficient between the solid and the aqueous phase. By neglecting the sorption onto mineral surfaces, the sorption of the non-polar compounds occurs mainly on the soil organic matter. Accordingly, K_d values can be estimated from the partitioning coefficient between organic carbon and water K_{oc} $[L^3M^{-1}]$ and the mass fraction of organic carbon f_{oc} [-] in solid matter:

$$K_d = K_{oc} f_{oc} \tag{3.7}$$

Equilibrium-controlled sorption isotherms are generally incorporated into the transport model through the use of the retardation factor as defined in Equation 3.8.

$$R = 1 + \frac{(1+n_e)}{n_e} \rho_s K_d \tag{3.8}$$

The mass density ρ_s of solid and effective porosity n_e are site dependent. Equations 3.6 and 3.8 show that in case of linear sorption isotherm, the retardation factor does not depend on the concentration, while it is concentration dependent in case of the non-linear sorption isotherm. For example, in case of Langmuir isotherm the retardation is large for smaller concentrations, and thus the concentration changes are slowed severely down at lower concentrations than at higher concentrations.

Accounting for the abovementioned physical considerations, it should be noted that the accuracy of the model should depend on its purpose. For example, if the objective is to achieve a complete site restoration, then the mass transfer reactions along with other processes such as diffusion from low-permeability zones and desorption from aquifer soil should be precisely described. However, in an advective control particle tracking-based optimization the transport simulation is used as a tool to describe the approximate contaminant mass removal. In other words, in advective control optimization the safety thresholds (i.e. containment of the plume and capture zone within the site premise) are determined using particle tracking, while transport simulation is only used to design the treatment station according the amount of extracted contaminants. Accordingly, equilibrium sorption described by a linear isotherm is assumed to be satisfactory for this purpose. Moreover, the organic carbon fraction is considered uniform through the model domain, thus the partitioning coefficient values K_d are assumed to be constant.

MT3MS (Zheng and Wang, 1999b) is used to simulate the transport processes for the 30 years design period. MT3DMS accounts for equilibrium conditions only with both linear and non-

linear (Freundlich, and Langmuir) isotherms. For transport simulation, MT3DMS uses an Eulerian-Lagrangian approach with hybrid method of characteristics (HMOC), which is a hybrid of the forward-tracking method of characteristics (MOC) and the backward-tracking modified method of characteristics (MMOC). The HMOC technique is an automatically adaptive scheme, which changes the solution technique depending to the nature of the concentration field. When sharp concentration fronts are present, the advection term is solved by the MOC technique through the use of moving particles distributed dynamically around each front, while away from such fronts the advection term is solved by the MMOC technique with fictitious particles placed at the nodal points tracked directly backward in time (Zheng and Wang 1999b).

3.1.4 Pump and Treat System Design and Cost Code

3.1.4.1 Design and Dimensioning of the Treatment Station

3.1.4.1.1 Technology Selection

Several water treatment alternatives were initially investigated in various combinations of technologies. The final water treatment alterative selected for this site is Palladium Catalytic Reduction (PCR) unit with Membrane Based Stripping (MBS) for the treatment of the CHC compounds, followed by a gradual activation carbon (GAC) unit for the treatment of both the BTEX compounds and any residual CHC contamination (Schueth,2003). GAC is selected for BTEX compounds due to their relatively high octanol water partitioning coefficient K_{ow} (i.e. high sorption capacity). On the other hand, CHC compounds have low K_{ow}, so treatment by GAC is very inefficient and results in higher costs compared to reductive catalysis treatment (Finkel et al., 2008), and thus PCR with MBS is more efficient. However, this study does not use the PCR-MBS and GAC units in series as proposed by (Schueth, 2003), but rather in parallel as proposed by Finkel et al. (2008). This point is further explained in Section 3.2.4 PTSDC Model. Anyway, the PTSDC code is flexible and can account for either case.

3.1.4.1.2 Catalytic Reduction Algorithm

3.1.4.1.2.1 Technology overview

Before describing the design and dimensioning algorithm of the catalytic redaction treatment unit, this sub-section provides a brief overview on the reductive catalysis and stripping technologies proposed by Schueth (2003). The selected catalytic reduction unit is PCR-MBS, which is a combination of hollow fiber membrane filtration to transfer the contaminants from the aqueous phase into the gas-phase, and a reduction unit for the treatment of the contaminated gas with palladium as a catalyst.

Reductive catalysis is very efficient, and ideally produces harmless products. It this case study, gaseous hydrogen is used as reductant and palladium as catalyst to degrade chlorinated methanes, ethenes and ethanes. The degradation pathways result in methane or ethane, and gaseous HCl as end products. The catalyst itself is not consumed in the reaction and can ideally operate for long periods.

Stripping of the dissolved aqueous phase contaminants into gaseous phase is needed prior to the reduction process. The dehalogenation of 1,2-DCA does not occur at ambient conditions, but rather need temperatures as high as 400°C, which is only possible in gaseous phase. In addition, running catalytic degradation in the gaseous phase has more advantages such as higher reaction rates (several orders of magnitude faster) due to the higher diffusion coefficients. Moreover, the methods for the prevention of catalyst poisoning by the removal of sulphur-containing compounds (e.g. zinc oxide ZnO) are more efficient for gaseous phase systems.

Instead of using ambient air, nitrogen is used as strip gas to prevent oxygen from entering the system, and thus minimizing the risk of precipitations of iron or manganese oxides as contaminated aquifer systems are in general anoxic.

For the stripping process, hollow fiber membrane modules are selected over conventional strip towers to reduce the gas-to-water ratio. The hollow fiber membrane module contains thousands of microporous polypropylene hollow fibers knitted into an array that is wound around a distribution tube and a central baffle. During operation, the contaminated groundwater enters the module at one side and the strip gas is applied in counter flow. The application of vacuum inside the hollow fibers in counter flow enhances the strip efficiency. Due to these enhanced properties, the hollow fiber membrane has less gas-to-liquid ratios than conventional strip towers. For example, assuming equilibrium conditions, while several strip towers would have to be operated in series with a gas-to-liquid ratio of up to 300:1 to strip the 1,2-DCA (Henry's Coefficient 0.04) to the gaseous phase, with hollow fiber membrane modules this ratio can drop to 3:1-7:1. Moreover, the modular design of the membrane modules allows scaling the treatment system according to the flow requirements and treatment goals. By running several modules in series removal efficiencies of the system can be increased as needed.

3.1.4.1.2.2 *Treatment Process*

The main components of the PCR-MBS treatment unit are illustrated in Figure 3.1.

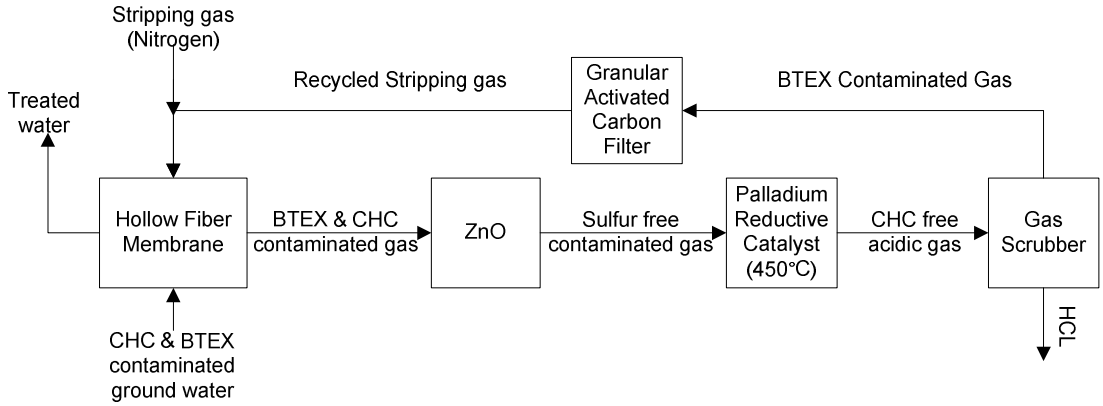

Figure 3.1 Schematic for the PCR-MBS treatment unit

The main components of the PCR-MBS treatment unit are summarized as follows:

- Aqueous phase contaminants are converted to gaseous phase using hollow fibre membrane with nitrogen flowing as a strip gas from top to bottom to counter the water flow
- Stripping efficiency is enhanced through a vacuum pump placed after the membrane module (~60 mbar absolute pressure)
- Contaminated gas flow to zinc oxide column to remove sulphur compounds
- Contaminated gas is heated up to 450°C using an electric heater and feed with hydrogen, which act as a reductant
- Gas flow through the reductive palladium catalyst column (0.5% Pd on Al_2O_3) to remove the CHCs
- CHC free acidic gas is feed to the gas-scrubber to wash out the HCL
- Washed gas is finally treated through an activated carbon filter to ensure a complete removal of CHC contaminants and for the treatment of any present BTEX compounds
- The exhaust gas can then be released to the atmosphere. The nitrogen can be recycled and re-fed to the air stripping unit, yet this option is not incorporated in the PTSDC code

3.1.4.1.2.3 Design and Dimensioning Algorithm

A code for the design and dimensioning the PCR-MBS unit is developed by Lantschner (2005). The design parameters of the main components used in this treatment unit is presented in this section. Data is based on the parameters used at the pilot treatment plant which Schueth (2003) operated at the site.

Stripping: The membrane contactor module taken for design of the treatment facility has an inner surface of 200 m^2. Operated under 60 mbar of absolute pressure, using a vacuum pump (water ring type) and keeping an N_2/water ratio of 5:1, a removal efficiency of 99 % could be assumed. The N_2 consumption is therefore directly determined as a function of the discharge rate. A N_2 generator is included in the design. The removal of 1,2-DCA from the liquid phase at the membrane contactor is assumed to be 99%. The removal rate for the rest of the COCs should be higher than the one for the 1,2-DCA being the one with lowest Henry constant value. However, for simplicity the code assumed the same removal rate.

Hydrogen injection: The volume of hydrogen required for injection into the gaseous stream is calculated taking into account the stoichometry of the hydro-dehalogenation reaction (one mole of H_2 for each chlorine atom present in the contaminant molecule), and the concentration of each contaminant. The calculations are done using the mean concentration of 5 years periods. A H_2 generator is included in the design.

Catalyst bed: The aluminum oxide/Pd material is assumed to be replaced every 5 years. The required volume V_{req} of aluminum oxide coated with palladium (0.5 % Pd on Al_2O_3) is calculated based on the N_2 flow rate Q_{N2} [m^3/hr] using a contact time $t_{contact}$ of 3.5 seconds, assuming an effective porosity n_e of 0.5 and an effective density of 0.5.

$$V_{req} = \frac{Q_{N2}}{t_{contact} \cdot n_e} \tag{3.9}$$

Neutralization: The amount of NaOH required for neutralization of the acid stream coming out of the scrubber is computed by considering the stoichometry of the neutralization reaction (1 mole of NaOH per atom of chlorine present in the contaminant molecule), and the concentration of each contaminant. The calculations are done using the mean concentration of 5 years periods.

3.1.4.1.3 Granular Activated Carbon Algorithm

Granular activated carbon is needed for two purposes:

- GAC aqueous unit for the treatment of the water current coming from the BTEX wells group mixed with the discharge of the PCR unit, which might has some residual contamination
- GAC air filter for the treatment of the exhaust air of the PCR unit, which might contain residual CHC, and any originally present BTEX (i.e. BTEX compounds do not break by reduction reactions)

The design and dimensioning algorithm of the GAC aqueous unit and GAC air filter as presented in this section is based on (Lantschner, 2005). The calculation of the GAC consumption is based on the assumption of non-competitive equilibrium sorption. The volume of the reactor is calculated taking the volume of activated carbon required V_{req} for a minimum operation time t_{oper} of 9 months for the highest consumption during that simulation period:

$$V_{req} = \frac{t_{oper} Q}{n_e R} \tag{3.10}$$

Where Q is discharge rate (water passing through the column), R is the retardation factor and n_e is the effective porosity of the activated carbon. Since sorption is described by Freundlich isotherm the partitioning coefficient between the solid and the aqueous phase K is concentration c_w dependent as shown by equation 3.11:

$$K = K_f {c_w}^{nf-1} \tag{3.11}$$

Where K_f and nf are Freundlich compound specific constants determined at certain temperature and concentration range, which differ from aqueous to gaseous phase sorption. The Freundlich adsorption parameters for the COCs are presented in the Annex (Table A.2). The retardation factor needed for the design equation 3.10 is obtained as follows

$$R = 1 + p_b \frac{K}{n_e} \tag{3.12}$$

Where p_b is the bulk density of the activated carbon. The V_{req} is thus calculated for each contaminant and interval, and the maximum volume is taken.

The properties of the used activated carbon are as follows:

- Granular activated carbon F400
- Effective porosity [-]=0.5
- Intra-particles Porosity [-]=0.4
- Buck density [g/cm^3]=0.57

The activated carbon is recycled estimating a 10% loss during recycling. The number of GAC refills required over the simulation time is computed and the required accumulated volume is obtained.

3.1.4.2 Cost Code

Similar to Lantschner (2005) investment costs and running costs are calculated for the Net Present Value (NPV) to account for the time value of money. The cost model assumes constant inflation and interest rate. The discount factor *Df* for investment cost, running cost and replacement are respectively as follows:

$$Df = \left[\frac{1+p}{1+i}\right]^{j-1} \tag{3.14}$$

$$Df = (1+p)\left[\frac{(1+i)^t-(1+p)^t}{(1+i)^t(i-p)}\right] \tag{3.15}$$

$$Df = (1+p_n)\left[\frac{(1+i_r)^n-(1+p_r)^n}{(1+i_r)^n(i_r-p_r)}\right] \tag{3.16}$$

$$i_r = (1+i)^{tr} - 1 \tag{3.17}$$

$$p_r = (1+p)^{tr} - 1 \tag{3.18}$$

Where p is the annual inflation rate, i is the annual interest rate, J is the number of years from present time, t is operation time (i.e. 30 years), n is the number of replacements during operation time, tr is the replacement period (years), and p_r and i_r are the inflation and interest rates of replacement respectively.

3.1.5 Optimization Code

Groundwater design optimization problems for hydraulic capture system are solved by classical programming methods such as linear (e.g. Ahlfeld et al, 1995), nonlinear (e.g. Mulligan and Ahlfeld, 1999), dynamic programming (e.g. Culver and Shoemaker, 1992) and dynamic programming with fuzzy interface system (Chu and Chang, 2009) or modern heuristic methods such as evolutionary strategies (e.g. Bayer and Finkel, 2004), genetic (e.g. McKinney and Lin, 1996), simulated annealing (e.g. Marryott et al., 1993), tabu search (e.g. Zheng and Wang, 1999a; Kalwij and Peralta,2006) and neural networks (e.g. Rogers and Dowla, 1994) algorithms. The most commonly used classical programming method are derivative based nonlinear programming methods. However, their ability to handle nonsmooth objective functions with numerous local minima and nonconvexity is criticized (Mayer et al., 2002). Moreover, in few studies to compare both methods (Aly and Peralta, 1999; Yoon and Shoemaker, 1999) the heuristic methods outperformed programming methods, yet at the expense of computational effort (Yoon and Shoemaker, 1999). In general, heuristic methods are becoming more common due to their ability of handling nonsmooth, nonlinear, discontinuous and nonconvex objective functions that have many local minima. For a comparative survey of different optimization methods the reader is referred to Beyer and Sendoff (2007) and Fowler et al. (2008).

Heuristic methods are experience-based techniques that control the problem solving. Simulation annealing mimics the physical annealing process in metallurgy; the Tabu search is inspired by the human memory process; the artificial neural networks are derived from the structure of biological neural networks and genetic algorithms use concepts from population genetics and evolution theory (Cunha, 2002). The simplest heuristic technique is "trial and error". The goal of heuristic methods applied in design optimization problem is to find a good solution, since the best possible solution with "trial and error" methods is only possible through exhaustive enumeration. If the search path is guided by a robust cognitive search process, it could converge rapidly to a good solution, which is in principle accurate and without cognitive biases. For example, in simulation annealing the degree of randomness for the replacement of the current solution with a new one depends on a global evolving parameter, and the degree of randomness decreases as this global parameter converges to zero. A comparative description of different heuristic methods is not covered here, but rather this section focuses on evolutionary algorithms and particularly evolution strategies.

The evolutionary algorithms such as genetic algorithm (GA) and evolution strategies (ES) are iterative, direct and stochastic search algorithms, which have been developed in parallel to one another since the 1960s (Schwefel,1995). Inspired by the evolutionary theory, these methods work on the basis of populations. Each population composes of a number (λ) of n-dimensional decision variables so-called individuals, which are in this case the well configurations. For example, a well configuration with 9 wells, where the well coordinates and pumping rate are the decision variables, is a 27-dimensional decision variables problem, which can have binary representation as most common GA variants or real-value decision parameters as in ES. An initial population, which donates the first generation, is randomly generated. By running the model, each individual is evaluated and a fitness value based on the objective function is calculated until the whole population is evaluated. The OF value is the measure of the fitness of the individual to survive. In a so-called selection process, the best individuals (μ) or more generally the information they carry are retained. To map the search space a new population is created by a recombination of the information of different selected individuals and a stochastic step so-called mutation, which is a probabilistic change of the selected individuals or their combinations (Bayer et. al,2008). Populations are iteratively created until a stopping criterion, which could be maximum generation number or a certain threshold, is reached.

CMA-ES, evolution strategies with covariance matrix adaptation (Hansen and Ostermeier, 2001; Hansen et al., 2003) is selected due to its proven superior performance in design optimization problems (Bayer and Finkel, 2004). The CMA-ES main feature is the adaptive mutation, which reduce the effect of noise and improve the global search properties by utilizing the covariance matrix that is adapted during the evolutionary search, yielding a strategy that is invariant against any linear transformation of the search space. A second important feature is that the utilization of the cumulative information collected over the whole evolutionary path, which makes it possible to adapt the covariance matrix at small population sizes, and thus the computational effort is significantly reduced. For comprehensive review of the CMA-ES algorithm the reader is referred to (Hansen, 2006). In addition, Bayer and Finkel (2007) provide a critical summary for the CMA-ES algorithm.

Two main optimization settings are discussed in this section, which are the stopping criterion and the optimization parameters.

Three different stopping criteria are examined in this study. A predefined number of generations is the CMA-ES default stopping criterion in which the search ends when the number is reached. A second criterion developed in this study is the improvement of the OF values, which calculates the percent improvement between the minimum and the maximum OF values for an array containing the OF values of all generation in a predefined generation range. The search terminates when of the objective function improvement (OFI) reaches a certain predefined minimum value. Thirdly, the variation of search points (VSP) is built-in stopping criterion in which the search stops if variation of the search points becomes considerably smaller in all coordinates than a predefined scalar value *tolX*, which is defined as $S / \sqrt{n}$, where n the number of problem dimensions and S is a scalar number with a default value S of 1E-7. Since the particle meaning of the VSP is not clear, several S values are examined and normalized to the OFI stopping criterion.

The stopping criteria tell the number of model runs (MR) required to reach to an optimal solution. However, the MR number is not the only factor that determines the robustness of the solution. It is evident that some optimization runs converge to a better solution than others, which is more a function of the search capacity.

Equations 3.19 and 3.20 define the default parameter setting for (μ_w, λ)-CMA-ES:

$$\lambda = 4 + \lfloor 3\ln(n) \rfloor \quad (3.19)$$

$$\mu = \lfloor \lambda/2 \rfloor \quad (3.20)$$

Where λ is number of individual per generation, μ the number of parent and n the dimensions of the problem. The selection of the λ and μ are comparatively uncritical and can be chosen in a wide range without disturbing the adaptation procedure (Hansen and Ostermeier, 2001). The optimization recommends the parent number μ to be $2 \leq \mu \lesssim n$, yet to provide a robust strategy, large μ and large ratio of μ/λ up to 0.5 are preferable (Hansen and Ostermeier, 1997). Accordingly, the default parent to population size ratio as presented by equation 3.20 is used.

To make the strategy more robust and explorative, λ can be enlarged. The range of $\lambda \geq 5$ and $2\mu \lesssim \lambda \lesssim 2n+10$ is a reasonable choice for the population size λ. Larger λ values linearly worsen progress rate and can linearly decrease the performance because the adaptation time in generations is independent of λ (Hansen and Ostermeier, 2001). Inserting the problem dimensions n=27 (9 wells x 3 decision variables) into equation 3.19 gives the population size according to the default setting which is 13 individuals per generation. From the recommended range, two other population sizes of 20 and 23 individuals are chosen. However, increasing the population size increases the number of MRs inside each generation range in which the OFI stopping criterion is evaluated. For example, for a range of 50 generation the number MRs required for the population sizes of 13, 20 and 23 are 650, 1000 and 1150 respectively. Using Case 4, 5 and 6, this extra computational effort is evaluated with respect to the improvement in the obtained solution.

3.2 Simulation Models

3.2.1 Flow Models

3.2.1.1 Model Design

The flow model comprises of two layers:

- Layer 1: unconfined aquifer with thickness ranging from 10 m to 20 m
- Layer 2: confining layer with thickness ranging from 5 m (East) to 45 m (West)

The model grid covers an area of 43.2 km² (7.2 km X 6.0 km) with an approximately 9 km² of inactive cells and 34.2 km² of active cells. Variable cell dimensions range from 25 m by 25 m in the center of the model at the site premise, to 100 m by 100 m in the model edges. The grid size is in the site vicinity is 25 X 25 m, which correspond to approximate a Peclet number of 2.5.

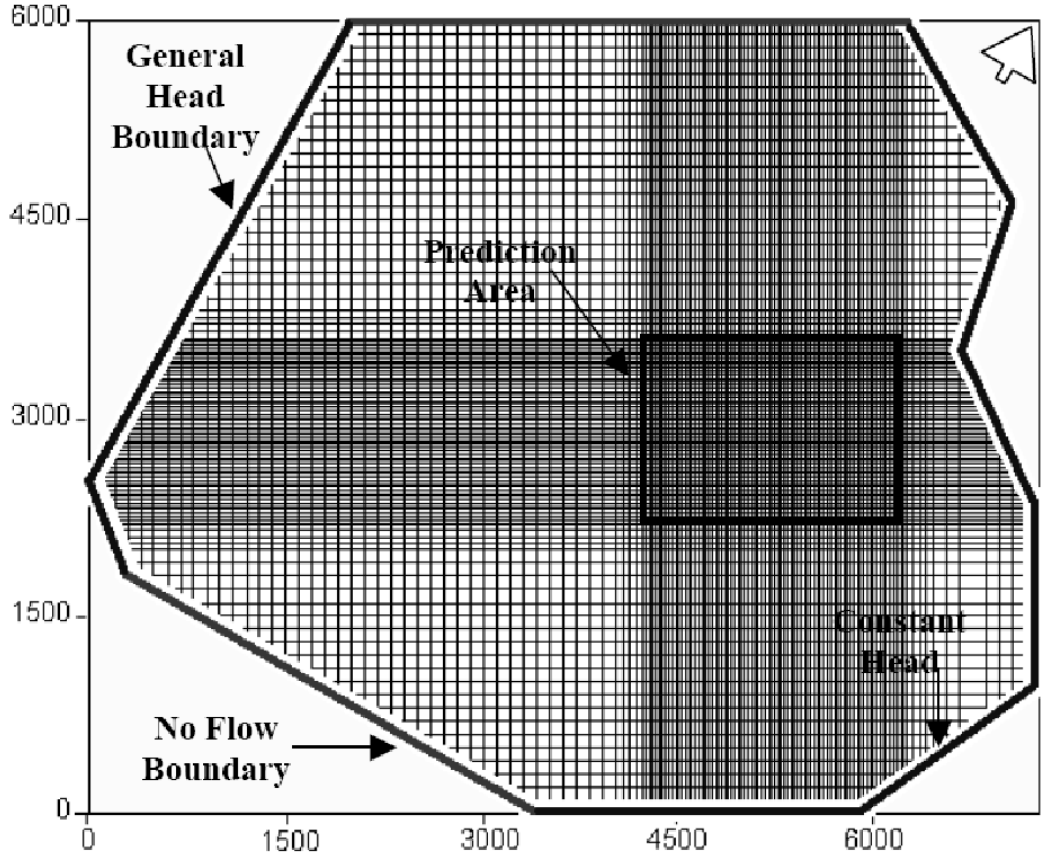

Figure 3.2 Model area, grid geometry and boundary conditions [source: Lantschner, 2005].

The model boundary condition at the Western side is specified as general head boundary, which allows exchange of flow across the model boundaries in response to hydraulic stresses applied to the flow system. It reaches its maximum level at the Western most cell and decreases with a linear gradient towards the South and the North. The Eastern boundary is specified as constant head (sea level). Both the Northern and the Southern sides are specified as no-flow boundaries, since they run parallel to groundwater flow direction.

Although some studies consider unsteady state flow models (e.g. Chang et al., 1992), yet steady state flow description is assumed to be sufficient for this study.

The model units are meter for length [L], days for time [T]. For example, the hydraulic conductivity is expressed in [m/day] and pumping rate in [m^3/day].

3.2.1.2 Multi-Scenarios Generation

Uncertainty in the aquifer parameters such as hydraulic conductivity and recharge rates, and auxiliary conditions such as boundary conditions and thickness of aquifer layers are handled deterministically through the generation of different deterministic flow models, which are herein donated as different scenarios. When the aquifer parameters are uncertain, then the reliability of the flow and transport models prediction is uncertain, which has a direct impact on the performance of the remediation system. Accordingly, the follow scenario, which presents more challenges for different proposed designs, is more reliable as a design scenario. This critical scenario can be identified using the ISA. In addition, the design that performs well for many scenarios is considered to be more reliable than the one that performs well for only few (Ranjithan et al. 1993). This design can be generated with the GSA. The generation of several scenarios is needed in order to identify the critical scenarios and the reliable designs.

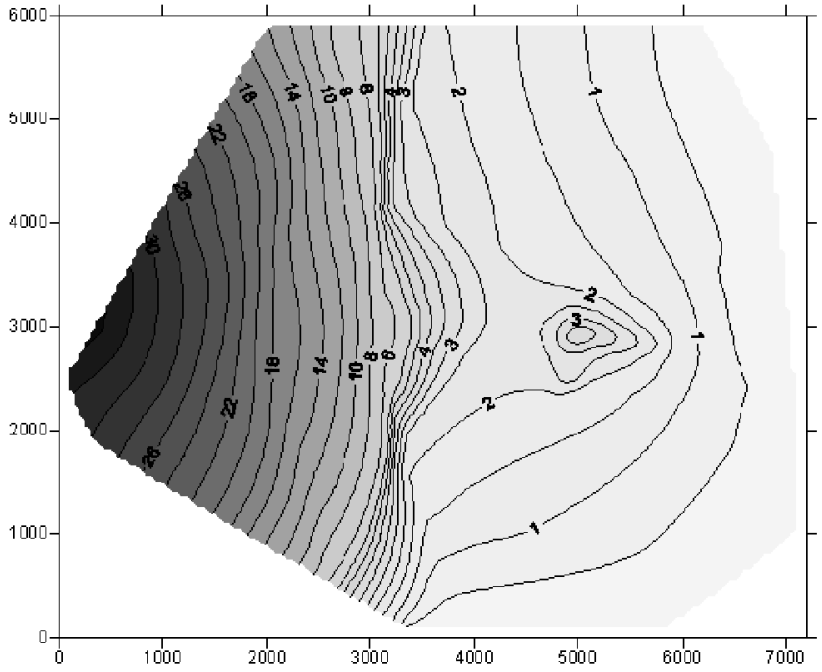

Figure 3.3 Scenario 1 equipotential lines (masl) [source: Lantschner, 2005]

Four different scenarios are generated for this case study. The original groundwater flow model referred to hereafter as Scenario 1 is used as the basic model for the generation of the different scenarios. The original groundwater flow model used for this study is developed by IMES GmbH (2002). The data used for defining the hydrogeological properties and boundary

conditions of the model is relatively sparse. The model is calibrated based on site information only, lacking regional hydraulic parameters. The hydraulic conductivity zonation is defined using the results from six pumping tests. Surface levels and depths to the aquiclude top (taken from bore-logs of observation wells) are used for defining the layers thickness and water levels in the prediction area. The boundary conditions, layer thickness and water level are estimated using topographical maps, and the identified pertinent features (e.g., creeks) during site visits. The equipotential lines (masl) for Scenario 1 are shown in Figure 3.3 showing an existing water table mound, which is probably due to artificial local recharge.

In Scenartion1, both layers are assumed to be anisotropic. Hydraulic conductivity in Layer 1 ranges from 2E-04 m/s to 1E-06 m/s as detailed in Figure 3.4. A continuous hydraulic conductivity of 1E-07 m/s is assigned to Layer 2. Two recharge rate zones are included in the prediction area (560 mm/yr and 2800 mm/yr) to reflect the local recharge. This recharge is assumed to have an artificial source (e.g. a broken water pipe). In the rest of the model area the recharge rate is set to 10 mm/yr for irrigated agricultural land, and no recharge for non-agricultural land as shown in Figure 3.4.

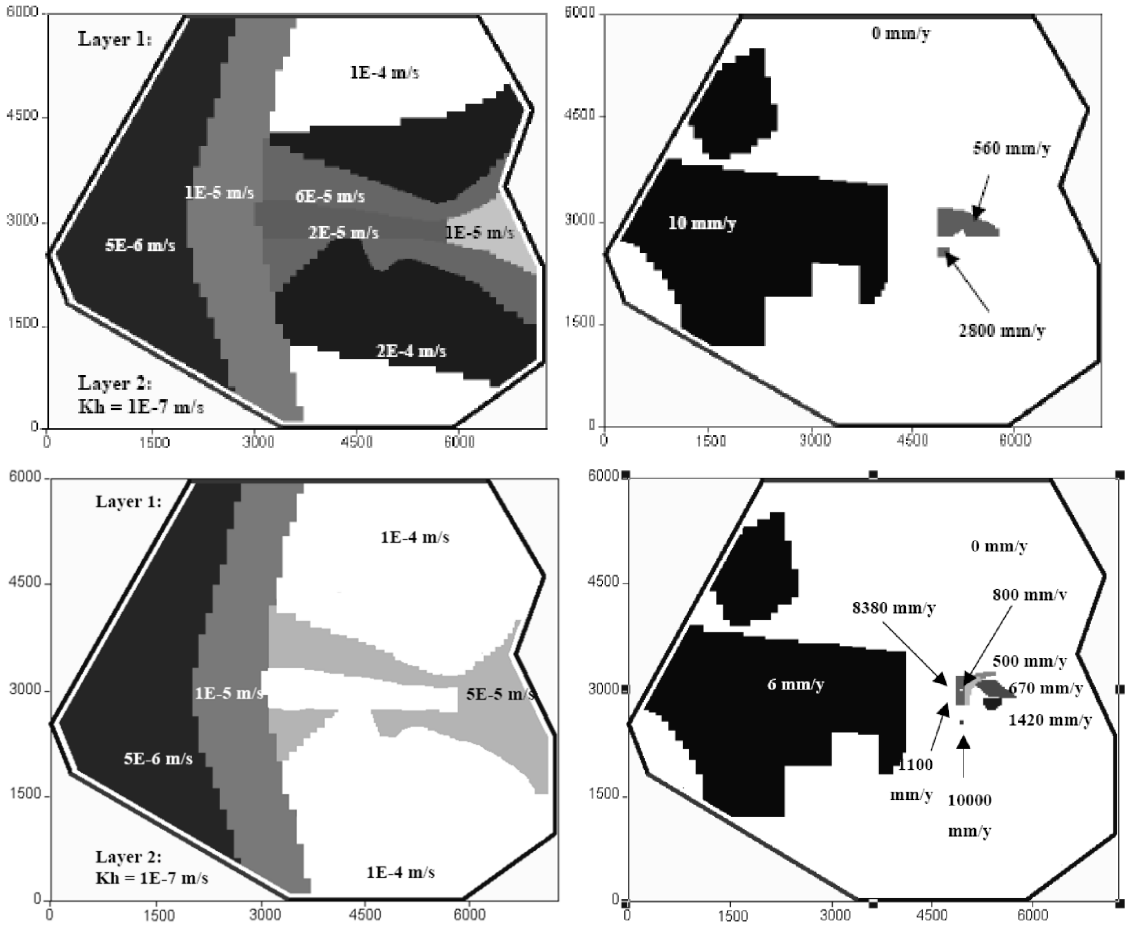

Figure 3.4 Hydraulic conductivity [m/s] and recharge rate [mm/y] for Scenario1 (top figure), and reduced hydraulic conductivity heterogeneity and increased recharge rate heterogeneity for Scenario 2 (bottom Figure) [source: Lantschner, 2005]

To account for uncertainty, different scenarios are generated by changing the hydraulic conductivity, recharge rate, general head boundary and the layer thickness. In Scenario 2, the water table mound shown in Figure 3.3 is explained by increased recharge rates heterogeneity, while reducing as much as possible the heterogeneity of hydraulic conductivity as shown in Figure 3.4. Recharge rates are used as the calibration parameter in this scenario.

Scenario 3 is identical to Scenario 1 except for the layers thickness. Since the aquifer thickness is only known within the site premise with no certain knowledge about the layers thickness in the rest of the model domain, the top of Layer 2 is lowered at the Western general head boundary by approximately 40%, and thus increasing the thickness of Layer 1. The thickness of the layers in the model domain is modified proportionally as shown in Figure 3.5

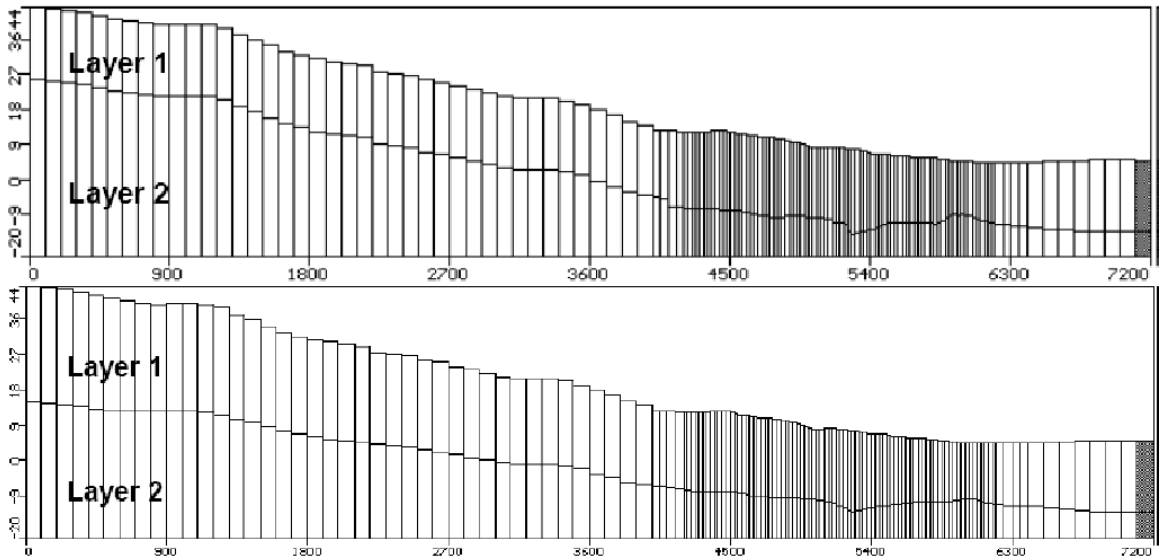

Figure 3.5 Vertical cross-sections at Row 71 indicating the lowering of Layer 2 outside the site area for Scenario 3 (bottom figure) from the original case of Scenario 1 (top figure) [source: Lantschner, 2005]

Scenario 4 is identical to Scenario 3 except that the level of the general head boundary at the Western boundary (WB) is reduced as much as possible (33%) without any cell falling dry. The goal of this scenario is to reflect the significance of the uncertainty associated with the water table depth in the model domain given that there is no available data outside the site premise.

The water balances of the hydrogeological scenarios as shown in Table 3.1 indicate that recharge represents the main input in all scenarios, and is much larger than the input through the Western general head boundary. Approximately 70% to 80% of the total recharge is originated inside the site premise by artificial recharge.

Table 3.1 Summary of the model parameters, auxiliary conditions, water balance and calibration results of the 4 hydrogeological scenarios

	Scenario 1	Scenario 2	Scenario 3	Scenario 4
Conductivity Heterogeneity	-	Reduced	Same as Scenario 1	Same as Scenario 1
Recharge Rate Heterogeneity	-	Increased	Same as Scenario 1	Same as Scenario 1
Thickness of Model Layers	-	Same as Scenario 1	Lowered outside site area (Layer 2)	Same as Scenario 3
General Head	-	Same as Scenario 1	Same as Scenario 1	Lowered by 33% at WB
Calibration Parameter	Hydraulic Conductivity	Recharge Rate	Hydraulic Conductivity	Hydraulic Conductivity
Water balance (m^3/day)	828	891	937	777
Fixed head (m^3/day)	80	82	181	23
Recharge (m^3/day)	747	807	755	755
Normalized RMS [%]	14.5	11.3	9.8	9.8

The water balance is generally a good indication for the solution accuracy. Percentage discrepancy between water input and output is smaller than 1% for all the scenarios indicating an accurate model design. Without any active pumps, 100% of the water exits the model at the Constant Head Boundary. Scenarios 3 and 4 show the best calibration results followed by Scenario 2 and finally Scenario 1.

3.2.2 Particle Distribution Configuration

The particles distribution configuration (PDC) delineates the aquifer zone that has to be captured by the well configuration. The particles distribution helps in formulating some of the optimization objectives such as capturing the plume fringe (Section 3.3.3.2), constraining the capture zone to the site premise (Section 3.3.3.3) and the disjoint capture of the two plume types (3.3.3.4).

Different particle configurations can be used. Lantschner (2005) uses two configurations in which one delineates the fringe of the BTEX and CHC plumes, and the second delineates the site premise. The former configuration, which is more robust particularly with respect to disjoint capturing, is used in this study.

Concentration data from 46 observation wells are interpolated to be used in developing the particle distribution configuration and to serve as an initial conditions for the transport model. Although Kriging interpolation method has become a fundamental tool in the field of geostatistics in the last decades, yet no variogram could be fitted to the small amount of

available concentrations data. Lantschner (2005) uses Natural Neighbor method for interpolation of concentrations data.

The concentration data are interpolated using the Natural Neighborhood method as the first step for setting up the PDC. Two limits are set for the interpolation, which are the allowable MCLs and alternate concentration levels (ACLs). Using the MCLs, the fringes of the CHC and BTEX plumes will overlap as shown in Figure 3.6, and thus the designation of two different capture zones for each plume type is not possible. In order to separate the two plume types, the plume fringes are delineated by higher concentration standards. Accordingly, ACLs are defined as shown in Table 3.2 in a way that enables the differentiation of the two plumes.

Table 3.2 Allowable MCLs for groundwater and alternative concentration levels that allow the plumes separation

Compound	MCL DM471/99 [µg/l]	ACL [µg/l]
Benzene	1	5
Toluene	15	15
1,1,2-TCA	0.2	20
1,2-DCA	3	60
Chloroform	0.15	10
DCM	NS	20
PCE	1.1	30
TCE	1.5	30
1,1-DCE	0.05	1
1,2-DCE	60	60
VC	0.5	30

The MCLs are raised to the limit that shall allow the separation of the two plume types in order to assign a different particle type for each of the two classes of contaminants namely the CHC and BTEX. The initial locations of the 1,2-DCA, TCE and Benzene plumes are illustrated in Figure 3.6 according to the MCLs and ACLs. The right hand side (RHS) of Figure 3.6 shows that CHC (1,2-DCA and TCE) and BTEX (Benzene) overlap in the upper right hand corner. Increasing the contraction limit from MCLs to the ACLs (left hand side plots) will avoid the overlap between the CHC and BTEX plumes, and thus allow the designation of two plume types.

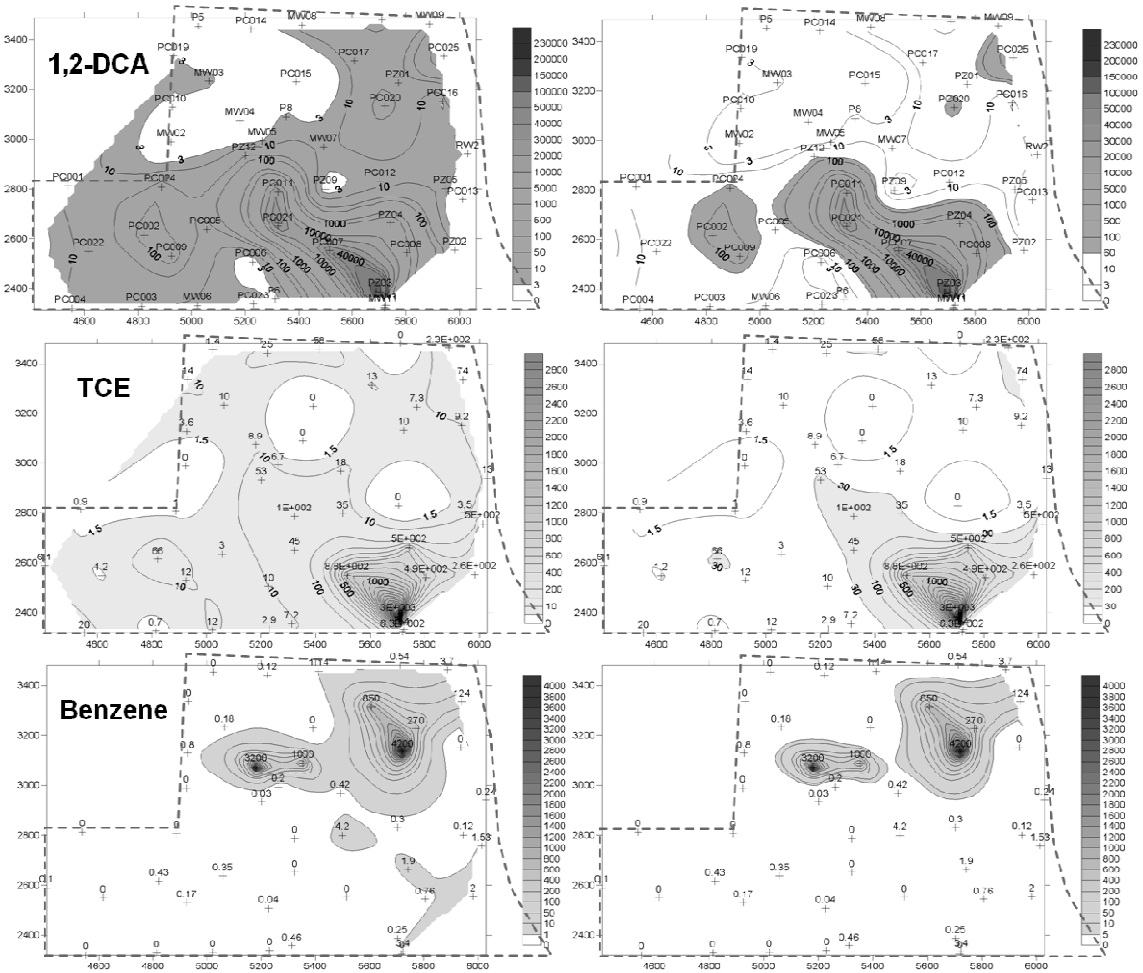

Figure 3.6 Left hand side plots shows that allowable MCLs and the right hand side plots show the ACLs that allow the setting to two plume types [Source: Finkel et al., 2008[1]]

By applying these ACLs for the 11 contaminants, the fringes of all the contaminants can be plotted in one plot to facilitate the mapping of the different plume types as shown in Figure 3.7.

[1] From Finkel et al. (2008) conference presentation with minor editing

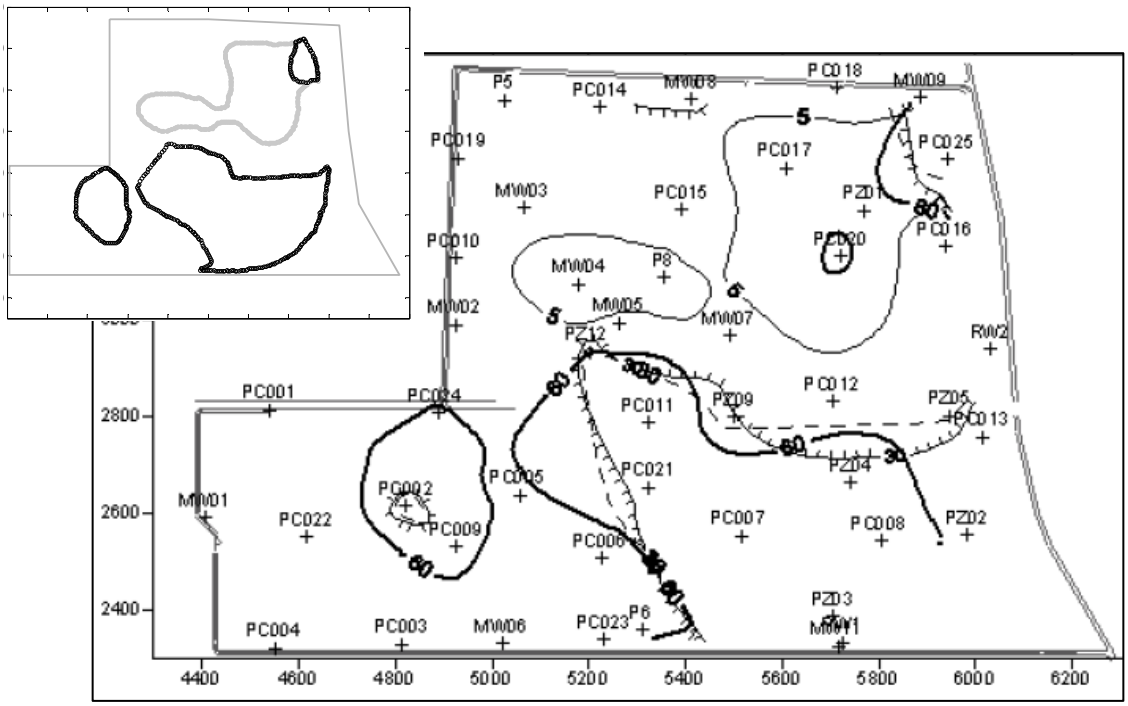

Figure 3.7 shows the ACL contour lines for Benzene (black, thin), 1,2-DCA (black, thick), PCE (hatched) and TCE (dashed) [source: Lantschner, 2005]. The inset depicts the delineated CHC plume (black) and BTEX plume (gray) according to the ACLs

3.2.3 Transport Model

The transport model uses the gradients determined by the flow model to simulate the transport processes in order to estimate the mass removed for each COC. The amount of removed mass for a simulation period of 30 years is used to design the water treatment units.

The model grid and parameters are used after Finkel et al. (2008). To insure accurate transport simulation the model grid should generally has a Peclet Number less than 2. In this study, the transport model utilizes the same model grid as the flow model, which corresponds to a Peclet Number of approximately 2.5. However, HMOC used by MT3DMS can provide accurate solutions to transport problems over the entire range of Peclet numbers from zero to infinity with virtually no numerical dispersion (Zheng and Wang 1999b). Accordingly, the used Peclet Number is valid.

The uncertain transport model parameters are generally the distribution coefficient K_d, mass transfer and reaction rates and dispersivity. However, carbon ratio is assumed constant through the model domain, so distribution coefficients K_d are constants. Mass transfer rates are calculated using equilibrium sorption assumption with a linear sorption isotherm. The retardation factors for the COCs are calculated using the K_d values shown in Table 3.3. No reactions are assumed. Longitudinal dispersivity is estimated to be 10m using the regression equation 3.21 presented by Xu and Eckstein (1995), which estimate dispersivity (α_x) based on the plume length (L_p).

$$\alpha_x = 0.83(\log L_p)^{2.4} \quad (3.21)$$

Horizontal and vertical transverse dispersivity are set to be one tenth and one hundredth of the longitudinal dispersivity respectively.

Table 3.3 Distribution coefficients and retardation factors used in transport model

Compound	K_{ow} [-]	K_{oc} [mg/l]	K_d [-] (f_{oc} 0.1%)	Retardation Factor R [-]
Benzene	100	84	8.36E-02	1.5
Toluene	500	304	3.04E-01	2.9
1,1,2-TCA	100	187	1.87E-01	2.2
1,2-DCA	30	18	1.83E-02	1.1
Chloroform	90	53	5.28E-02	1.3
DCM	10	9	8.76E-03	1.1
PCE	800	470	4.70E-01	3.9
TCE	300	163	1.63E-01	2.0
1,1-DCE	100	84	8.36E-02	1.5
1,2-DCE	70	45	4.49E-02	1.3
VC	4	2	2.47E-03	1.0

Beside the model parameters, the initial plume distribution is another source of uncertainties, yet this point is not accounted. Only one initial distribution is accounted for in this study.

Table 3.4 Initial mass of the COCs
[Source: Lantschner, 2005]

Compound	Maximum Concentration [µq/l]	Initial Mass [kg]
Benzene	4200	380
Toluene	4900	210
1,1,2-TCA	2500	840
1,2-DCA	240	28000
Chloroform	5500	110
DCM	2050	44
PCE	3000	970
TCE	5100	1800
1,1-DCE	2780	55
1,2-DCE	3100	490
VC	7000	460

The COCs and their distribution obtained for particle tracking are used in the transport model. The model assumes no active contamination source, since no source was identified during the site investigation. The initial contaminant mass dissolved in the aquifer at the site is calculated by Lantschner (2005) as the integration of contaminants concentrations over the site area as shown in Table 3.4. The total initial mass is estimated to be 33.4 tones.

3.2.4 Pump and Treat System Design and Cost Model

The water treatment calculations are done using the concentration data obtained by the transport model for the simulation period of 30 years. Time discretization (length of each time step) is automatically set by MT3DMS, ranging from 20 to 40 days.

The pumping rates and the amount of mass removed obtained by the optimization module and transport simulation are the main inputs to the PTDSC, which calculate the total pumping rate, designate the number of active wells and dimension the two treatment units:

- Treatment Unit 1 (PRC-MBS + GAC Air Filter), which is hereinafter named as CAT unit for the treatment of the CHC current
- Treatment Unit 2 (GAC Aqueous unit), which is hereinafter named as GAC unit for the treatment of the BTEX current

For both the GAC and CAT units, the PTSDC model calculates the major running cost items such as GAC, NaOH, N_2, H_2, Zeolite-Pd, electricity and so on. The code then uses these key components to calculate the total cost of the PTS.

The parameters for cost calculation are used after Lantschner (2005). The individual cost items and other parameters for both the three main PTS components, which are the GAC unit, CAT unit and pumping wells, are shown in the Annex (Table A.3).

3.3 Optimization Problem Formulation

3.3.1 Problem Statement

The problem of finding an optimal design can be stated after Mayer et al. (2002) as:

$$\min_{z \in \Omega_z} f(\boldsymbol{z}) \tag{3.22}$$

Where *f* is the objective function, **z(u,w)** is a vector of decision variables consisting of a vector **u** of state variables and a vector **w** of decision variables, $\Omega_z = \Omega_u \cup \Omega_w$ is the feasible region of the decision variables **z** represented by a set of constraint equations, Ω_u represent the feasible region of the state variable **u**, and Ω_w represent the feasible region of the decision variables **w**.

The decision variables could be real number such as injection or/and extraction rate (e.g. Bear and Sun, 1998) or cleanup time (e.g. Ko et al., 2005), integer such as the number of pumping wells (e.g. Chu et al., 2005) or their locations (e.g. Huang and Mayer, 1997). The choice of a unit process from a set of possible processes is an example of a third type of variables called categorical variables. The variables are discrete quantities that are part of the design space and for which only certain values maybe specified in order for the objective function to be evaluated and return a valid quantity (Mayer et al., 2002).

State variables represent the state of the physical system being considered, which can be explicitly represented in terms of concentration levels or implicitly represented by a capture zone or risk levels. The state variables formulations can be sub-divided into three categories, which are (1) a flow-based hydraulic control, (2) transport-based concentration control and (3)

particle tracking-based advective control (Mulligan and Ahlfeld, 1999). The hydraulic control formulation is based on a pre-defined head difference, gradient or velocity constraints at selected points (e.g. Gorelick, 1987). Although this method is fast because it is only based on flow modeling and allows the utilization of response matrix technique, yet a major disadvantage arises from the predefinition of the constraints, which requires a predefinition of the shape of the capture zone (Bayer and Finkel, 2004). In concentration control formulation the well configuration is a valid configuration, if the concentration levels (e.g. Guan and Aral, 1999; Bayer and Finkel, 2007) or the risk levels (e.g. Ren and Minsker, 2005) at certain points do not exceed a certain predefined values. Such formulation are based on transport simulation, so they are computationally demanding, and to ensure accurate results non-equilibrium processes acting on all relevant contaminants should be included(Mulligan and Ahlfeld, 1999). Accordingly, this method is applicable to site where sufficient data is available to develop reliable transport model. The particle tracking-based advective control formulation, which is used in this study, delineates the capture zone through particle tracking, so in contrast to the hydraulic control it does not bias the results of the optimization because no prejudgment concerning the capture zone must be made (Bayer and Finkel, 2004). However, this formulation is only limited to cases dominated by macroscale heterogeneity sufficiently described by the flow model, since hydrodynamic dispersion is neglected. Thus, advective control formulation is selected in this case because it is the most suitable solution for problems with limited amount of transport data.

In the flowing sub-sections the design of the decision variables and optimization objectives/constraints are explained. Based on this discussion, the objective function formulation, which incorporates optimization objectives/constraints, is presented for the different optimization strategies (i.e. IDCO and DCO) and approaches (i.e. ISA and GSA). The final part in this section discusses the number of ORs needed to provide a reliable basis for the analysis, and an overview on the statistical methods used in the analysis of the optimal solutions produced by these several ORs.

3.3.2 Decision Variables

Two decision variables are used in this problem, which are the pumping rate and the location of the pumping wells, with the formal being a real number and the later being an integer. The pumping rate for each well P_i is constrained between $0 < P_i < 100$ m^3/day. The well locations are constrained within the site boundaries as described in Section 3.3.3.1. The number of wells is not an explicit decision variable, but rather a constant number of 9 pumping wells are used. However, the optimization algorithm could propose a well configuration with zero pumping rates for one or several wells, and thus the number of pumping wells can be implicitly altered.

3.3.3 Optimization Objectives and Constraints

3.3.3.1 Restriction of the Pumping Wells to the Site Premise

This constraint is mainly of a practical rather than technical implication. For a regular geometric shape site boundary it can be easily implemented by rejecting the candidate wells that lie outside certain row and column coordinates. For irregular site boundary as in this case, each well has to be checked against a site grid area, which contains ones for all cells that lie in the site

premise and zeros for all cells in the rest of the model domain. This file can even be extended to signify areas inside the site premise, in which wells cannot be installed such as roads, buildings and so on. Moreover, a penalty factor can be assigned to unfavorable well locations inside the site premise. These last two options are not taken into account for simplification. The well placement area, which coincides with the site boundaries, is shown as dotted line in Figure 3.8.

3.3.3.2 Capturing of the Plume Fringe

A total of 731 particles are equally distributed over the contaminated zone as illustrated in Figure 3.8. Ideally, the capture zone shall be demarcated at the plume boundary according to the groundwater MCLs. In case the plumes overlap, then the plume fringe can be demarcated by concentration levels higher than the MCLs to allow the establishment of disjoint capture zones. This process is explained in details in Section 3.2.2 Particle Distribution Configuration. Although this demarcation might not ensure a complete capture of the plume fringes according the groundwater MCLs, yet this can be verified after selecting the final well configuration by inserting down gradient observation points at the site boundary.

This constraint is designed by forwardly tracking the particles along the locally varying head gradients to calculate the captured particles ratio $R_{cap,i}$ for each well *i*.

$$R_{cap,i} = \frac{n_{particles,captured\ by\ well\ i}}{n_{particles,total}} \tag{3.23}$$

The summation of the ratios of all the captured particles $\sum_{i=1}^{n_{w,tot}} R_{cap,i}$ for the total number of wells $n_{w,tot}$ is then used in the OF as a direct indicator of the plume containment.

3.3.3.3 Constraining the Capture Zone to the Site Premise

To avoid any legal or financial liability the plume must not only be captured and contained, but rather the capture zone should be located within the site boundaries. In other words, the proposed well configuration should ensure that all particles route from the original position to the pumping well is within the site boundaries. This can be easily implemented through analyzing the pathline file generated by MODPATH. The route of each particle is scanned over that site grid in order to calculate the travel time in each cell inside the site premise ($t_{IN,i}$). By subtracting the t_{IN} from the particle total travel time $t_{TOT,i}$, the travel time outside the site boundaries $t_{OUT,i}$ is calculated. By summing up for all particles, the time ratio (TR) of out-site to in-site particles travel time is obtained,

$$TR = \frac{\sum_i^N t_{OUT,i}}{\sum_i^N t_{IN,i}} \tag{3.24}$$

in which *N* is the number of particles. The TR [-] can be given a certain weight factor and used in the OF as penalty for particles traveling outside the site premise, which accordingly limit the capture zone to the site premise. Using Case 1 and 2, the validity of the TR concept and its effectiveness are discussed in the results Section 4.1.

3.3.3.4 Disjoint Capture of the Different Plume Types

The concept of disjoint capture in design optimization is introduced by Finkel et al. (2008). The establishment of disjoined capture zones for each contaminant class (i.e. BTEX, CHC, PAH etc.) shall facilitate the separate treatment of each class of contaminants. To achieve this objective, each capture zone is delineated by specific particle group.

The penalty term for this disjoint capture is based on the cross captured coefficient CC_i. As shown in Figure 3.8., two plume types are specified, n_{plume}= 2. The three CHC plumes are delineated by 472 particles and the BTEX plume is delineated by 259 particles. The overlap between the small CHC plume and the BTEX plume near the upper right site boundary is inevitable.

The two particle types are used to calculate the cross capture coefficient:

$$CC_i = \frac{min_j R_{cap,i,j}}{max_j R_{cap,i,j}} \tag{3.23}$$

With $R_{cap,i,j}$[-] being the plume-type-specific ratio of captured particles:

$$R_{cap,i,j} = \frac{n_{particles\ of\ type\ j,captured\ by\ well\ i}}{n_{particles\ of\ type\ j,total}} \forall i \in [1 \dots n_{w,tot}] \& j \in [1 \dots n_{plume}] \tag{3.24}$$

Where $n_{w,tot}$ is the total number of pumping wells.

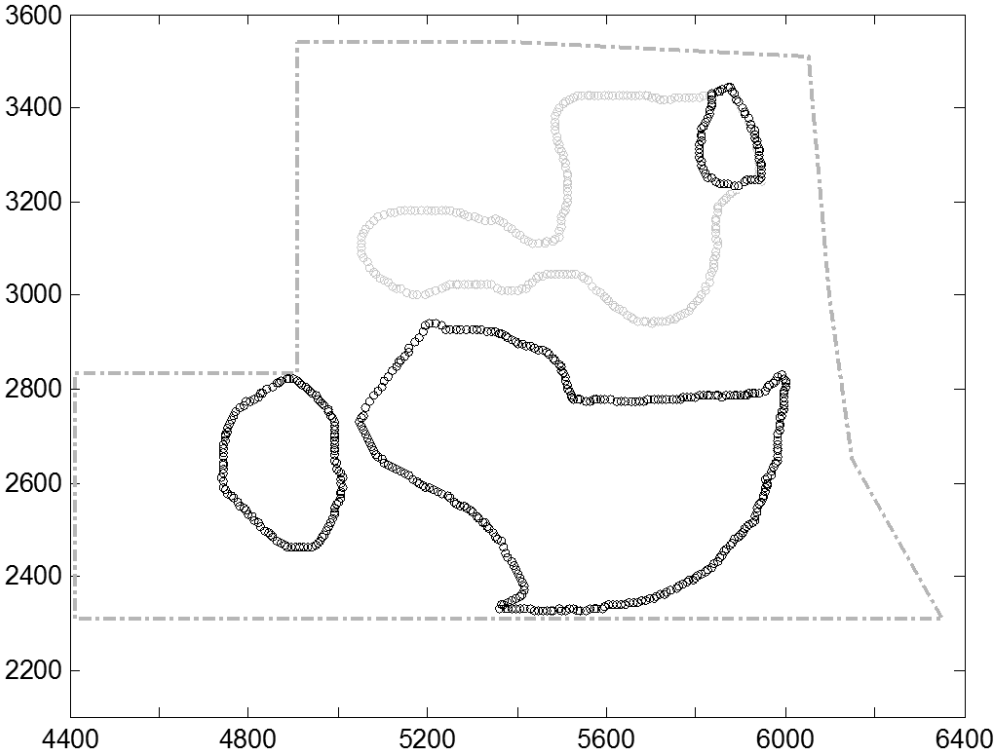

Figure 3.8 CHC plumes delineated by 472 particles (black) and the BTEX plume by 259 particles (gray)

By summing the cross captured coefficient CC_i for all wells and multiplying by a weighting factor, this constitute the penalty term for the disjoint capture. Lower cross captured coefficient indicates that the two contaminant types are differentiated, where a $\Sigma CC_i=1$ indicates a full differentiation of the two particle types by two separate well groups. Thus, the two contaminant types are collected and treated separately each according to its properties. This shall increase the treatment efficiency and thus reduce the overall treatment cost. Using Case 7 and 8, the correlation between the disjoint capture and the overall treatment cost is evaluated in the result Section 4.3.3.

3.3.3.5 Minimizing the Pumping Rate

Minimizing the total pumping rate Q_{tot} of candidate wells is a common objective for long-term hydraulic control problems (e.g. Bayer and Finkel, 2004; Finkel et al., 2008). This formulation is based on the assumption that the pumping cost and water treatment cost are non-linear functions of the continuous decision variable $Q_{tot}= \Sigma Q_i$ with strong direct correlation. The degree of correlation between the pumping rate and the PTS cost is assessed in Section 4.4.

3.3.4 Objective Function

The OF used for the IDCO strategy for both ISA and GSA is similar to Finkel et al. (2008), expect for the additional term for the travel time ratio *TR*.

$$OF = (1 + w_{out}.P_{out}).\left(1 + w_c.\left(1 - \sum_{i=1}^{n_{w,tot}} R_{cap,i}\right) + w_{cc}.\sum_{i=1}^{n_{w,tot}} CC_i\right).\sum_{i=1}^{n_{w,tot}} Q_i\,.(1 + TR^{w_{TR}}) \tag{3.25}$$

Where w_{out} [-], w_c [-], w_{cc} [-], and w_{TR} [-] are weight factors, $n_{w,tot}$ is the total number of wells, P_{out} is zero if all the wells are located within the site boundaries , $R_{cap,i}$ [-] is the ratio of the captured particles, Q_i [m^3/day] is the pumping rate for well i, CC_i [-] is the cross capture coefficient and TR [-] is the time ratio of the out-site to in-site particles travel time. The fitness value for each scenario in the ISA (Eq. 3.26) is the OF value of that scenario. On the other hand, the summation of the OF values for all scenarios is the fitness value in the GSA (Eq.3.37).

$$F_j = OF_j \; \forall \; j \in [1 \ldots n_{scenarios}] \tag{3.26}$$

$$F = \sum_{j=1}^{n_{scenarios}} OF_j \tag{3.27}$$

The $n_{scenarios}$ is the number of scenarios. The objective function for the DCO strategy is given as:

$$OF = (1 + w_{out}.P_{out}).\left(1 + w_c.\left(1 - \sum_{i=1}^{n_{w,tot}} R_{cap,i}\right)\right).\sum_{i=1}^{n_{w,tot}} Q_i\,.(1 + TR^{w_{TR}}) \tag{3.28}$$

Eq. 3.28 is similar to Eq.3.25, except for the cross-capture coefficient term. As explained in the introduction that since transport simulation for the DCO strategy is simultaneously linked to

the flow simulation, real concentration for each class of contaminants are obtained. These concentrations are passed to the PTSDC model as part of the optimization procedure and not as part of an additional post-processing step such as the case of the IDCO strategy. The result of the DCO strategy is one final value that is the total cost in this case. Accordingly, the fitness value for the DCO is the total cost, yet subject to practical and safety constraints.

The only practical constraint is that all the proposed pumping wells should be located in the site boundaries (i.e. P_{out}=0). The safety constraints are the plume capturing and the location of the capture zone. To ensure that all the plumes are captured the ratio of the captured particles to the total number of particles$\sum_{i=1}^{n_{w,tot}} R_{cap,i}$ should be equal to unity. In addition, to ensure that the capture zone is mostly located within the site premise the *TR* should be less than a maximum predefined ratio (TR_{max}).

If these 3 constraints are fulfilled, the fitness value is the total cost C [€] estimated by the PTSDC model, otherwise a predefined maximum cost C_{max} [€] is scaled according the OF value to enable the optimization algorithm to converge. The scaling is done by normalizing the OF value by multiplying it with a weighting factor w_{OF} to be in the same order of magnitude as the total cost. This shall enable the addition of the OF value to the C_{max} [€]. This method proved to be more robust than multiplying the maximum cost with a normalized OF value. Although Hilton and Culver (2000) shows that multiplicative penalty method (MPM) is more robust than additive penalty method (APM), yet it is noticed in this study that APM when accurately developed is more robust that MPM.

The formulation of the fitness function for the DCO strategy for the ISA and GSA are respectively the following:

$$F_j = \begin{Bmatrix} C & \boldsymbol{if} \quad TR < TR_{max}, P_{out} = 0, \sum_{i=1}^{n_{w,tot}} R_{cap,i} = 1 \\ & (w_{OF}.OF_j) + C_{max} \end{Bmatrix} \quad \forall\, j \in [1 \dots n_{scenarios}] \tag{3.29}$$

$$F = \max(F_j)\, \forall\, j \in [1 \dots n_{scenarios}] \tag{3.30}$$

The fitness for the GSA as represented in equation 3.30 has the same formulation of the ISA (Eq. 3.29) expects that the fitness is the cost of the single scenario with the highest cost.

3.3.5 Optimization Runs

Because of the stochastic features of the evolutionary algorithms, any randomly initialized optimization run (OR) shows a different search path and provide different results even if the parameter settings are not changed (Bayer and Finkel, 2004). Thus to provide a reliable basis for the analysis the optimization is performed repeatedly for each task under study. In doing so the stochastic influences on the evaluation and interpretation of the results is reduced. In most of the used cases, 5 ORs are performed on the 4 flow scenarios resulting in a set of 20 data points for each objective under study. Although 20 data points are not sufficient enough to obtain statistically representative results, but it is believed to be sufficient in the comparison between the objectives understudy.

For the compression between data sets, one-way ANOVA is performed to compare the means of several data sets of the investigated objective. The ANOVA1 function returns the *p*-value, which is derived from the CDF of the F-statistic, under the null hypothesis that the data samples are drawn from populations with the same mean. If the p-value is near zero, it casts doubt on the null hypothesis and suggests that at least one sample mean is significantly different from the other sample means. A p-value below 0.05 is a common significance level. The box plots of the data columns are visual representation of the size of the F-statistic and the p-value. Large differences in the center lines of the boxes correspond to large values of F and correspondingly small p values.

4 Results and Discussion

4.1 Optimization Performance

The number of model runs and individuals per generation are two important variables that directly affect the robustness of the optimization search.

The first objective of this section is to study the relationship between the improvements in the objective function (OF) values as the optimization progress in order to develop a practical stopping criterion. In contrast to the built-in stopping criteria, the proposed stopping criterion can be adopted to real and non-scaled variables. In this case, the OF values are chosen as the stopping criterion variable. The proposed stopping criterion simply terminates the optimization if the objective function improvement (OFI) over a certain predefined generation range reached a considerably small predefined improvement value. Case 3 (308 Generations) and Case 4 (750 Generations) as described in Table1.1 are used in this evaluation. In addition, using Case 9 IDCO-$S_{n.}$, the built-in stopping criterion VSP is normalized with OFI stopping criterion. This normalization is then validated using the results of Case 10 IDCO and Case 11 DCO.

The second objective of this section is to evaluate the effect of increasing the population size λ on the optimization performance in terms of approaching a better solution, and to assess the computational cost associated with increasing the population size. Case 4 GSA-13λ, Case 5 GSA-20λ and Case 6 GSA-23λ are used in this assessment. The GSA cases are chosen for the evolution of the CMA-ES optimization performance because GSA is more complex and computationally demanding, since one well configuration must successfully perform on all the scenarios.

The default stopping criterion for the CMA-ES optimization is a fixed number of iterations, which are also known as model runs (MR). The problem with this approach is that the number of model runs is not know from the beginning and several trails have to be initially performed to determine a suitable number of MRs. Moreover, this approach could be inefficient since the optimization can converge to a solution early resulting in additional MRs with no significant variations in the search points. Conversely, the optimization can prematurely terminate before the evolutionary path containing wide range of diverse successful search points converges. To explore all these possibilities Case GSA 3 is used with MRs= 4000 (13λ x 308 Generations). Five optimization runs (OR) are performed. The progress of a single OR for the 4 scenarios is shown in Figure 4.1.

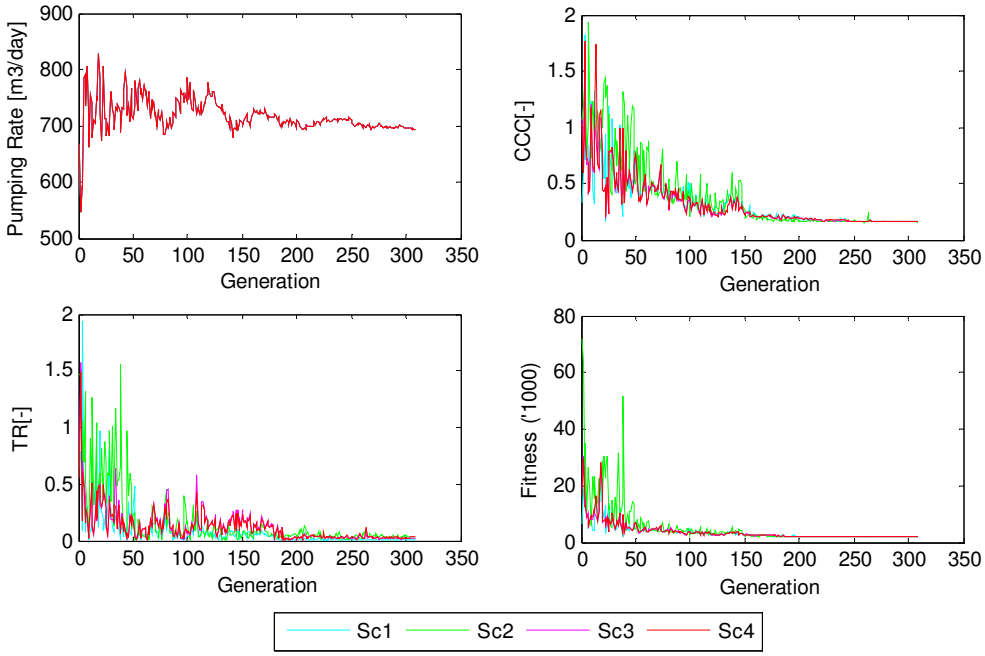

Figure 4.1 Case 3 GSA: Progress of OR5

Three primarily remarks can be drawn from the results of these 5 ORs. Although Figure 4.1 shows that the optimization variables are leveling-off, yet visual judgment is not a clear indication that no further improvement is possible. Figure 4.2 illustrates this point by determining the difference between the minimum and maximum normalized OF values (normalized to the best fitness value of all the ORs and MRs, and expressed in terms of percent deviation from that best fitness) over last the 100 generations. The difference is as high as 10%, which indicates that further improvement in the OF value is still possible. This point is verified by the two additional ORs shown in the right hand side plot in Figure 4.2.

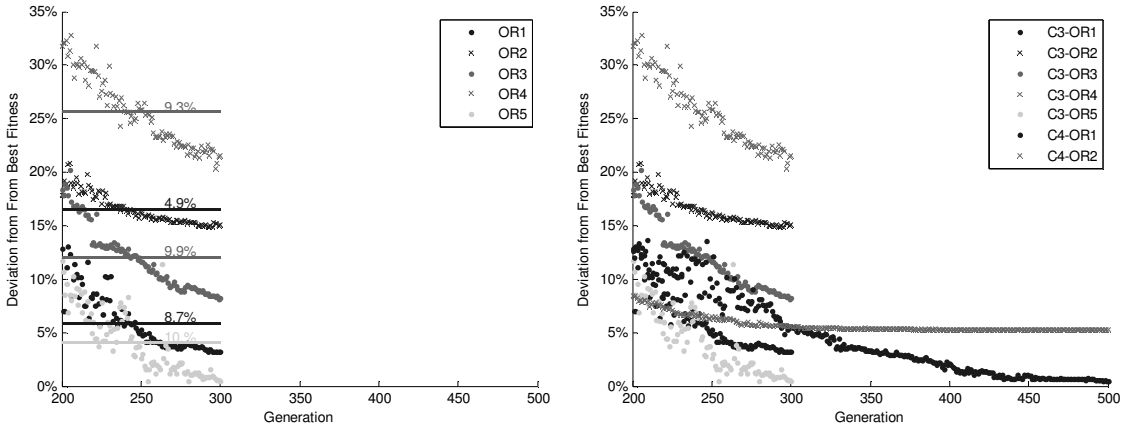

Figure 4.2 Case 3 GSA: normalized fitness values for the 5 ORs over the last 100 generations (left hand plot) and two addition ORs to prove that further improvement in the OF value is still possible (right hand plot)

The second remark is that there is a wide range of deviations in the fitness values and optimization variables between the proposed results. These deviations can be visualized in Figure 4.3. The 5 ORs results shown for Scenario 2 indicate a wide range of values among different ORs with OR5 showing the best fitness and OR2 and OR4 being the worst.

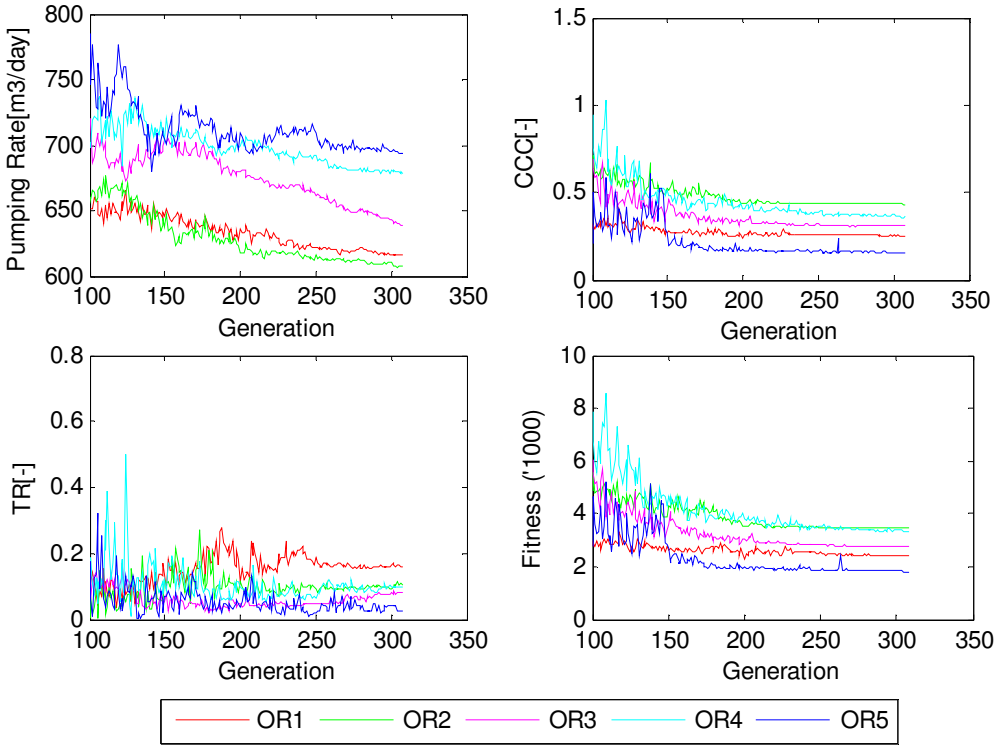

Figure 4.3 Case 3 GSA: Progress of the 5 ORs for Scenario 2

The final remark is that some ORs converge to significantly better solutions than other. For example, although some ORs succeed in dis-jointly capturing the two plumes such as OR5, other such as OR2 failed to find a solution that separates the CHC and BTEX plumes.

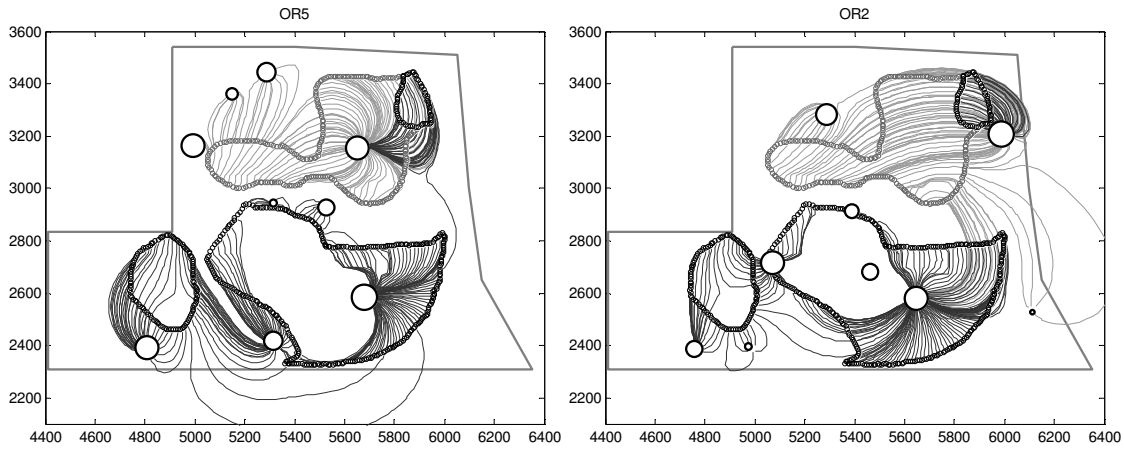

Figure 4.4 Case 3 GSA Scenario 2: OR5 and OR2 performance compared

The above three remarks are not only due to the stochastic nature of the solution method, but also are function of the number of MRs and population size. Accordingly, finding a stopping

criterion that insure that on significant improvement in the objective function values is further possible and determining the population size that insure that enough search space is explored are crucial for reaching a robust solution.

A simple and straight forward stopping criterion, which is directly based on the improvement of the OF values, is proposed. This criterion simply assesses the objective function improvement (OFI) by calculating the percent improvement between the minimum and the maximum OF values for an array containing the OF values of each generation for a predefined generation range (a→ b):

$$OFI_{a\to b} = \frac{Max(OF)_{a\to b} - Min(OF)_{a\to b}}{Max(OF)_{a\to b}} x100 \qquad (4.1)$$

A suitable generation range (a→b) for evaluating the OFI is 50 generations. This range could vary depending on the complexity of the problem. The termination criterion is a predefined minimum improvement value OFI_{MIN}. If the OFI in the examined range $OFI_{a\to b}$ is below the OFI_{MIN} the optimization terminate. An OFI_{MIN} of 0.1% is reasonably sufficient.

The effect of increasing the population size λ on the global search capacity is explored, and variation in the required MR number with population size is assessed using the OFI stopping criterion.

The results of the 6 ORs of Cases 4, 5 and 6 show that higher population sizes (20 and 23) enhance the global search capacity and thus converges to better solutions compared to the default population size, yet more MRs are needed by large populations to reach the 0.1% OFI stopping criterion.

Further analysis of the results as shown in Figure 4.6 indicates that the OFI is a valid stopping criterion, since the OFI continuously decreases as the optimization progress. The OFI is evaluated over a range of 50 generations. At the first OFI evaluation (i.e. period from generation1-50), the OFI for the 6 ORs ranges from 90-100% decreasing to 2 – 10% at fifth evaluation (i.e. from generation 200-250) and followed by 0.02 to 0.5 % at the tenth evaluation. By the last OFI evaluation (i.e. generation 700-750) the OFI dropped as low as 0.02 to 0.006 %.

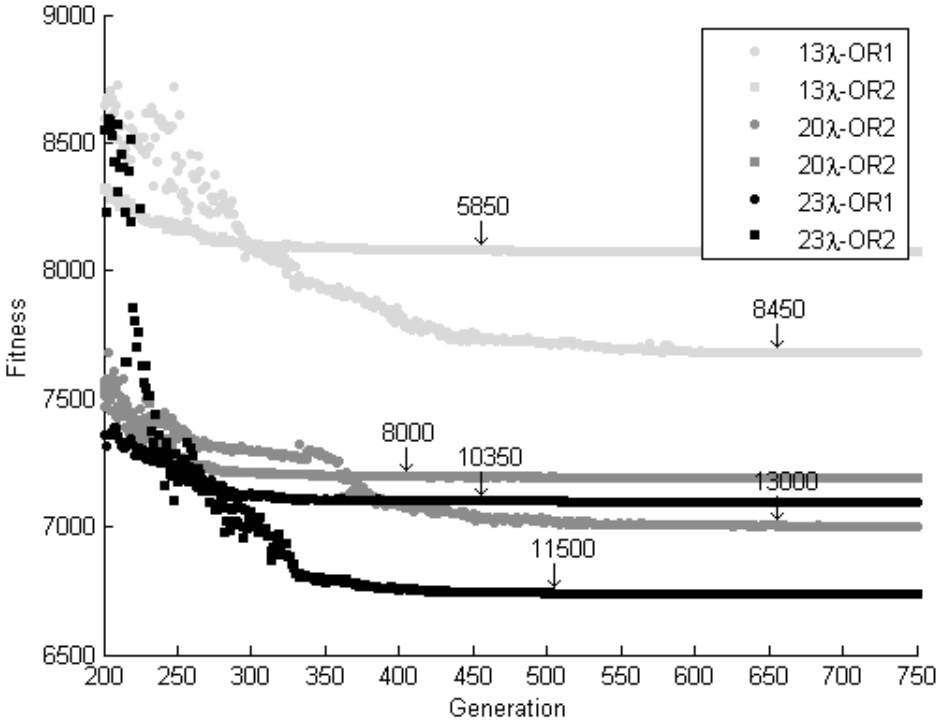

Figure 4.5 Case 4 GSA- 13λ, Case 5 GSA- 20λ and Case 6 GSA- 23λ: performance of different population sizes (the number above the arrow indicates the number of MRs required to reach the 0.1% OFI_{MIN} stopping criterion)

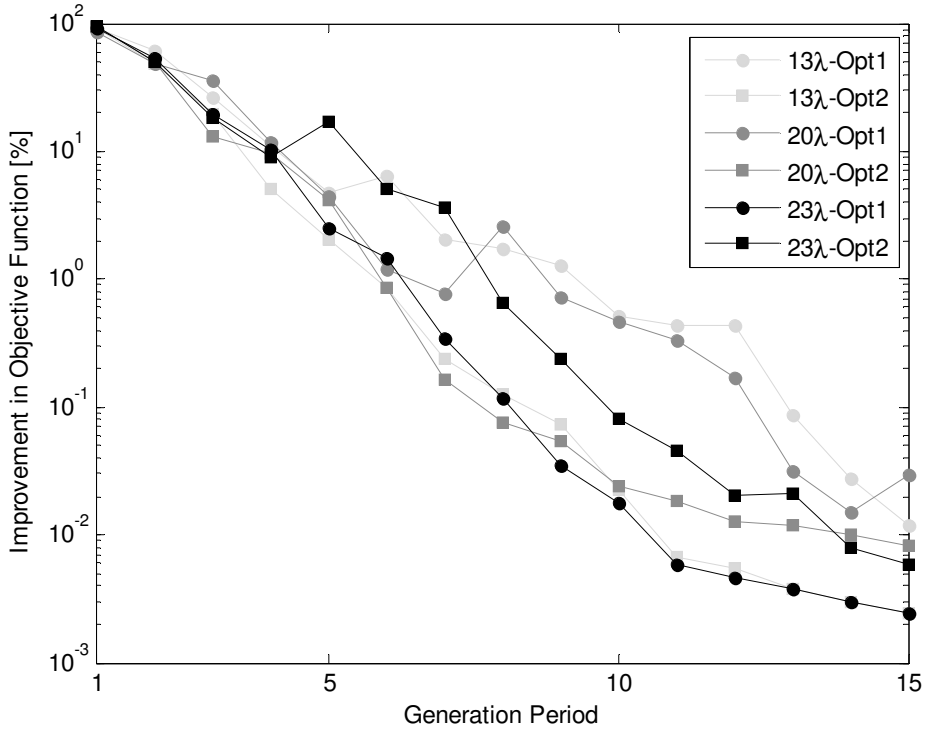

Figure 4.6 Case 4 GSA- 13λ, Case 5 GSA- 20λ and Case 6 GSA- 23λ: OFI continuous decrease as the optimization progress

This concept is validated by applying OFI stopping criterion to the differentiated capture (DC) and non differentiated capture (NDC) cases (i.e. Case 7 and Case 8) using a termination criterion OFI_{MIN} of 0.1%. The result is shown in Table 4.1.

Table 4.1 Case 7 GSA-DC and Case 8 GSA-NDC: OFI for different generation periods

Case	OR	Gen	Target OFI [%]	OFI [%] within each period										
				0-50	50-100	100-150	150-200	200-250	250-300	300-350	350-400	400-450	450-500	500-550
DC	1	400	0.1	89.85	55.50	30.10	11.57	4.10	0.74	0.12	0.05			
DC	2	350	0.1	87.22	44.44	27.56	3.85	1.90	0.48	0.08				
DC	3	450	0.1	92.03	44.87	14.10	4.86	3.92	1.90	0.78	0.15	0.09		
DC	4	550	0.1	85.02	61.17	38.18	6.58	3.23	1.90	2.61	2.44	0.78	0.20	0.04
DC	5	550	0.1	92.04	40.45	12.29	5.04	2.93	2.89	1.64	1.08	1.00	0.29	0.07
NDC	1	300	0.1	96.06	7.57	2.75	1.66	0.62	0.10					
NDC	2	350	0.1	95.11	11.50	2.41	1.88	0.64	0.14	0.04				
NDC	3	400	0.1	96.97	8.26	3.64	0.94	0.65	0.82	0.43	0.07			
NDC	4	350	0.1	91.29	10.02	1.62	1.17	0.40	0.15	0.04				
NDC	5	400	0.1	96.05	10.26	4.17	1.47	1.20	0.43	0.18	0.05			

As previously observed the OFI values are continuously decreasing as the optimization progresses, which shows that the OFI is a valid stopping criterion. Also, the result shows that since the DC case is more computational demanding the termination criterion for all the 5 ORs is reached at within generations 400 to 550, compared to 300 to 400 for the NDC.

Before moving to the next objective, it is worth mentioning that the fitness values are the stopping criterion variable in this case. Other optimization objectives such as CCC or TR, or decision variables such as pumping rate could be also used as a stopping criterion variable. However, fitness is preferred in this case because it is more representative.

The second objective of this section is to normalize the variation of search points (VSP) stopping criterion to the objective function improvement (OFI) stopping criterion. In VSP stopping criterion, the search stops if variation of the search points becomes considerably smaller in all coordinates than a predefined scalar value *tolX*, which is defined as $S / \sqrt{n}$, where n the number of problem dimensions and S is a scalar number with a default value S= 1E-7. The meaning of VSP stopping criterion is not clear to the user since it does not have a direct meaning to any of the optimization objectives, but rather corresponds to the variations in scaled decision parameters, which are not meaningful a priori. Yet a practical use of VSP is that it allows nonbiased comparison between different objective functions. For example, VSP is perfect if the objective is to compare the IDCO (Case 10), which objective function yields fitness values, with the DCO (Case 11) which objective function gives total cost. However, the practical meaning of the termination criterion tolX should be understood beforehand by normalizing it to a known value. Different values of *tolX* are normalized to OFI as presented in Table 4.2.

Table 4.2 Case 9 IDCO-S_n : normalization of the S values to the OFI

OR	S	Gen	Fitness	OFI [%] within each period							
				0-50	50-100	100-150	150-200	200-250	250-300	300-350	350-400
1	1	34	22314	88.5							
2	0.5	89	7982	90.3	72.3						
3	0.1	177	9508	79.5	19.6	64.9	55.4				
4	0.03	339	1079	97.1	53.4	39.4	9.5	6.5	2.8	1.6	1.5
5	0.02	335	1078	98.5	64.3	29.5	17.7	9.6	3.0	1.2	
6	0.02	356	1070	96.4	29.3	23.4	10.3	3.7	1.9	1.3	0.2

Table 4.2 shows that choosing an S value of below 0.03 ensures that the IMP will be below 5%. A high OFI_{MIN} 5% is chosen for the DCO case because running MT3DMS for multi-compounds is time consuming. Using a 1.67 GHz Core II processor, the average CPU time for one generation containing 13 individuals is approximately 40 seconds for the IDCO and 3200 seconds for the DCO. Accordingly, obtaining an ultra-refined solution is irrelevant for this comparison purpose. If the objective is to obtain a final solution, then the number of individuals per generation should increase and an OFI_{MIN} should be 0.1% as previously suggested. Thus, S value of 0.03 is used in the comparison between Case 10 IDCO and Case 11 DCO for achieving $OFI_{a\rightarrow b} < 5\%$.

The result as presented in the Annex (Table.A4) shows that the mean $OFI_{a\rightarrow b}$ at termination is 1±0.3%, with the highest $OFI_{a\rightarrow b}$ being 2.8% and lowest being 0.1%.

4.2 Comparison between Individual and Grouped-Scenarios Approaches

As explained in the methodology section several scenarios are generated to account for uncertainty. The first objective of this section is to cross evaluate the reliability of a well configuration proposed for one scenario on other scenarios in order to determine the critical scenarios. The second objective is to compare the technical parameters (i.e. pumping rate, TR, CCC …) of both the ISA and GSA solutions.

Using the formulation of Case 1 ISA-TR, 5 ORs are performed on each of the 4 scenarios resulting in 20 optimal well configurations. Table 4.4 presents the five optimal solutions for each of the four scenarios.

Table 4.4 indicates that for the 20 ORs the optimization succeed in placing the pumping wells within the site boundary and capturing all particles. The cross capture coefficient in most of the ORs is brought to its lower possible limit (i.e. the lowest limit ≈0.14 since the BTEX and CHC overlap in the North East side as shown in Figure 3.8). The fitness values of the 20 ORs have a wide range from 1070 to 2360. While the statistical mean for the fitness values for scenarios 1, 3 and 4 is 1150 ± 59, Scenario 2 has a mean of 1828±383. This definitely proves that scenario 2 is more demanding.

Table 4.4 Case 1 ISA-TR: Optimal Solutions of the 5 ORs for the four scenarios

Sc. No.	OR No.	Number of Wells outside [-]	Total Pumping Rate [m^3/day]	Particles Not Captured [-]	CCC [-]	TR [-]	Particle Mean Travel Time [year]	Fitness
1	1	0	456	0	0.14	0.01	20	1111
	2	0	518	0	0.14	0.02	20	1232
	3	0	456	0	0.15	0.04	18	1143
	4	0	454	0	0.15	0.05	21	1184
	5	0	487	0	0.14	0.02	21	1159
2	1	0	619	0	0.28	0.02	11	2361
	2	0	614	0	0.17	0.02	17	1669
	3	0	654	0	0.17	0.01	25	1770
	4	0	635	0	0.18	0.00	17	1766
	5	0	572	0	0.17	0.03	12	1575
3	1	0	444	0	0.14	0.02	43	1070
	2	0	535	0	0.15	0.06	12	1399
	3	0	476	0	0.15	0.02	28	1181
	4	0	459	0	0.15	0.05	13	1169
	5	0	452	0	0.15	0.06	12	1173
4	1	0	437	0	0.14	0.01	19	1066
	2	0	447	0	0.14	0.04	15	1099
	3	0	452	0	0.15	0.03	13	1141
	4	0	489	0	0.15	0.04	19	1254
	5	0	451	0	0.14	0.02	14	1096
Mean		0	505	0	0.16	0.03	19	1331
Stdev		0	73	0	0.03	0.02	7	335
Max		0	654	0	0.28	0.06	43	2361
Min		0	437	0	0.14	0.00	11	1066

In conclusion, this results show that the almost all the proposed 20 well configurations are successful in terms of meeting the optimization objective, except for the configuration proposed by OR 1 for Scenario 2 due to the high CCC. However, the performance of a specific well configuration of one scenario on the other three scenarios remains as a further challenge.

To insure a successful performance of a certain well configuration produced for specific scenario on the other scenarios, post-processing is needed. This analysis follows the following procedure:

1. Retrieve the most optimal well configuration form each optimization run (OR) for the four scenarios , which results in 20 well configurations (Table 4.4)
2. Post-process these 20 well configurations on each scenario, which results in 20 fitness values for each scenario (e.g. Table 4.5)

3. For each well configuration, sum up the fitness values of the four scenarios
4. Sort the cumulative fitness values to obtain the top configurations (Table 4.6)
5. Determine the critical scenario based on the top configurations

Each of the 20 configurations shown in Table 4.4 is post-proceeded to evaluate its performance on the other 3 scenarios. The performance of these configurations on Scenario 1 is shown in Table 4.5. Similar post-processed results for the other three scenarios are shown in the Annex (Table A.5).

Table 4.5 Case 1 ISA-TR: Performance of the optimal solutions of the other 3 scenarios on Scenario 1

Sc. No.	OR No.	Number of Wells outside [-]	Total Pumping Rate [m^3/day]	Particles Not Captured [-]	CCC [-]	TR [-]	Particle Mean Travel Time [year]	Fitness
1	1	0	456	0	0.14	0.01	20	1111
	2	0	518	0	0.14	0.02	20	1232
	3	0	456	0	0.15	0.04	18	1143
	4	0	454	0	0.15	0.05	21	1184
	5	0	487	0	0.14	0.02	21	1159
2	1	0	619	0	0.60	0.03	19	4402
	2	0	614	0	0.26	0.18	14	2496
	3	0	654	0	0.42	0.01	18	3418
	4	0	635	0	0.31	0.09	23	2729
	5	0	572	0	0.52	0.08	14	3710
3	1	0	444	162	0.59	2.22	96	46508
	2	0	535	0	0.81	0.18	18	5500
	3	0	476	110	0.09	2.11	91	27802
	4	0	459	63	0.12	1.94	44	15895
	5	0	452	52	0.11	2.09	38	14278
4	1	0	437	162	0.08	3.06	71	50487
	2	0	447	56	0.11	0.96	39	8456
	3	0	452	20	0.14	0.57	27	3518
	4	0	489	39	0.13	1.03	51	7570
	5	0	451	61	0.10	1.16	40	10235
Mean		0	505	36.25	0.25	0.79	35	10642
Stdev		0	73	53	0.21	0.97	25	14542
Max		0	654	162	0.81	3.06	96	50487
Min		0	437	0	0.08	0.01	14	1111

The post-processed results in Table 4.5 indicate that the optimal well configurations proposed for Scenarios 3 and 4 fails completely to perform on Scenario 1. The results of Scenario 2 show a good performance in terms of capturing all the particles and relatively in containing the plume

within the site boundary, but the performance in terms of the CCC is generally poor. The performance of OR2-Sc2 and OR3-Sc2 on Scenario 1 are relatively acceptable.

The next step in the result analysis is to determine the best well configurations, which can successfully perform on the multiple scenarios. Thus, the fitness of all the post-proceeded results is compiled and ranked in an ascending order as shown in Table 4.6.

Table 4.6 Case 1 ISA-TR: Cross performance of the 20 ORs ranked by fitness values

Scenario-OR No.	Fitness ('1000)				
	Scenario-1	Scenario-2	Scenario-3	Scenario-4	ΣFitness / OR
2-3	3.4	1.8	4.1	4.1	13
2-5	3.7	1.6	4.9	4.8	15
2-1	4.4	2.4	5.0	5.1	17
2-2	2.5	1.7	13.4	5.6	23
2-4	2.7	1.8	14.5	12.0	31
3-2	5.5	23.4	1.4	1.5	32
1-4	1.2	40.6	2.4	3.8	48
4-3	3.5	45.2	1.3	1.1	51
1-3	1.1	43.4	4.7	3.5	53
3-4	15.9	36.7	1.2	1.9	56
3-5	14.3	45.2	1.2	1.2	62
4-2	8.5	55.8	1.4	1.1	67
4-5	10.2	63.0	1.4	1.1	76
1-5	1.2	37.1	80.1	1.5	120
4-4	7.6	117.1	1.5	1.3	127
1-2	1.2	115.0	6.4	7.6	130
4-1	50.5	152.8	1.4	1.1	206
3-3	27.8	200.8	1.2	3.4	233
3-1	46.5	207.6	1.1	6.0	261
1-1	1.1	245.0	30.7	28.4	305
Σ Fitnes / Scenario	213	1438	179	96	1926

Since Scenario 2 is the most demanding scenario, the well configurations of the other scenarios performed poorly on Scenario 2 making the summation of the total fitness values of all the ORs the highest as shown in the bottom row of Table 4.6. In turn, the well configurations of Scenario 2 perform superiorly on the other scenarios resulting in relatively low total fitness value per single OR as shown in the last column. The top 5 well configurations are the results of the 5 ORs of Scenario 2. Following the same analogy, since Scenario 4 is the least demanding, only one optimal solution of its 5 ORs is among the top ten well configurations. The performance of the top five well configurations on each of the 4 scenarios is detailed in Table 4.7 to assess the technical qualification of the top selected solutions.

Table 4.7 Case 1 ISA-TR: performance of the top five optimal solutions on the four scenarios

Sc-OR	Post processed on Sc No.	Number of Wells outside [-]	Total Pumping Rate [m^3/day]	Particles Not Captured [-]	CCC [-]	TR [-]	Particle Mean Travel Time [year]	Fitness	Total Fitness ('1000)
2-3	1	0	654	0	0.42	0.01	18	3418	13.3
2-3	2	0	654	0	0.17	0.01	25	1770	
2-3	3	0	654	0	0.52	0.01	12	4089	
2-3	4	0	654	0	0.52	0.01	12	4065	
2-5	1	0	572	0	0.52	0.08	14	3710	14.9
2-5	2	0	572	0	0.17	0.03	12	1575	
2-5	3	0	572	0	0.66	0.16	9	4852	
2-5	4	0	572	0	0.66	0.15	10	4777	
2-1	1	0	619	0	0.60	0.03	19	4402	16.9
2-1	2	0	619	0	0.28	0.02	11	2361	
2-1	3	0	619	0	0.67	0.09	11	5029	
2-1	4	0	619	0	0.67	0.09	11	5067	
2-2	1	0	614	0	0.26	0.18	14	2496	23.2
2-2	2	0	614	0	0.17	0.02	17	1669	
2-2	3	0	614	6	0.45	2.13	38	13440	
2-2	4	0	614	0	0.46	0.69	20	5627	
2-4	1	0	635	0	0.31	0.09	23	2729	31.0
2-4	2	0	635	0	0.18	0.00	17	1766	
2-4	3	0	635	30	0.30	1.65	24	14492	
2-4	4	0	635	25	0.31	1.42	22	12010	
Mean		0	619	3.05	0.41	0.35	17	4967	20
St. dev		0	28	9	0.18	0.63	7	3834	7
Max		0	654	30	0.67	2.13	38	14492	31
Min		0	572	0	0.17	0.00	9	1575	13

As expect the best well configurations are those of Scenario 2. Sc2-OR3 shows the lowest fitness. This well configuration succeeds in containing the capture zone within the site boundary as indicated from the TR being as low as 0.01 for all scenarios. Yet as illustrated in Figure 4.7, Sc2-OR3 well configuration among all the other well configurations shown in Table 4.7 performed poorly in terms of the CCC being over 0.5 for some scenarios, which renders the dis-joint capture and treatment approach ineffective. . The second best well configuration (Sc2-OR5) did not only fail to dis-jointly capture the two plumes, but also in effectively containing the plume within the site boundary as shown in Figure 4.8.

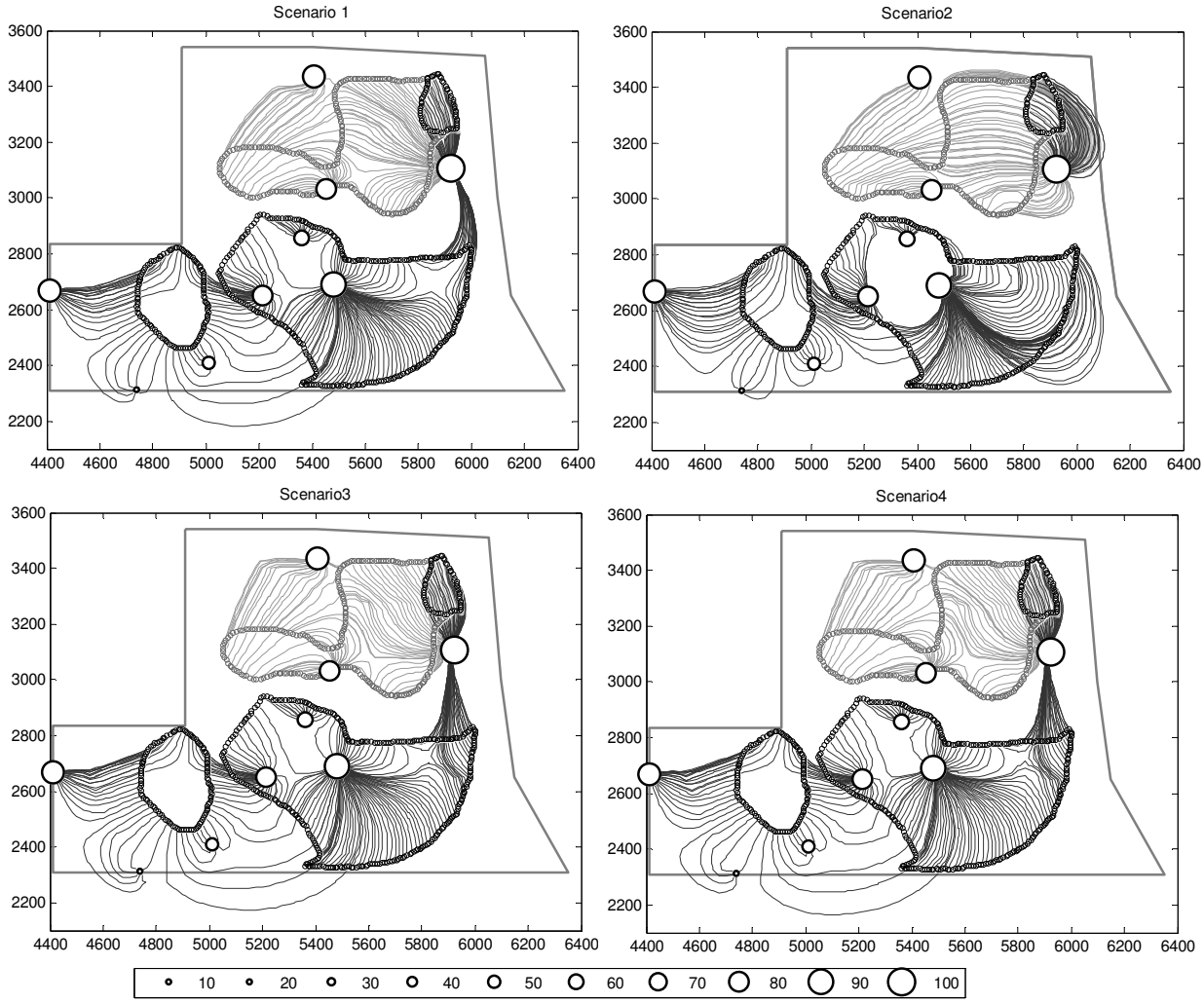

Figure 4.7 Case 1 ISA-TR: Performance of Sc2-OR3 on the four scenarios (well locations and pumping rates are represented by the circles)

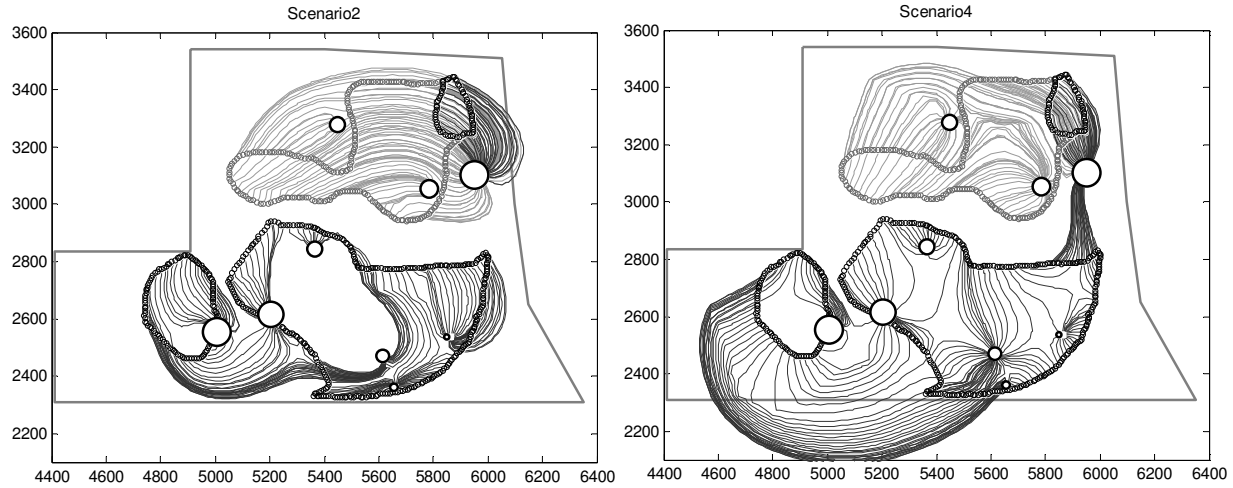

Figure 4.8 Case1 ISA-TR: Performance of Sc2-OR5 on Scenario 2 and 4

To overcome these drawbacks, a more conservative approach will be the grouped-scenarios approach (GSA). In this approach the optimization runs on the four scenarios simultaneously resulting in 1 optimal well configuration, which is valid for the four scenarios. Analysis method for this approach is simple because the optimal result does not need to be post-processed. Using the optimization formulation of Case 3 GSA, the optimal well configurations proposed by the 5 ORs are shown in Table 4.8.

Table 4.8 Case 3 GSA: Optimal Solutions of the 5 ORs for the four scenarios

OR No.	Sc. No.	Number of Wells outside [-]	Total Pumping Rate [m^3/day]	Particles Not Captured [-]	CCC [-]	TR [-]	Particle Mean Travel Time [year]	Fitness	Total Fitness ('1000)
1	1	0	616	0	0.18	0.07	7	1828	7.6
	2	0	616	0	0.25	0.16	14	2415	
	3	0	616	0	0.16	0.08	11	1672	
	4	0	616	0	0.16	0.07	11	1657	
2	1	0	608	0	0.17	0.00	13	1625	8.4
	2	0	608	0	0.43	0.10	10	3450	
	3	0	608	0	0.17	0.00	9	1671	
	4	0	608	0	0.17	0.00	9	1669	
3	1	0	639	0	0.19	0.00	6	1829	7.9
	2	0	639	0	0.31	0.08	12	2730	
	3	0	639	0	0.16	0.03	9	1669	
	4	0	639	0	0.16	0.02	9	1657	
4	1	0	678	0	0.17	0.02	13	1827	8.8
	2	0	678	0	0.37	0.10	12	3354	
	3	0	678	0	0.17	0.01	12	1830	
	4	0	678	0	0.17	0.01	12	1832	
5	1	0	693	0	0.16	0.01	13	1837	7.3
	2	0	693	0	0.15	0.03	23	1781	
	3	0	693	0	0.16	0.03	9	1854	
	4	0	693	0	0.16	0.03	9	1864	
Mean		0	647	0	0.20	0.04	11	2003	8.0
St dev		0	34	0	0.08	0.04	3	548	0.6
Max		0	693	0	0.43	0.16	23	3450	8.8
Min		0	608	0	0.15	0.00	6	1625	7.3

In contrast to the ISA, the GSA succeeds in finding a solution that performs successfully on the four scenarios. All the ORs succeed in containing the capture zone within the site boundary for the four scenarios as shown in Figure 3.9. Although not a single well configuration in the ISA case is able to dis-jointly capture the two plumes, some GSA well configurations such as these of OR1 and OR5 succeed in dis-jointly capturing the plumes, yet this success is on the expense of the pumping rate.

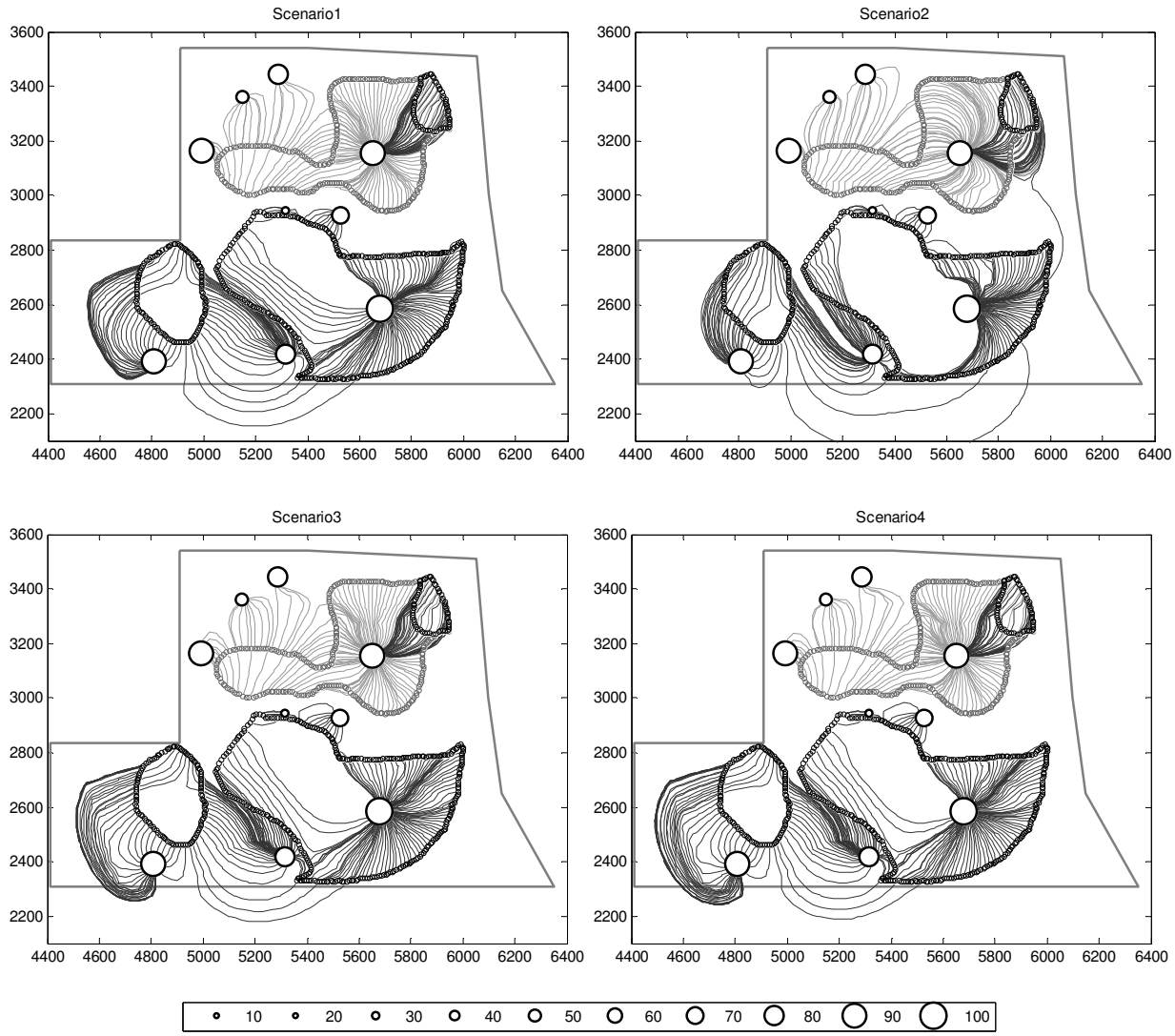

Figure 4.7 Case 1 GSA: Performance OR5 on the four scenarios (well locations and pumping rates are represented by the circles)

One-way ANOVA is performed on ISA and GSA cases to quantitatively compare their main optimization variables which are CCC, TR and pumping rate. The F-distribution of the means can be visualized in Figure 4.10. Large differences in the center lines of the boxes correspond to large values of F and correspondingly small values of P indicating that there is a significant difference between the means of the two data sets.

To ensure a fair comparison, the data set of the top 5 well configurations of ISA (Table 4.7) is compared with results of the 5 ORs of GSA. Using significance level of 0.05 for the P-values, Figure 4.10 confirms that the GSA shows significant improvement in terms of the CCC and TR on the expense of the pumping rate. The improvement in the overall fitness values compared to the ISA (Table 4.7) is due to the successful performance of the candidate well configurations on the 4 scenarios.

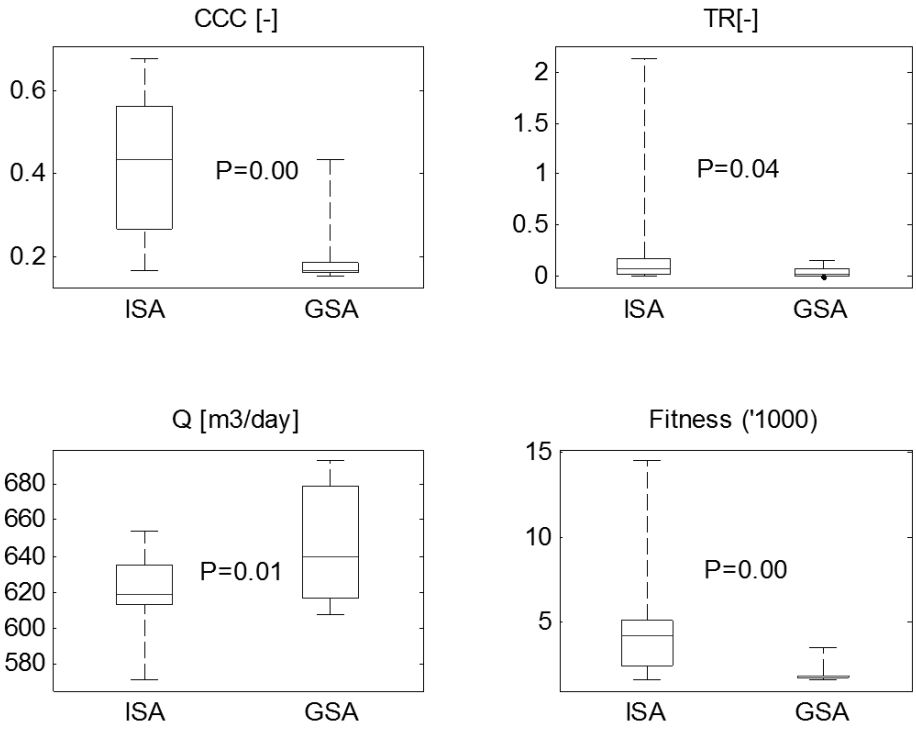

Figure 4.10 Case 1 ISA and Case 3 GSA: comparison between the main optimization variables

4.3 Constraining the Capture Zone to the Site Premise

Case 1 ISA-TR accounts for the time ratio of the out to in site particles travel time, while Case 2 ISA-NTR does not. Before comparing the ISA-TR and ISA-NTR, a quick overview on the results of Case-2 ISA-NTR is essential. The results in Table 4.9 indicate that the optimization succeeds in proposing a well configuration within the site boundary, which is able to dis-jointly capture the two plumes, yet fails to contain the capture zone within the site boundary for most of the well configurations as indicated by the high TR.

One-way ANOVA is used to quantify the difference in TR between the two data sets, which are Cass 1 ISA-TR (Table 4.4) and Case 2 ISA-NTR (Table 4.9). A P-value of 3E-5 is obtained indicating a significant difference between the two data sets. The results of Case 1 ISA-TR show that the capture zone is successfully contained within the site boundary. The mean TR for the 20 ORs is 0.03±0.01. Some OR such as Sc2-OR4 succeeds in totally containing the capture zone within the site boundary as shown in Figure 4.11. On the other hand, the mean TR for Case 2 ISA-NTR is 0.77±0.33, and some ORs such as Sc2-OR1 completely fails in containing the capture zone within the site boundaries.

Table 4.9 Case 1 ISA-NTR: Optimal Solutions for the 5 ORs for the four scenarios

Sc. No.	OR No.	Number of Wells outside	Pumping Rate [m^3/day]	Particles Not Captured	CCC [-]	TR [-]	PMTT [year]	Fitness
1	1	0	453	0	0.14	0.25	20	1280
	2	0	453	0	0.14	0.84	27	1951
	3	1	450	0	0.15	0.08	15	1431
	4	0	455	0	0.14	0.59	21	1635
	5	0	448	0	0.14	0.14	19	1166
2	1	0	542	0	0.17	3.13	37	7163
	2	0	602	0	0.33	0.48	16	3681
	3	1	574	0	0.18	1.71	23	5704
	4	0	560	0	0.21	1.72	29	5075
	5	0	618	0	0.17	1.12	28	3607
3	1	0	444	0	0.14	0.61	19	1648
	2	0	445	0	0.14	0.53	16	1585
	3	0	442	0	0.14	0.43	21	1427
	4	0	444	0	0.14	0.54	22	1590
	5	0	450	0	0.14	0.24	15	1289
4	1	0	437	0	0.14	0.86	23	1892
	2	0	440	0	0.14	0.35	19	1379
	3	0	449	0	0.14	0.71	31	1808
	4	0	446	0	0.14	0.82	20	1911
	5	0	442	0	0.14	0.40	20	1432
Mean		0	480	0	0.16	0.78	22.03	2433
St dev		0	61	0	0.05	0.71	5.79	1705
Max		0	618	0	0.33	3.13	36.95	7163
Min		0	437	0	0.14	0.08	14.57	1166

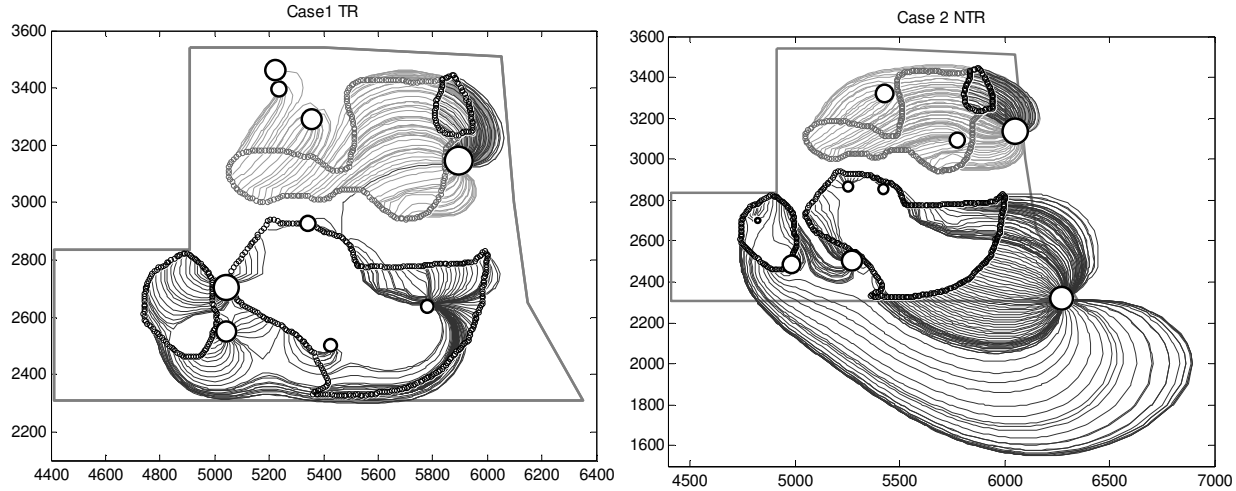

Figure 4.11 Case 1 ISA-TR and Case 2 ISA-NTR: Case1-OR4-Sc2 succeeds in containing the capture zone within the site premise; Case2-OR1-Sc2 shows a complete failure

In conclusion, the objective function that incorporates TR as an additional constraint is successfully formulated. This shows that the concept of using the time ratio of the particles travel time out and is-side the site premise is a valid approximation for the particle locations (i.e. travel path inside and outside the site boundaries).

4.4 Disjoint Capture of Different Plume Types

Another optimization objective is to capture the BTEX and CHC plumes separately to decrease the treatment cost. The cross capture coefficient (CCC) as explained in Section 3.3.3.4 measures the degree of separation. In this section the relationship between the CCC and total cost is evaluated. To perform this assessment, Case 8 GSA-DC is used according to the optimization formulation presented in Table 1.1. Case 7 GSA-NDC is used a as reference case for comparison. In addition, the sensitive variables are identified to determine its main drivers of the system.

In the indirect cost optimization (IDCO), the transport model is used to calculate the breakthrough curves for all the COCs using the well configurations proposed by the optimization algorithm. These concentrations along with the pumping rates are the inputs of the PTSDC model, which analyzes the concentration profiles and calculates the removed mass, and designs and dimensions both the GAC and CAT treatment units. In addition, it calculates the total cost of the GAC and CAT treatment units, pumping wells and all other cost items in the PTS.

The outputs of the optimization, transport simulation and cost calculations for the 10 ORs of both DC and NDC cases are presented in Table 4.10. The breakthrough curves for GSA-DC Sc1-OR2 and the corresponding cost calculation for the GAC and CAT treatment units are shown in Figure 4.12.

Table 4.10 Case 7 GSA-DC and Case 8 GSA-NDC: Optimization result, and the post-processed mass removal rates and cost calculations

Optimization Run			Optimization Result			Pumping Rate [m3/day]			Removed Mass [Kg]			Treated Mass [Kg]		Cost [€ 1E6]		
Case	OR	Sc	CCC	TR	Fitness	GAC	CAT	Total	BTEX	CHC	Total	GAC	CAT	GAC	CAT	Total
DC	1	1	0.20	0.01	1.7	6.7	100	477	577	144	3781	3925	171	3754	0.81	1.32	2.97
		2	0.24	0.05	2.0					164	2996	3160	166	2994	0.55	1.31	2.70
		3	0.15	0.03	1.5					131	2879	3010	193	2816	0.93	1.31	3.09
		4	0.15	0.03	1.5					132	2924	3056	195	2861	0.94	1.31	3.09
DC	2	1	0.17	0.00	1.7	7.0	287	361	648	136	4167	4303	185	5849	1.72	1.09	3.93
		2	0.16	0.05	1.7					143	3236	3378	184	3672	1.82	1.07	3.69
		3	0.17	0.01	1.8					121	3187	3308	215	6069	1.85	1.09	3.30
		4	0.17	0.01	1.8					120	3193	3313	218	6161	1.85	1.09	3.27
DC	3	1	0.16	0.01	1.6	8.6	178	413	591	132	6190	6322	213	4090	1.97	1.11	3.30
		2	0.51	0.11	3.8					152	5529	5680	209	3169	1.73	1.11	3.57
		3	0.16	0.04	1.6					105	5534	5639	189	3119	1.34	1.11	3.25
		4	0.16	0.04	1.6					103	5546	5649	186	3127	1.31	1.11	3.23
DC	4	1	0.18	0.01	1.6	6.9	129	440	569	149	4688	4837	175	5709	1.62	1.09	3.31
		2	0.27	0.14	2.3					162	3216	3378	202	4325	1.93	1.07	2.88
		3	0.16	0.01	1.5					142	3688	3830	137	5882	1.68	1.09	3.33
		4	0.16	0.02	1.5					143	3736	3879	136	5906	1.68	1.09	3.32
DC	5	1	0.18	0.03	1.7	7.4	99	492	592	146	5917	6063	199	6123	1.23	1.23	3.13
		2	0.29	0.16	2.6					165	4707	4873	221	5459	1.52	1.21	2.83
		3	0.15	0.06	1.6					129	4126	4255	166	5473	1.20	1.22	3.17
		4	0.15	0.05	1.6					129	4148	4277	164	5485	1.17	1.22	3.17
NDC	1	1	1.65	0.01	9.6	28.1	199	349	548	127	5907	6034	216	4444	1.67	1.13	3.65
		2	1.26	0.01	7.5					139	3718	3857	214	2115	1.59	1.11	3.73
		3	1.03	0.01	6.2					147	6137	6284	222	4072	1.81	1.13	3.77
		4	0.76	0.01	4.8					149	6229	6378	227	4102	1.84	1.13	3.78
NDC	2	1	0.68	0.02	4.2	24.3	207	339	546	117	5767	5884	205	4632	1.21	1.27	3.55
		2	1.22	0.00	7.2					145	4382	4527	172	3206	0.78	1.26	3.84
		3	1.13	0.01	6.7					85	5934	6019	206	3624	1.23	1.26	3.61
		4	1.02	0.01	6.1					84	5959	6043	208	3671	1.22	1.26	3.61
NDC	3	1	0.99	0.02	6.1	27.3	185	360	545	152	4509	4660	225	5508	1.81	1.05	3.64
		2	0.75	0.01	4.6					157	2173	2330	233	3424	2.24	1.02	3.54
		3	1.5	0.03	8.9					153	4141	4294	221	5532	2.01	1.05	3.78
		4	1.3	0.02	7.7					155	4174	4329	223	5563	2.00	1.05	3.80
NDC	4	1	1.05	0.02	6.3	22.5	227	327	554	147	5585	5733	186	5878	0.91	1.38	3.70
		2	0.7	0.02	4.5					154	3503	3657	172	4701	0.62	1.37	4.11
		3	0.42	0.03	2.8					138	5614	5752	190	4066	0.96	1.37	3.90
		4	1.5	0.03	8.9					138	5648	5786	188	4089	0.96	1.37	3.89
NDC	5	1	1.31	0.02	7.7	21.5	218	319	537	153	6309	6462	224	6238	1.81	1.06	3.70
		2	1.04	0.02	6.3					161	4946	5107	231	4876	2.18	1.04	4.06
		3	0.71	0.01	4.5					150	6335	6485	220	6265	1.62	1.06	3.52
		4	0.45	0.02	3.0					150	6446	6596	221	6375	1.68	1.06	3.58

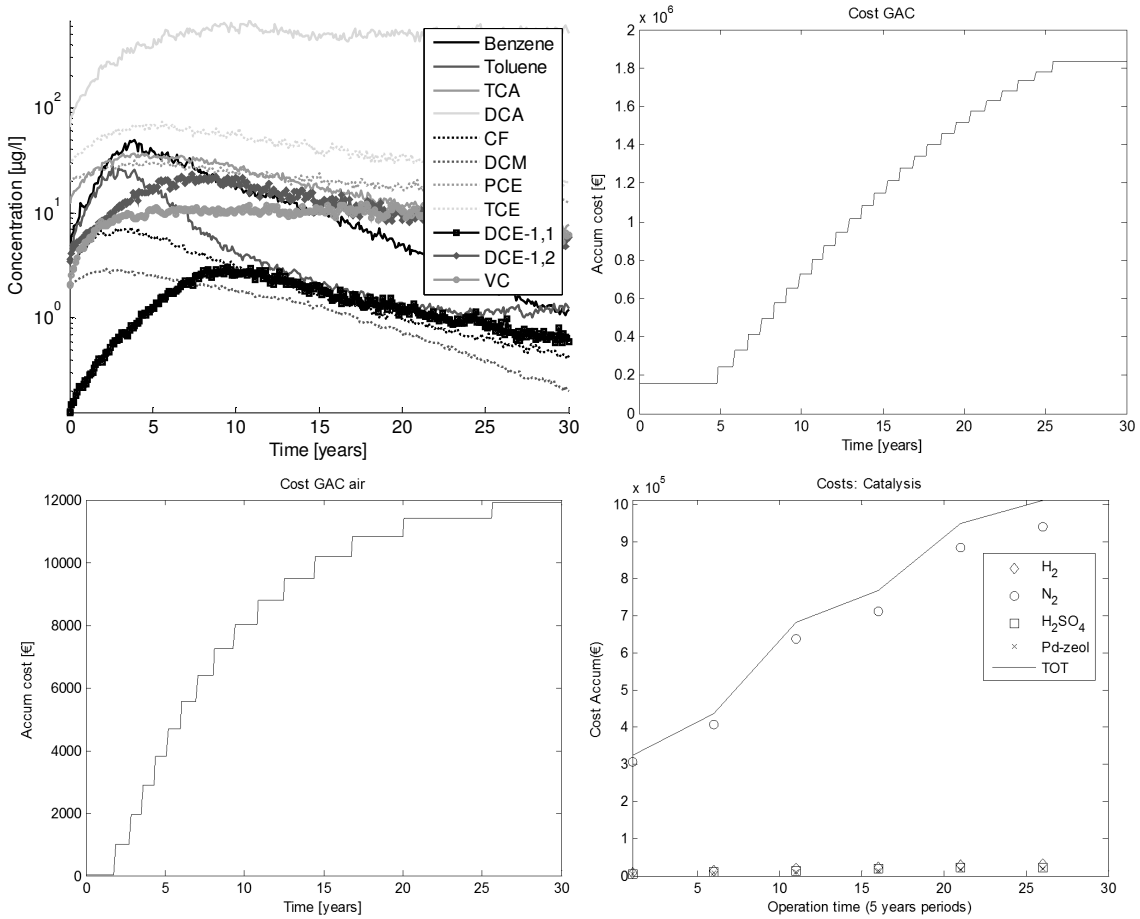

Figure 4.12 the breakthrough curves for the 11 COCs and the corresponding water treatment cost during the 30 years operation period

The following general remarks can be drawn from the results of the 10 ORs:

- The pumping rate for the DC tends to be higher than NDC
- No specific scenario tends to be more cost demanding than others
- Cost deviation between scenarios for a single OR ranges from € 1.3E5 (NDC-OR1) to €6.7E5 (DC-OR2) with an average of €3.8E5 for the 10 ORs
- Significant cost reduction is achieved by the DC (average cost € 3.23±0.27 million) compared to the NDC (average cost € 3.89±0.15 million)

A quantitative compression for the mean values using one way ANOVA for different ORs and cost variables is shown in Figure 4.13. The P-values for the technical variables approach zero for CCC [-] and Q [m^3/day] indicating a significant difference between the data means, and 0.01 for TR [-] indicating a slight increase in the TR mean for the DC data over the NDC. This slight difference in TR and significant difference in pumping rate is not surprising. Having the CCC as an additional constraint is overcome by increasing the pumping rate and by slightly scarifying the TR, which has less weight in the objective function.

The clear improvement in the CCC for the DC over the NDC is reflected in a significant improvement in the total cost. The P-values approach zero for all cost variables.

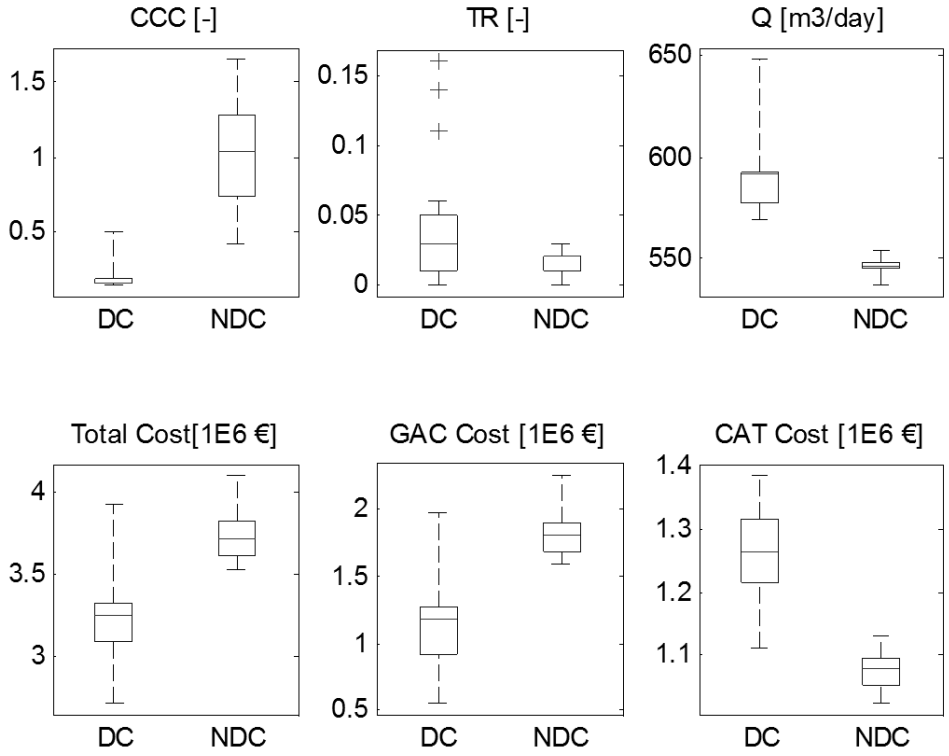

Figure 4.13 Case 7 GSA-DC and Case 8 GSA-NDC: main trends in the DC and NDC cases.

The box plots for the one way ANOVA illustrate that the total PTS cost positively correlate with the GAC treatment unit cost and negatively correlate with the CAT treatment unit cost. This relationship is further investigated by performing a cost breakdown for the major components of the PTS. The PTS can be divided into three main components, which are the Pumping Wells (PW), GAC Unit and CAT Unit. The cost of each of these components can be further sub-divided into investment costs and running costs. The ratios of the major cost items of the PTS are presented in Figure 4.14.

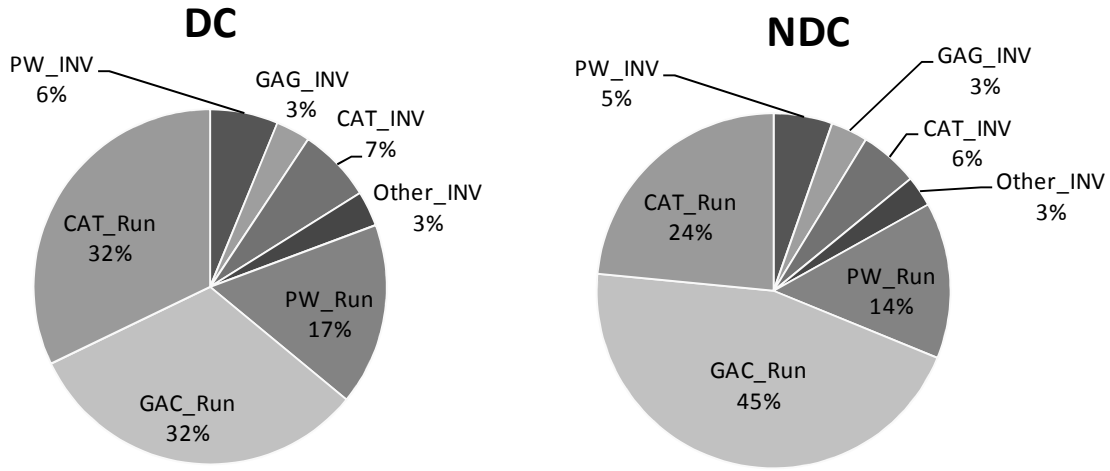

Figure 4.14 Case 7 GSA-DC and Case 8 GSA-NDC: pie chart for the main cost variables

The pie chart in Figure 4.14 indicates that the investment costs for both DC and NDC are similar, and that the major variables are the running costs of the GAC and CAT units. Ratios presented in Figure 4.14 are prepared based on average values for the 5 ORs for each of the DC and NDC cases. Taking the range of these cost items over all the ORs, it is clear that this range is highly variable from one cost item to another. PW investment and running costs and CAT investment cost is almost constant among all the ORs. The GAC investment cost and CAT running cost is moderately variable. The running cost of the GAC is highly variable with more than fourfold increase between the ORs. Table 4.11 summarizes the ranges of the major cost items of the PTS.

Table 4.11 Case 7 GSA-DC and Case 8 GSA-NDC: Cost breakdown showing the ranges of the investment and running costs for the main PTS components

Cost Breakdown [million €]		Investment Cost					Running Cost				
		PW	GAC Unit	CAT Unit	Other	Sub-total	PW	GAC Unit	CAT Unit	Sub-total	Total
DC	Min	0.20	0.08	0.21	0.10	0.61	0.54	0.47	0.90	2.10	2.70
	Mean	0.20	0.10	0.22	0.10	0.62	0.54	1.03	1.04	2.60	3.23
	Max	0.20	0.14	0.22	0.11	0.66	0.54	1.83	1.16	3.28	3.93
NDC	Min	0.20	0.12	0.20	0.10	0.62	0.53	1.48	0.82	2.89	3.52
	Mean	0.20	0.13	0.20	0.11	0.63	0.53	1.70	0.88	3.11	3.74
	Max	0.20	0.13	0.21	0.11	0.64	0.54	2.11	0.92	3.47	4.11

From the above analysis it is clear that the major cost components are the running cost of the GAC and CAT treatment units with the GAC being highly variable over the different ORs, while the CAT is relatively constant. Thus the running cost of the GAC treatment unit is the most variable component and the main cost driver of the system.

Based on the obtained results the following remarks are drawn:

- The CAT treatment is relatively concentration independent, since the major cost item in the CAT unit is N_2 as shown in Figure 4.12, which correlates with the flow rate rather than the concentration. On the other hand, GAC treatment is concentration dependent
- GAC unit shows very high treatment costs for significantly smaller contamination loads than the CAT unit
- GAC air filter responsible for treating the BTEX and residual CHC contaminations in the CAT current is more cost efficient than the GAC aqueous unit because the Freundlich coefficients for the liquid phase are lower than the gas phase. For example, benzene has Freundlich coefficient in the air phase kf =281 $(mg/g)(L/mg)^{0.25}$ compared to kf =16.6 $(mg/g)(L/mg)^{0.4}$ in the liquid phase

Accordingly, it is expected that decreasing the flow rates and contamination loads going to the GAC unit will result in significant cost reduction. The same applies for decreasing the volumetric flow rate to the CAT unit. These remarks are verified by performing a direct cost optimization, in which the optimization automatically selects between the entire interrelated variable.

4.5 Comparison between Indirect and Direct Cost Optimization

In this comparison the optimization configuration of Case 10 indirect cost optimization (IDCO) and Case 11 direct cost (DCO) as shown in Table 1.1 are used. DCO strategy gives the optimization search the freedom to automatically select between different variables in the system in order to satisfy a single objective, which is the cost in this case, subject to some constraints. Eleven ORs are performed for each case in order to obtain statistically representative results. The results of the two cases are shown in Table 4.12.

Table 4.12 Case 10 IDCO and Case 11 DCO: Results of the 11 ORs of each case

Optimization Run				Optimization Result			Pumping Rate [m3/day]			Removed Mass [%]			Treated Mass [%]		Cost [€ 1E6]			
Case	Sc	OR	Gen	CCC	TR	Fitness	GAC	CAT	Total	BTEX	CHC	Total	GAC	CAT	PW	GAC	CAT	Total
IDCO	1	1	335	0.14	0.01	1078	98	357	455	0.4	17.2	17.6	0.7	16.97	0.73	1.05	1.13	3.00
IDCO	1	2	356	0.14	0.02	1070	98	353	451	0.5	8.4	8.8	0.6	8.20	0.73	1.11	1.06	2.99
IDCO	1	3	399	0.14	0.01	1079	110	341	451	0.5	19.1	19.5	0.6	18.88	0.73	1.18	1.09	3.10
IDCO	1	4	305	0.14	0.01	1073	109	341	450	0.4	17.4	17.9	0.7	17.24	0.73	1.17	1.07	3.06
IDCO	1	5	327	0.14	0.02	1126	146	317	463	0.4	18.8	19.2	0.6	18.56	0.73	1.57	1.08	3.48
IDCO	1	6	332	0.14	0.02	1082	114	338	451	0.4	11.3	11.7	0.6	11.05	0.73	1.24	1.06	3.13
IDCO	1	7	298	0.14	0.02	1110	137	325	463	0.5	6.5	6.9	0.7	6.25	0.73	1.45	1.01	3.29
IDCO	1	8	410	0.14	0.02	1108	123	329	451	0.4	18.4	18.9	0.6	18.24	0.73	1.17	1.07	3.06
IDCO	1	9	346	0.14	0.02	1106	120	342	462	0.5	13.7	14.1	0.6	13.49	0.73	1.18	1.07	3.08
IDCO	1	10	242	0.14	0.02	1118	128	333	461	0.4	18.6	19.1	0.6	18.44	0.73	1.33	1.09	3.25
IDCO	1	11	326	0.14	0.01	1088	126	327	453	0.4	9.9	10.4	0.6	9.74	0.73	1.20	1.03	3.05
DCO	1	1	199	0.77	0.04	5114	207	366	574	0.2	1.6	1.8	0.1	1.75	0.74	0.15	1.07	2.06
DCO	1	2	400	1.02	0.05	5791	96	410	506	0.4	11.3	11.7	0.1	11.67	0.73	0.15	1.18	2.16
DCO	1	3	258	1.82	0.04	10900	104	452	557	0.4	6.0	6.4	0.2	6.29	0.74	0.15	1.26	2.24
DCO	1	4	217	0.73	0.04	4030	24	450	473	0.4	5.0	5.4	0.0	5.41	0.73	0.10	1.26	2.18
DCO	1	5	332	0.87	0.05	5757	241	336	577	0.3	1.5	1.7	0.1	1.61	0.74	0.15	1.00	1.99
DCO	1	6	394	0.99	0.04	5143	0	461	461	0.4	1.5	1.9	0.0	1.91	0.65	0.00	1.24	1.98
DCO	1	7	252	0.29	0.01	2356	298	297	595	0.4	3.5	3.9	0.5	3.38	0.74	0.26	0.97	2.06
DCO	1	8	274	0.60	0.04	3271	0	459	459	0.4	1.4	1.8	0.0	1.81	0.65	0.00	1.24	1.98
DCO	1	9	306	1.44	0.04	8463	167	369	536	0.3	2.4	2.8	0.1	2.73	0.73	0.14	1.08	2.05
DCO	1	10	247	1.61	0.04	8890	94	416	510	0.2	4.0	4.1	0.1	4.01	0.73	0.14	1.17	2.13
DCO	1	11	332	1.28	0.04	7281	121	395	516	0.4	3.3	3.7	0.1	3.56	0.73	0.14	1.14	2.10
Minimum			199	0.14	0.01	1070	0	297	450	0.2	1.4	1.7	0.0	1.61	0.65	0.00	0.97	1.98
Median			327	0.22	0.02	1741	117	348	462	0.4	7.4	7.9	0.6	7.24	0.73	0.65	1.08	2.61
Mean			313	0.59	0.03	3592	121	369	490	0.4	9.1	9.5	0.4	9.1	0.72	0.68	1.11	2.61
Maximum			410	1.82	0.05	10900	298	461	595	0.5	19.1	19.5	0.7	18.88	0.74	1.57	1.26	3.48

A significant reduction in the total cost from € 3.14± 0.10 million (IDCO) to € 2.08± 0.06 million (DCO) accompanied by a decrease in the total removed mass from 15± 3% (IDCO) to 4± 2% (DCO) is obvious. The results clearly show that the DCO strategy shows significant cost reduction compared to the IDCO strategy due to the decrease in the total mass treated by the GAC unit. To get a more rigorous view a quantitative compression for the main variable using one way ANOVA is conducted as shown in Figure 4.15.

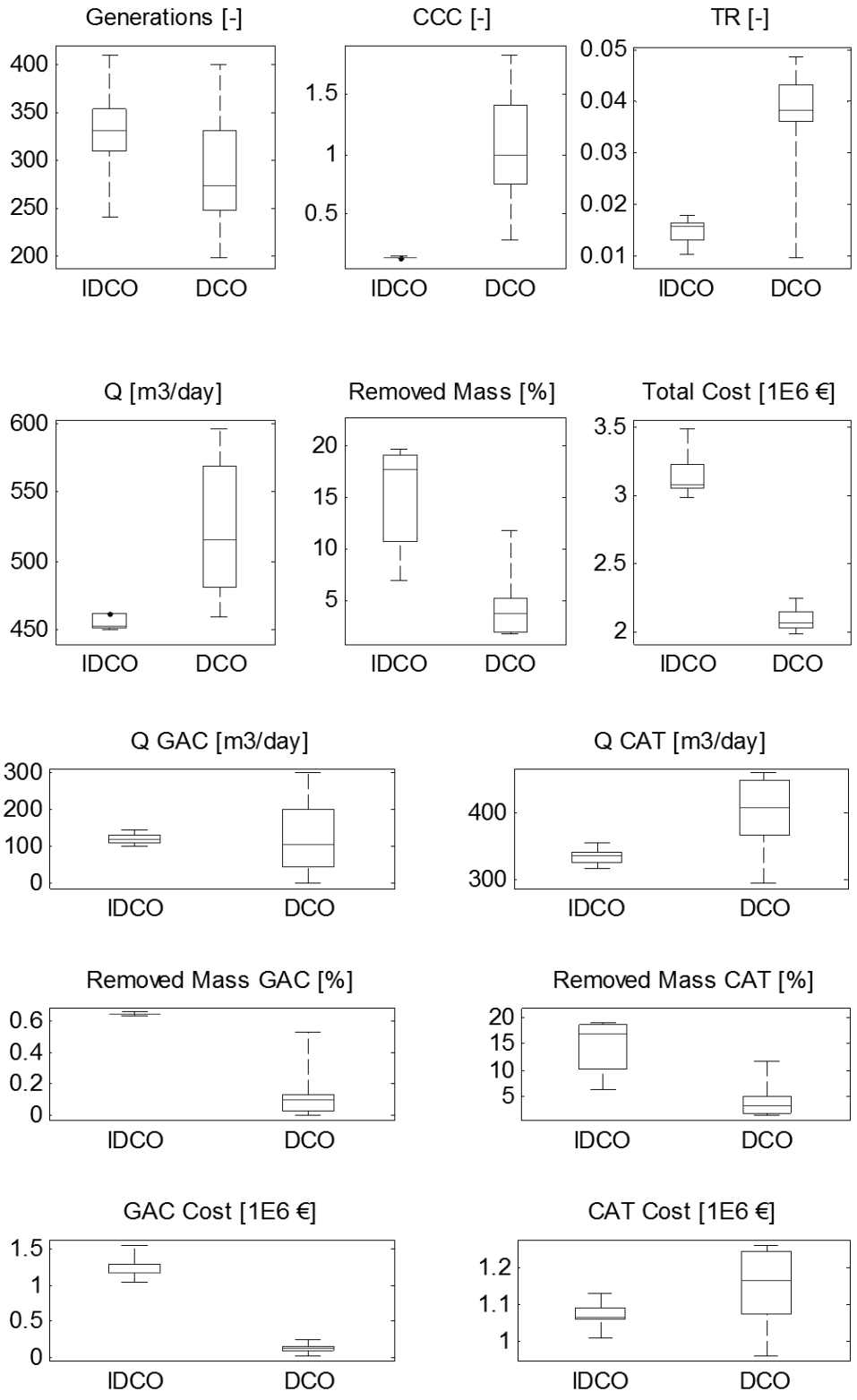

Figure 4.15 Case 10 IDCO and Case 11 DCO: Main trends

The following general trends can be observed from the results:

- For both the IDCO and DCO similar number of generations are required to reach the stopping criterion with the DCO showing slightly less number of iterations
- CCC does not correlate with cost because DCO implements a different strategy for reaching the optimal solution. The DCO tends to decrease the concentration in the water current going to the GAC unit, and decrease the overall extracted mass. Accordingly, the adverse effect resulting from the mixing of the two classes of contaminants becomes less significant. In other words, the concentrations in the BTEX current and the amount of extracted mass, has more impact on the total cost than the CCC (i.e. the degree of separation of the two contaminant types)
- Q for DCO strategy is 524±32 m^3day compared to 455±4 m^3/day for IDCO strategy. This is mainly because the PW cost is less significant cost item (i.e. range over all the ORs from €6.5E5 to 7.4E5) compared to the treatment cost. In other words, the attempt of the DCO strategy to decrease the contaminant concentrations going to the GAC unit is done on the expense of the pumping rate

The DCO strategy does not only show a tendency to decrease concentrations in the GAC current but rather to eliminate the GAC unit at all. This point is further analyzed by studying the correlation between the costs of the GAC and CAT units with the major optimization variables, which are volumetric flow to each treatment unit (i.e. Q_{GAC} and Q_{CAT}), the amount of treated mass by each unit and the removed mass for each class of contaminants. The correlation coefficients are shown in Table 4.13.

Table 4.13 Case 11 DCO: Correlation coefficients for the main optimization variables correlated with costs of the GAC and CAT units

Cost [€]	Q[m^3/day]		Treated Mass [%]		Removed Mass [%]	
	GAC	CAT	GAC	CAT	BTEX	CHC
GAC Unit	-0.1	-	0.9	-	0.5	0.8
CAT Unit	-	0.9	-	-0.2	-0.1	-0.1

As expected, the correlation coefficients in Table 4.13 confirm the same remarks observed in the previous sections, which can be summarized as follows:

- GAC unit cost is insensitive to volumetric water flow to the unit Q_{GAC} [m^3/day], but rather it correlates with the concentration (correlation coefficient of 0.9)
- CAT unit cost correlates with the Q_{CAT} (correlation coefficient 0.9) and is concentration independent (correlation coefficient -0.2)
- 1,2-DCA , which dominates the CHC current, has a liquid phase Freundlich coefficient *kf* of 5.12 $(mg/g)(L/mg)^{0.53}$, which is lower than benzene being 16.6 $(mg/g)(L/mg)^{0.4}$ and toluene being 97 $(mg/g)(L/mg)^{0.43}$, and thus treating BTEX by GAC is more cost efficient than CHC. Accordingly, the GAC unit cost is more sensitive to the CHC concentration (correlation coefficient 0.8).

5 Conclusion and Recommendations

According to Becker et al. (2006), based on competitive bids the cost of applying the simulation-optimization methods are between $40,000 and $120,000, including site visits, report generation and project management, which is conducted over a period of approximately 4 months. Still applying S/O is valuable, since the potential savings easily exceeds their cost (Zheng and Wang, 2002). Having in mind that time and money are the two constraints that restrict the effort an engineer can spend on a design, a general aim of research in this area is to develop practical methods capable of finding reliable and cost efficient solutions. Several topics are discussed in this thesis to develop robust and computationally efficient design optimization method for ground water remediation systems for complex real world plumes, which can be readily and efficiently applied on an average desktop computer.

The first objective of this thesis is to develop a practical stopping criterion. The built-in scaled stopping criterion VSP, which does not has a practical meaning a priori, is normalized to this real variable stopping criterion. This shall save unnecessary computations and allow the search to stop at the desired accuracy level.

A second topic, which addresses the number of individuals per generations, shows that a higher population size enhances the global search capacity, and thus allows the algorithm to converge to a better solution compared to the default population size. Yet this is accompanied by extra computations. To decrease the computational burden it is recommended to incorporate an adaptive artificial neural network algorithm (e.g. Yan and Minsker, 2006) or recursive function (e.g. Zheng and Wang, 2002), which act as surrogate for the time consuming flow or transport models. In addition, a novel algorithm reported as non-revisiting (Yen and Chow, 2009), which remember every position it searched and has a novel non-parameter adaptive mutation operator, shows a superior performance over CMA-ES. It is recommended to compare this algorithm with CMA-ES to assess if it shows significant improvements in terms of the computational time or search capacity for a real world complex problem with large search space and dimensions as this one.

The constraints that control the state variables for the advective control formulation developed by Lantschner (2005) is complimented in this study be developing an additional constraint. Adding the time of contaminant migration in ground water as an additional constraint in the objective function insures that not only the plume is captured, but also the capture zone is restricted to the site premise. A specific degree of containment can also be predefined. The result shows that using the contaminants travel time ratio outside and inside the site premise is adequate for the task, and is effectively formulated.

Hilton and Culver (2005) and Ko and Lee (2009) are two studies that compare the deterministic and scholastic approaches used to account for uncertainty. While the formal study concludes that either homogenous or heterogeneous deterministic aquifer description results in significant underdesign and poor remediation performance, the later study concludes that deterministic optimization approach is viable enough to design reliable remediation strategies. In any case, it is obvious that lack of data often constitutes a major limitation that ultimately may produce an over designed system, and/or a certain degree of non-compliance. Accordingly, in the presence of uncertain parameters it is recommended to incorporate in advance the value of data into the

optimal design of the PTS as proposed by Bau and Mayer (2007). Anyway, this is not possible in this case study, since the site investigation has already been carried out.

To make the best out of the available data, uncertainty is tackled deterministically by two approaches, which are ISA (i.e. critical scenarios) or GSA (i.e. robust configuration). Critical scenarios are these scenarios that present more challenges for the candidate well configurations. The result shows that critical scenarios can be simply identified, since they positively correlate with the OF value. Accordingly, to save the computational effort the optimization instead of running on all scenarios it can only run on the critical scenario. The candidate well configuration can then be post-processed on any number of scenarios. On the other hand, a more conservative approach will be the GSA. Through incorporating data from several scenarios, one robust configuration that successfully performs on all the scenarios is identified. Generally, GSA proposes more robust candidates than ISA, yet this also could imply overdesign. Either way, this deterministic method for addressing uncertainty can still be further enhanced by incorporating a method proposed by Lee and Kitanidis (1991), which under limited data, can still express uncertainty by deterministic and stochastic control terms.

The concept of disjoint capture developed by Finkel et al. (2008) is further assessed in this study. The results show that the concept is generally valid, and can produce more cost efficient solutions over non-differentiated capture technique with mean cost being €3.23±0.27 millions for DC and €3.89±0.15 millions for NDC. However, this concept is unsuitable for this case due to the physiochemical properties of contaminates as shown by the comparison between the IDCO and DCO strategies.

The fifth and the last objective of this thesis is to compare the IDCO strategy, which is stepwise procedure consisting of technical optimization followed by economic assessment of the feasible solution, while the DCO strategy that is a one-step full economic optimization. With a mean cost of €2.08±0.06 millions, the DCO strategy shows a substantial cost savings over the IDCO, which has a mean cost of 3.13±0.10 millions.

This large difference in cost between the IDCO and DCO strategies can be explained by looking at the used treatment units, which are the GAC aqueous unit and CAT unit (PCR-MBS followed by GAC air filter). The results show that these two treatment units are controlled by two main factors. Firstly, while the cost of the GAC units (i.e. aqueous unit and air filter) is concentration dependent, the cost of the PCR-MBS is flow dependent. Secondly, GAC aqueous unit shows significantly higher treatment costs over the GAC air filter, due to the lower Freundlich coefficients of the treated compounds for the liquid phase compared to the gas phase. Having these two factors in mind it is clear that the optimization shall increase the volumetric flow rate and decrease the contaminant concentrations for the GAC unit current, and decrease the volumetric flow rate in the CAT unit current. Such objective cannot be formulated through practical tracking alone. This shows that the incorporation of the time consuming transport simulation is inevitable in this case

In addition, some ORs especially those that presented the lowest costs tend to eliminate at all the GAC unit. Thus, it is recommended to conduct several ORs with CAT unit only and compare them with the results of Case 11 (i.e. DCO with GAC & CAT units). This might not only reduce the cost, but also decrease the problem complexity. Also, the PTSDC code can be

modified to mix the water coming from different wells in a way that reduces the concentrations below the MCLs for certain group of wells to be directly discharge without treatment, and the remaining water can then be sent to the CAT unit. This shall decrease the treatment cost since cost of the CAT unit positively correlate with the volumetric flow rate.

In this study the management strategy is not to achieve a complete aquifer restoration, but rather to hydraulically contain the contaminants within the site premise at the minimum possible cost. However, since CAT unit is relatively concentration independent, higher concentration can be extracted without any significant increase in cost. For example, 5 ORs are conducted with similar settings as Case 11 except that the contaminants extraction rate for the 30 year design period is set to be at least 17% of the total mass initially present[2]. The mean cost for these ORs is found to be €2.19±0.12 millions, which does not differ significantly from Case 11, which has a mean cost of €2.08±0.06 millions for a mass removal rate of 4± 2%. Thus, it is recommended to incorporated Niched Pareto algorithm (e.g. Erickson et al. 2002), which can generate trade-off curve between mass removal rates and cost of the PTS. In addition, if the management strategy shifted towards aquifer restoration instead of only contaminants containment, then the treatment system can be supplemented with enhanced natural attenuation (Park et al. 2007).

It should be clear that the objective of this study is to compare between different concepts in order to improve the problem formulation, and not to recommend a final solution. Accordingly, several ORs are carried out for each case in order to get the main statistical feature of the task under study. The next step is to recommend a final well configuration to be implemented. This later point is not discussed in this thesis. Freeze et al. (1990) proposes a decision analysis framework, which is further developed by Russell and Rabideau (2000) to facilitate such selection process. Hence, it is recommended to continue this work by incorporating a reliability analysis that defines the probability and cost of failure in order to have a guided method for the selection between the different candidate solutions of the several ORs.

[2] The result is presented in the Annex (Table A.6)

6 References

Ahlfeld, D. P., R. H. Page, and G. F. Pinder (1995), OPTIMAL GROUNDWATER REMEDIATION METHODS APPLIED TO A SUPERFUND SITE - FROM FORMULATION TO IMPLEMENTATION, *Ground Water*, *33*(1), 58-70.

Aksoy, A., and T. B. Culver (2004), Impacts of physical and chemical heterogeneities on aquifer remediation design, *Journal of Water Resources Planning and Management-Asce*, *130*(4), 311-320.

Aly, A. H., and R. C. Peralta (1999), Optimal design of aquifer cleanup systems under uncertainty using a neural network and a genetic algorithm, *Water Resources Research*, *35*(8), 2523-2532.

Ayvaz, M. T., and H. Karahan (2008), A simulation/optimization model for the identification of unknown groundwater well locations and pumping rates, *Journal of Hydrology*, *357*(1-2), 76-92.

Babbar, M., and B. S. Minsker (2006), Groundwater remediation design using multiscale genetic algorithms, *Journal of Water Resources Planning and Management-Asce*, *132*(5), 341-350.

Bau, D. A., and A. S. Mayer (2007), Data-worth analysis for multiobjective optimal design of pump-and-treat remediation systems, *Advances in Water Resources*, *30*(8), 1815-1830.

Bau, D. A., and A. S. Mayer (2008), Optimal design of pump-and-treat systems under uncertain hydraulic conductivity and plume distribution, *Journal of Contaminant Hydrology*, *100*(1-2), 30-46.

Bayer, P., and M. Finkel (2004), Evolutionary algorithms for the optimization of advective control of contaminated aquifer zones, *Water Resources Research*, *40*(6).

Bayer, P., and M. Finkel (2007), Optimization of concentration control by evolution strategies: Formulation, application, and assessment of remedial solutions, *Water Resources Research*, *43*(2).

Bayer, P., C. M. Burger, and M. Finkel (2008), Computationally efficient stochastic optimization using multiple realizations, *Advances in Water Resources*, *31*(2), 399-417.

Bayer, P., E. Duran, R. Baumann, and M. Finkel (2009), Optimized groundwater drawdown in a subsiding urban mining area, *Journal of Hydrology*, *365*(1-2), 95-104.

Bear, J., and Y. W. Sun (1998), Optimization of pump-treat-inject (PTI) design for the remediation of a contaminated aquifer: multi-stage design with chance constraints, *Journal of Contaminant Hydrology*, *29*(3), 225-244.

Becker, D., B. Minsker, R. Greenwald, Y. Zhang, K. Harre, K. Yager, C. M. Zheng, and R. Peralta (2006), Reducing long-term remedial costs by transport modeling optimization, *Ground Water*, *44*(6), 864-875.

Beyer, H. G., and B. Sendhoff (2007), Robust optimization - A comprehensive survey, *Computer Methods in Applied Mechanics and Engineering*, *196*(33-34), 3190-3218.

Chang, L. C., C. A. Shoemaker, and P. L. F. Liu (1992), OPTIMAL TIME-VARYING PUMPING RATES FOR GROUNDWATER REMEDIATION - APPLICATION OF A CONSTRAINED OPTIMAL-CONTROL ALGORITHM, *Water Resources Research*, *28*(12), 3157-3173.

Chang, L. C., H. J. Chu, and C. T. Hsiao (2007), Optimal planning of a dynamic pump-treat-inject groundwater remediation system, *Journal of Hydrology*, *342*(3-4), 295-304.

Chu, H. J., and L. C. Chang (2009), Application of Optimal Control and Fuzzy Theory for Dynamic Groundwater Remediation Design, *Water Resources Management*, *23*(4), 647-660.

Chu, H. J., C. T. Hsiao, and L. C. Chang (2005), Optimal remediation design in groundwater systems by intelligent techniques, *Knowledge-Based Intelligent Information and Engineering Systems, Pt 2, Proceedings*, *3682*, 628-634.

Culver, T. B., and C. A. Shoemaker (1992), DYNAMIC OPTIMAL-CONTROL FOR GROUNDWATER REMEDIATION WITH FLEXIBLE MANAGEMENT PERIODS, *Water Resources Research*, *28*(3), 629-641.

Cunha, M. D. (2002), Groundwater cleanup: The optimization perspective (a literature review), *Engineering Optimization*, *34*(6), 689-702.

Endres, K. L., A. Mayer, and D. W. Hand (2007), Equilibrium versus nonequilibrium treatment modeling in the optimal design of pump-and-treat groundwater remediation systems, *Journal of Environmental Engineering-Asce*, *133*(8), 809-818.

Erickson, M., A. Mayer, and J. Horn (2002), Multi-objective optimal design of groundwater remediation systems: application of the niched Pareto genetic algorithm (NPGA), *Advances in Water Resources*, *25*(1), 51-65.

Espinoza, F. P., and B. S. Minsker (2006), Effects of local search algorithms on groundwater remediation optimization using a self-adaptive hybrid genetic algorithm, *Journal of Computing in Civil Engineering*, *20*(6), 420-430.

Finkel, M., H. Schad, P. Bayer and L. Lantschner (2008), Disjoined capture and treatment of multiple contaminant plumes in groundwater to improve cost efficiency of remediation. In: Groundwater Quality: Securing Groundwater Quality in Urban and Industrial Environments.- IAHS Publ. no. 324, 94-101.

Fowler, K. R., et al. (2008), Comparison of derivative-free optimization methods for groundwater supply and hydraulic capture community problems, *Advances in Water Resources*, *31*(5), 743-757.

Freeze, R.A, J. Massmann, L. Smith,T. Sperling, and B. James (1990), HYDROGEOLOGICAL DECISION-ANALYSIS .1. A FRAMEWORK, *Ground Water*, *28*(5), 739-766.

Guan, J., and M. M. Aral (1999), Optimal remediation with well locations and pumping rates

selected as continuous decision variables, *Journal of Hydrology*, *221*(1-2), 20-42.

Guan, J. B., and M. M. Aral (2005), Remediation system design with multiple uncertain parameters using fuzzy sets and genetic algorithm, *Journal of Hydrologic Engineering*, *10*(5), 386-394.

Guo, X., C. M. Zhang, and J. C. Borthwick (2007), Successive equimarginal approach for optimal design of a pump and treat, *Water Resources Research*, *43*(8).

Gorelick, S.M. (1987), Sensitivity analysis of optimal groundwater contaminant capture curves: spatial variability and robust solutions, in: Proceedings of the Solving Ground Water Problems with Models Conference, National Water Well Association, Denver, CO, 1987.

Hansen, N. (2006), The CMA evolution strategy: A comparing review, in Towards a New Evolutionary Computation: Advances in Estimation of Distribution Algorithms, edited by J. A. Lozano et al. pp. 75-102, Springer, New York.

Hansen, N., S.D. Mueller, and P. Koumoutsakos (2003), Reducing the time complexity of the derandomized evolution strategy with covariance matrix adaptation (CMA-ES), Evolutionary Computation 11, 1-18.

Hansen, N. and A. Ostermeier (2001), Completely derandomized self-adaptation in evolution strategies, Evolutionary Computation 9, 159-195.

He, L., G. H. Huang, and H. W. Lu (2009), A coupled simulation-optimization approach for groundwater remediation design under uncertainty: An application to a petroleum-contaminated site, *Environmental Pollution*, *157*(8-9), 2485-2492.

He, L., G. H. Huang, G. M. Zeng, and H. W. Lu (2008a), An integrated simulation, inference, and optimization method for identifying groundwater remediation strategies at petroleum-contaminated aquifers in western Canada, *Water Research*, *42*(10-11), 2629-2639.

He, L., G. H. Huang, H. W. Lu, and G. M. Zeng (2008b), Optimization of surfactant-enhanced aquifer remediation for a laboratory BTEX system under parameter uncertainty, *Environmental Science & Technology*, *42*(6), 2009-2014.

Herke HH, U. Hornung, Y. Kelanemer, M. Slodicka, S. Schumacher (1999), Optimal control of soil venting: mathematical modeling and applications. Basel, Switzerland: Birkhauser

Hilton, A. B. C., and T. B. Culver (2000), Constraint handling for genetic algorithms in optimal remediation design, *Journal of Water Resources Planning and Management-Asce*, *126*(3), 128-137.

Hilton, A. B. C., and T. B. Culver (2005), Groundwater remediation design under uncertainty using genetic algorithms, *Journal of Water Resources Planning and Management-Asce*, *131*(1), 25-34.

Huang, C. L., and A. S. Mayer (1997), Pump-and-treat optimization using well locations and pumping rates as decision variables, *Water Resources Research*, *33*(5), 1001-1012.

IMES GmbH (2003), Feasibility Study of alternative clean-up strategies for a groundwater contamination at the site, in cooperation with the University of Tübingen and Prantner Verfahrenstechnik GmbH.

Kalwij, I. M., and R. C. Peralta (2006), Simulation/optimization modeling for robust pumping strategy design, *Ground Water*, *44*(4), 574-582.

Khan, F. I., T. Husain, and R. Hejazi (2004), An overview and analysis of site remediation technologies, *Journal of Environmental Management*, *71*(2), 95-122.

Ko, N. Y., and K. K. Lee (2008), Reliability and remediation cost of optimal remediation design considering uncertainty in aquifer parameters, *Journal of Water Resources Planning and Management-Asce*, *134*(5), 413-421.

Ko, N. Y., and K. K. Lee (2009), Convergence of deterministic and stochastic approaches in optimal remediation design of a contaminated aquifer, *Stochastic Environmental Research and Risk Assessment*, *23*(3), 309-318.

Ko, N. Y., K. K. Lee, and Y. Hyun (2005), Optimal groundwater remediation design of a pump and treat system considering clean-up time, *Geosciences Journal*, *9*(1), 23-31.

Kobayashi, K., R. Hinkelmann, and R. Helmig (2008), Development of a simulation-optimization model for multiphase systems in the subsurface: a challenge to real-world simulation-optimization, *Journal of Hydroinformatics*, *10*(2), 139-152.

Kourakos, G., and A. Mantoglou (2008), Remediation of heterogeneous aquifers based on multiobjective optimization and adaptive determination of critical realizations, *Water Resources Research*, *44*(12).

Kourakos, G., and A. Mantoglou (2009), Pumping optimization of coastal aquifers based on evolutionary algorithms and surrogate modular neural network models, *Advances in Water Resources*, *32*(4), 507-521.

Lantschner, L. (2005), Cost-efficient remediation of multiple contaminant plumes using differentiated capture approach, M.Sc. Master Thesis,, Applied Environmental Geoscience, University of Tuebingen, Tuebingen.

Lee, S. I., and P. K. Kitanidis (1991), OPTIMAL ESTIMATION AND SCHEDULING IN AQUIFER REMEDIATION WITH INCOMPLETE INFORMATION, *Water Resources Research*, *27*(9), 2203-2217.

Liu, W. H., M. A. Medina, W. Thomann, W. T. Piver, and T. L. Jacobs (2000), Optimization of intermittent pumping schedules for aquifer remediation using a genetic algorithm, *Journal of the American Water Resources Association*, *36*(6), 1335-1348.

Mantoglou, A., and G. Kourakos (2007), Optimal groundwater remediation under uncertainty using multi-objective optimization, *Water Resources Management*, *21*(5), 835-847.

Marryott, R. A., D. E. Dougherty, and R. L. Stollar (1993), OPTIMAL GROUNDWATER-MANAGEMENT .2. APPLICATION OF SIMULATED ANNEALING TO A FIELD-SCALE CONTAMINATION SITE, *Water Resources Research*, *29*(4), 847-860.

Massmann, J., R. A. Freeze, L. Smith, T. Sperling, and B. James (1991), HYDROGEOLOGICAL DECISION-ANALYSIS .2. APPLICATIONS TO GROUNDWATER CONTAMINATION, *Ground Water*, *29*(4), 536-548.

Mayer, A. S., C. T. Kelley, and C. T. Miller (2002), Optimal design for problems involving flow and transport phenomena in saturated subsurface systems, *Advances in Water Resources*, *25*(8-12), 1233-1256.

McDonald, M.G. and A.W. Harbaugh (1988), A modular three-dimensional finite-difference ground water flow model. U.S. Geol. Surv. Tech. Water Resour. Invest., Book 6.

McKinney, D. C., and M. D. Lin (1996), Pump and treat ground-water remediation system optimization, *Journal of Water Resources Planning and Management-Asce*, *122*(2), 128-136.

Medina, M. A., T. L. Jacobs, W. C. Lin, and K. C. Lin (1996), Ground water solute transport, optimal remediation planning, and decision making under uncertainty, *Water Resources Bulletin*, *32*(1), 1-12.

Mulligan, A. E., and D. P. Ahlfeld (1999), Advective control of groundwater contaminant plumes: Model development and comparison to hydraulic control, *Water Resources Research*, *35*(8), 2285-2294.

Mulvey, J. M., R. J. Vanderbei, and S. A. Zenios (1995), ROBUST OPTIMIZATION OF LARGE-SCALE SYSTEMS, *Operations Research*, *43*(2), 264-281.

Ndambuki, J. M., F. A. O. Otieno, C. B. M. Stroet, and E. J. M. Veling (2000), Groundwater management under uncertainty: A multi-objective approach, *Water Sa*, *26*(1), 35-42.

Park, C. H., and M. M. Aral (2004), Multi-objective optimization of pumping rates and well placement in coastal aquifers, *Journal of Hydrology*, *290*(1-2), 80-99.

Park, D. K., N. Y. Ko, and K. K. Lee (2007), Optimal groundwater remediation design considering effects of natural attenuation processes: pumping strategy with enhanced-natural-attenuation, *Geosciences Journal*, *11*(4), 377-385.

Peralta, R. C., I. M. Kalwij, and S. J. Wu (2008), Practical remedial design optimization for large complex plumes, *Journal of Water Resources Planning and Management-Asce*, *134*(5), 422-431.

Pollock, D. W., (1994). User's Guide for MODPATH/MODPATH-PLOT, Version 3: A particle trackingp ost-processinpga ckagef or MODFLOW, the U.S. GeologicalS urveyf inite-differenceg roundwater flow model, U.S. Geol. Surv. Open File Rep., 94-464.

Qin, X. S., G. H. Huang, and L. He (2009), Simulation and optimization technologies for petroleum waste management and remediation process control, *Journal of Environmental Management*, *90*(1), 54-76.

Rana, T., S. Khan, and M. Rahimi (2008), Spatio-temporal optimisation of agricultural drainage using groundwater models and genetic algorithms: an example from the Murray Irrigation Area, Australia, *Hydrogeology Journal*, *16*(6), 1145-1157.

Ranjithan, S., J. W. Eheart, and J. H. Garrett (1993), NEURAL NETWORK BASED SCREENING FOR GROUNDWATER RECLAMATION UNDER UNCERTAINTY, *Water Resources Research*, *29*(3), 563-574.

Ren, X. L., and B. Minsker (2005), Which groundwater remediation objective is better: A realistic one or a simple one?, *Journal of Water Resources Planning and Management-Asce*, *131*(5), 351-361.

Ricciardi, K. L., G. F. Pinder, and G. P. Karatzas (2007), Efficient groundwater remediation system design subject to uncertainty using robust optimization, *Journal of Water Resources Planning and Management-Asce*, *133*(3), 253-263.

Rogers, L. L., F. U. Dowla, and V. M. Johnson (1995), OPTIMAL FIELD-SCALE GROUNDWATER REMEDIATION USING NEURAL NETWORKS AND THE GENETIC ALGORITHM, *Environmental Science & Technology*, *29*(5), 1145-1155.

Russell, K. T., and A. J. Rabideau (2000), Decision analysis for pump-and-treat design, *Ground Water Monitoring and Remediation*, *20*(3), 159-168.

U.S. EPA (2002), Pilot project to optimize superfund-finance pump and treat systems: Summary report and lessons learned. EPA/542/R-02/008A.

U.S. EPA (2004), Cleaning up the nation's waste sites: markets and technology trends, Washington D.C., U.S. EPA.

Schaerlaekens, J., J. Mertens, J. Van Linden, G. Vermeiren, J. Carmeliet, and J. Feyen (2006), A multi-objective optimization framework for surfactant-enhanced remediation of DNAPL contaminations, *Journal of Contaminant Hydrology*, *86*(3-4), 176-194.

Schueth, C. (2003), Application of innovative cleanup technologies alternative to pump-andtreat at the site, feasibility study report, Centre of Applied Geoscience, University of Tuebingen, Tuebingen

Schwefel, H.-P. (1995), Evolution and Optimum Seeking, John Wiley, Hoboken, N. J.

Singh, A., B. S. Minsker, and A. J. Valocchi (2008), An interactive multi-objective optimization

framework for groundwater inverse modeling, *Advances in Water Resources*, *31*(10), 1269-1283.

Sinha, E., and B. S. Minsker (2007), Multiscale island injection genetic algorithms for groundwater remediation, *Advances in Water Resources*, *30*(9), 1933-1942.

Testo Unico (2006), Decreto Legislativo recante Norme in material ambientale, 2006-03-29 TU (allegati).

Tiedeman, C., and S. M. Gorelick (1993), ANALYSIS OF UNCERTAINTY IN OPTIMAL GROUNDWATER CONTAMINANT CAPTURE DESIGN, *Water Resources Research*, *29*(7), 2139-2153.

Wu, J. F., L. Zheng, and D. P. Liu (2007), Optimizing groundwater development strategies by genetic algorithm: a case study for balancing the needs for agricultural irrigation and environmental protection in northern China, *Hydrogeology Journal*, *15*(7), 1265-1278.

Xu, M. J., and Y. Eckstein (1995), USE OF WEIGHTED LEAST-SQUARES METHOD IN EVALUATION OF THE RELATIONSHIP BETWEEN DISPERSIVITY AND FIELD-SCALE, *Ground Water*, *33*(6), 905-908.

Yan, S. Q., and B. Minsker (2006), Optimal groundwater remediation design using an Adaptive Neural Network Genetic Algorithm, *Water Resources Research*, *42*(5).

Yoon, J-H and C.A. Shoemaker (1999), Comparison of Optimization Methods for Groundwater Bioremediation, J. Water Resour. Plann. Manag., 125 (1), 54-63.

Yuen, S. Y., and C. K. Chow (2009), A Genetic Algorithm That Adaptively Mutates and Never Revisits, *Ieee Transactions on Evolutionary Computation*, *13*(2), 454-472.

Zheng, C. M., and P. P. Wang (1999a), An integrated global and local optimization approach for remediation system design, *Water Resources Research*, *35*(1), 137-148.

Zheng, C., and P. P. Wang (1999b), Mt3dms: A modular three-dimensional multispecies transport model for simulation of advection, dispersion and chemical reactions of contaminants in groundwater systems: Documentation and user's guide, Contract Rep., SERDP-99-1, U.S. Army Eng. Res. and Dev. Cent., Vicksburg, Miss

Zheng, C. M., and P. P. Wang (2002), A field demonstration of the simulation optimization approach for remediation system design, *Ground Water*, *40*(3), 258-265.

7 Annex

Table A-1 Chemical compounds detected in GW samples from monitoring wells (July 2001)

	Nr. of wells analyte detected	Range (µg/l)	Detection Limit (µg/l)	MCL (DM 471/99) (µg/l)
Inorganic Compounds				
Arsenic	44	1-230	0.1	10
Chromium	31	0.3-61	0.1	50
Hexavalent Chromium	0	-	5	5
Mercury	12	0.1-0.8	0.1	1
Lead	42	0.1-210	0.1	10
Copper	41	0.2-1400	0.1	1000
Organic Compounds				
Aromatic hydrocarbons				
Benzene	30	0.03-4200	0.03	1
Ethylbenzene	31	0.03-550	0.03	50
Styrene	39	0.23-440	0.2	25
Toluene	30	0.11-4900	0.08	15
o-Xylene	24	0.06-480	0.06	NS
m-Xylene	23	0.03-380	0.03	NS
p-Xylene	21	0.06-400	0.06	10
Polycyclic aromatic hydrocarbons				
Naphthalene	45	0.01-135	0.01	NS
Acenaphthene	30	0.01-10	0.01	NS
Fluorene	26	0.01-14	0.01	NS
Phenanthrene	32	0.01-28.5	0.01	NS
Anthracene	20	0.01-5.9	0.01	NS
Fluoranthene	15	0.01-2.7	0.01	NS
Pyrene	24	0.01-4.8	0.01	NS
Chrysene	9	0.01-1.3	0.01	NS
Dibenzo(a,h)pyrene	5	0.01-0.04	0.01	NS
Dibenzo(a,l)pyrene	2	0.01-0.01	0.01	NS
Benzo(a)anthracene	9	0.01-2.1	0.01	NS
Benzo(b)fluoranthene	5	0.01-0.25	0.01	NS
Benzo(k)fluoranthene	7	0.02-0.5	0.01	NS
Benzo(j)fluoranthene	4	0.01-0.25	0.01	NS

(Continuated)	Nr. of wells analyte detected	Range (µg/l)	Detection Limit (µg/l)	MCL (DM 471/99) (µg/l)
Benzo(a)pyrene	6	0.02-0.8	0.01	0.01
Indeno(1,2,3-cd)pyrene	3	0.02-0.09	0.01	NS
Dibenzo(a,h)anthracene	2	0.02-0.09	0.01	NS
Benzo(g,h,i)perylene	4	0.02-0.08	0.01	NS
Halogenated Organic Compounds				
Carcinogenic Chlorinated Hydrocarbons				
Chloromethane	1	0.22-0.22	0.05	1.5
Dichloromethane	26	0.19-2050	0.05	NS
Chloroform	31	0.1-5500	0.04	0.15
Vynil Chloride	30	0.04-7000	0.04	0.5
1,2-Dichloroethane	42	0.12-240000	0.02	3
1,1-Dichloroethylene	29	0.14-2780	0.05	0.05
1,2-Dichloropropane	10	0.08-8.5	0.02	0.15
1,1,2-Trichloroethane	37	0.2-2500	0.08	0.2
Trichloroethylene	45	0.26-5100	0.02	1.5
1,2,3-Trichloropropane	4	0.14-0.77	0.09	0.001
1,1,2,2-Tetrachloroethane	29	0.1-1880	0.05	0.05
Tetrachloroethylene	41	0.7-3000	0.05	1.1
Hexachlorobutadiene	12	0.1-40	0.1	0.15
Non Carcinog. Chlorinated Hydrocarbons				
1,1-Dichloroethane	22	0.11-2300	0.05	810
1,2-Dichloroethylene	24	0.11-3100	0.06	60
1,1,1-Trichloroethane	3	0.35-2.3	0.04	NS
Brominated Hydrocarbons				
Bromoform	4	0.14-500	0.05	0.3
1,2-Dibromoethane	2	0.3-0.3	0.05	0.001
Dibromochloromethane	5	0.6-270	0.07	0.13
Bromodichloromethane	5	0.09-14	0.03	0.17
Chlorobenzenes				
Chlorobenzene	31	0.06-15	0.03	40
1,2-Dichlorobenzene	23	0.07-730	0.05	270
1,4-Dichlorobenzene	14	0.09-30	0.04	0.5
1,2,4-Trichlorobenzene	7	0.09-3.7	0.09	190
1,2,4,5-Tetrachlorobenzene	43	0.01-19	0.01	1.8
Pentachlorobenzene	40	0.01-24	0.01	5
Hexachlorobenzene	36	0.01-13.5	0.01	0.01

Note: NS stands for Not Specified.

Table A-2 Adsorption parameters of the COCs

Compound	Liquid Phase		Experiment Parameters		Source	Gaseous Phase		Source
	Kf ((mg/g)(L/mg)^{nf})	nf	Conc. Range (µg/l)	Temp. (°C)		Kf ((mg/g)(L/mg)^{nf})	nf	
Benzene	16.6	0.4	10-2000	20	Weber et al., 1981	281	0.25	Bayer (200?)
Toluene	97	0.43	2-900	20	Speth et al., 1988			
1,1,2-TCA	13	0.53	10-900	20	Speth et al., 1988			
1,2-DCA	5.12	0.53	43-717	24	Speth, 1990	299	0.26	Bayer (200?)
Chloroform	11.3	0.53	8-1180	11	Crittenden, 1985			
DCM	1.58	0.8	18-715	24	Speth, 1990			
PCE	246	0.46	4-1170	11	Crittenden, 1985			
TCE	31.9	0.47	3-528	21	Crittenden, 1985			
1,1-DCE	16.5	0.52	7-392	24	Speth, 1990			
1,2-DCE	11.7	0.59	5-615	24	Speth, 1990			
VC	0.165	0.64	-	-	Bayer (200?)	23	0.39	Bayer (200?)

Note: Parameters taken from AdDesignS (Mertz, K. A., Gobin, F. et al., 1994), except for Bayer (…).

Table A.3 Basic and specific parameters for cost calculation obtained from Lantschner (2005)

Description	Value	Unit
Basic Parameters		
Operation Time	50	years
Annual Interest Rate	0.05	of 1
Annual Price Increase Rate	0.02	of 1
Maintenance Period Well/Treatment Equipment	5	years
Replacement Period Wells	20	years
Investment: Unit Cost		
Site Installation – Wells	20000	€
Well Installation Costs Per Well	15000	€/well
Well Equipment Costs Per Well	5000	€/well
Operation & Maintenance: Unit Cost		
Annual Costs Per Well (Care & Control)	1,000.00	€/year & well
Unit pumping energy demand	0.10	KWh/m^3
Annual Costs Treatment GAC (Care & Control)	2,000.00	€/year
Annual Costs Treatment Catalysis (Care & Control)	4,000.00	€/year
Additional Costs per Reactor Refill - GAC	5,000.00	€/refill
Additional Costs per Replacement of Catalysis Treatment Unit(s)	40,000.00	€/replacement
Unit Costs GAC Material incl. Disposal	4.00	€/kg

Description	Value	Unit
Operation & Maintenance: Unit Cost (cont.)		
Unit Costs Electricity	0.10	€/KWh
Unit Costs Zeolite/ Pd material	300.00	€/kg
Unit Costs NaOH for Neutralisation	250.00	€/m3 (NaOH)
Specifications Concerning Catalysis		
Electricity Consumption Nitrogen Production + Compressor	10	KW
Replacement Period 1 for Catalysis Equipment	20	years
Replacement Period 2 for Vacuum Stripping & Catalysis	5	years
Replacement Period Stripping/Catalysis Equipment	5	years
Membrane module cost (200 m^2 surface area)	12000	€
Membrane module performance	3	€/m3
Vacuum pump cost	20000	€/pump
H_2 generator + flow controller cost	5500	€/generator
N_2 generator cost (N_2 flow < 120 m3/h, 98 % purity)	100000	
N_2 generator cost (N_2 flow < 200 m3/h, 98 % purity)	170000	
N_2/water ratio	5	-
Specifications Concerning Sorptive Removal		
Minimum Refilling Period GAC	9	months

The investment associated with the GAC treatment units was estimated using the regression equation after Bayer (200?), as a function of the total pumping rate Q:

Investment GAC for liquid stream (€):	Investment GAC for gaseous stream (€):
$I = 3000 + 4000\ Q_{liq}^{0.52}$	$I = 3720 + 10.5\ Q_{liq} - 3.9E\text{-}4\ Q_{liq}^{2}$

The site installation investment, accounting for general items not included in other categories, was estimated in 20 % of the total investment.

Usage of electrical energy by the N_2 generator was calculated using the regression equation based on the parameters given by a N_2 generator producer (N2 Generation Ltd., 2005):

$$\mathbf{E_{N2} = (9.0E\text{-}4\ Q_{N2}^2 + 0.27\ Q_{N2})\ 24}$$

where:

E_{N2}: electrical energy usage by N_2 generator (KWh)

Q_{N2}: gaseous nitrogen flow (m3/h)

Table A.4 Values obtained at termination for few selected parameters

Case	OR	Gen	Normalized Fitness	OFI [%]
IDCO	1	335	1007	1.19
IDCO	2	356	1000	0.19
IDCO	3	399	1008	1.51
IDCO	4	305	1003	0.40
IDCO	5	327	1052	0.91
IDCO	6	332	1011	1.04
IDCO	7	298	1037	2.76
IDCO	8	410	1036	0.87
IDCO	9	346	1034	1.43
IDCO	10	242	1045	2.09
IDCO	11	326	1017	1.19
DCO	1	199	1043	0.98
DCO	2	400	1091	2.16
DCO	3	258	1133	0.44
DCO	4	217	1105	0.49
DCO	5	332	1006	0.66
DCO	6	394	1002	0.55
DCO	7	252	1043	0.82
DCO	8	274	1000	0.39
DCO	9	306	1039	0.08
DCO	10	247	1078	1.45
DCO	11	332	1065	0.75
Minimum		199	1000	0.08
Median		327	1036	0.89
Maximum		410	1133	2.76
ST. DEV.		60	37	0.68

Table A.5 Post-processing of each of Scenario 2, 3 and 4 on the other scenarios respectively (Results continued from Table 4.5, Section 4.2)

ISA for Scenario 2

Sc. No.	OR No.	Number of Wells outside [-]	Total Pumping Rate [m^3/day]	Particles Not Captured [-]	CCC [-]	TR [-]	Particle Mean Travel Time [year]	Fitness
1	1	0	456	512	0.72	4.37	17	245021
	2	0	518	731	1.00	1.00	-	115036
	3	0	456	215	0.56	1.51	10	43369
	4	0	454	179	1.20	1.31	7	40619
	5	0	487	193	0.60	1.23	8	37063
2	1	0	619	0	0.28	0.02	3	2361
	2	0	614	0	0.17	0.02	5	1669
	3	0	654	0	0.17	0.01	7	1770
	4	0	635	0	0.18	0.00	5	1766
	5	0	572	0	0.17	0.03	3	1575
3	1	0	444	432	0.83	4.35	12	207582
	2	0	535	101	0.63	1.06	5	23427
	3	0	476	731	1.00	1.00	-	200765
	4	0	459	199	0.43	1.37	6	36719
	5	0	452	218	0.91	1.41	6	45192
4	1	0	437	340	1.02	3.86	13	152773
	2	0	447	265	0.25	1.89	10	55832
	3	0	452	231	0.54	1.50	9	45245
	4	0	489	378	0.19	2.77	11	117133
	5	0	451	305	0.13	1.91	12	63047
Mean		0	505	252	0.55	1.53	8	71898
Stdev		0	73	222	0.35	1.37	4	75512
Max		0	654	731	1.20	4.37	17	245021
Min		0	437	0	0.13	0.00	3	1575

ISA for Scenario 3

Sc. No.	OR No.	Number of Wells outside [-]	Total Pumping Rate [m^3/day]	Particles Not Captured [-]	CCC [-]	TR [-]	Particle Mean Travel Time [year]	Fitness
1	1	0	456	193	0.15	1.27	17	30698
	2	0	518	31	0.14	0.87	6	6367
	3	0	456	17	0.15	1.10	9	4698
	4	0	454	5	0.16	0.68	7	2402
	5	0	487	731	0.00	0.68	7	80054
2	1	0	619	0	0.67	0.09	3	5029
	2	0	614	6	0.45	2.13	10	13440
	3	0	654	0	0.52	0.01	3	4089
	4	0	635	30	0.30	1.65	6	14492
	5	0	572	0	0.66	0.16	3	4852
3	1	0	444	0	0.14	0.02	11	1070
	2	0	535	0	0.15	0.06	3	1399
	3	0	476	0	0.15	0.02	7	1181
	4	0	459	0	0.15	0.05	4	1169
	5	0	452	0	0.15	0.06	3	1173
4	1	0	437	3	0.14	0.17	7	1381
	2	0	447	2	0.14	0.20	4	1372
	3	0	452	1	0.15	0.18	4	1342
	4	0	489	2	0.15	0.15	4	1511
	5	0	451	2	0.14	0.21	4	1393
Mean		0	505	51	0.23	0.49	6	8956
Stdev		0	73	166	0.19	0.62	4	18193
Max		0	654	731	0.67	2.13	17	80054
Min		0	437	0	0.00	0.01	3	1070

ISA for Scenario 4

Sc. No.	OR No.	Number of Wells outside [-]	Total Pumping Rate [m^3/day]	Particles Not Captured [-]	CCC [-]	TR [-]	Particle Mean Travel Time [year]	Fitness
1	1	0	456	197	0.16	1.09	15	28370
	2	0	518	32	0.14	1.13	7	7587
	3	0	456	17	0.16	0.62	6	3486
	4	0	454	17	0.16	0.77	7	3837
	5	0	487	0	0.16	0.20	4	1472
2	1	0	619	0	0.67	0.09	3	5067
	2	0	614	0	0.46	0.69	5	5627
	3	0	654	0	0.52	0.01	3	4065
	4	0	635	25	0.31	1.42	6	12010
	5	0	572	0	0.66	0.15	3	4777
3	1	0	444	48	0.13	0.58	16	5982
	2	0	535	0	0.17	0.05	3	1486
	3	0	476	17	0.14	0.59	13	3437
	4	0	459	7	0.14	0.26	5	1854
	5	0	452	0	0.15	0.07	3	1181
4	1	0	437	0	0.14	0.01	5	1066
	2	0	447	0	0.14	0.04	4	1099
	3	0	452	0	0.15	0.03	3	1141
	4	0	489	0	0.15	0.04	5	1254
	5	0	451	0	0.14	0.02	4	1096
Mean		0	505	18	0.24	0.39	6	4795
Stdev		0	73	44	0.18	0.44	4	6214
Max		0	654	197	0.67	1.42	16	28370
Min		0	437	0	0.13	0.01	3	1066

Table A.6 Optimization for DCO with 17 % minimal mass removal

Optimization Run				Optimization Result			Pumping Rate [m3/day]			Removed Mass [%]			Treated Mass [%]		Cost [€ 1E6]			
Case	Sc	OR	Gen	CCC	TR	Fitness	GAC	CAT	Total	BTEX	CHC	Total	GAC	CAT	PW	GAC	CAT	Total
DCO17	1	1	367	1.5	0.02	9063	184	368	552	0.12	16.94	17.06	0.14	16.92	0.74	0.15	1.2	2.14
DCO17	1	2	303	0.5	0.02	3170	62.9	436	499	0.41	17.17	17.57	0.03	17.54	0.73	0.12	1.3	2.23
DCO17	1	3	343	0.8	0.04	5113	180	363	543	0.34	16.70	17.04	0.08	16.96	0.73	0.15	1.1	2.11
DCO17	1	4	323	0.6	0.05	3876	198	363	561	0.32	16.91	17.23	0.08	17.15	0.74	0.15	1.1	2.11
DCO17	1	5	338	0.5	0.04	3110	55.9	482	538	0.41	16.71	17.12	0.10	17.02	0.73	0.15	1.4	2.34
Minimum			303	0.47	0.02	3110	56	363	499	0.1	16.7	17.0	0.0	16.92	0.73	0.12	1.12	2.11
Mean			335	0.78	0.03	4866	136	403	539	0.3	16.9	17.2	0.1	17.1	0.73	0.15	1.20	2.18
Maximum			367	1.53	0.05	9063	198	482	561	0.4	17.2	17.6	0.1	17.54	0.74	0.15	1.35	2.34
St. Dev.			24	0.44	0.01	2481	70	54	24	0.12	0.19	0.22	0.04	0.25	0.00	0.01	0.10	0.10